METEOROLOGICAL-TOWER INDUCED WIND-FIELD PERTURBATIONS

by

G. Hsi and J. E. Cermak

Prepared under
U. S. Army Research Grant DA-AMC-28-043-64-G-9
U. S. Army Materiel Command
Washington 25, D. C.

FLUID MECHANICS PROGRAM
ENGINEERING RESEARCH CENTER
COLLEGE OF ENGINEERING
COLORADO STATE UNIVERSITY
FORT COLLINS, COLORADO

Technical Report

METEOROLOGICAL-TOWER INDUCED WIND-FIELD PERTURBATIONS

by

G. Hsi and J. E. Cermak

Prepared under

U. S. Army Research Grant DA-AMC-28-043-64-G-9
U. S. Army Materiel Command
Washington 25, D. C.

Fluid Mechanics Program
College of Engineering
Colorado State University
Fort Collins, Colorado

October 1965 CER65GH-JEC49

TABLE OF CONTENTS

TABLE OF CONTENTS--Cont'd

ACKNOWLEDGEMENTS

The authors wish to express their appreciation to Professor E. J. Plate and H. Maynard, Resident Research Meteorologist, U. S. Army, who both gave many valuable suggestions and guidance during the period of this research.

ABSTRACT

The objective of this study was to determine how the presence of a typical meteorological tower disturbs the local wind pattern. This study provides data which can be used to correct wind speeds measured by anemometers in the field. Experimental results in this paper are based on data taken upstream of, around, and downstream from a 1:4 scale model of a 20 ft segment of the prototype tower.

LIST OF FIGURES

LIST OF SYMBOLS

Symbol	
E	Eastward transverse direction from wind-tunnel center
g	Gravitational acceleration, ft/sec^2
Δh	m.m. of mercury
L	Characteristic length
Δp	Static and dynamic pressure difference
U	Local wind velocity, ft/sec
U_a	Free-stream wind velocity, ft/sec
W	Westward transverse direction from wind-tunnel center
Y	Transverse distance
z	Vertical distance
$\frac{\sqrt{\overline{u^2}}}{U_a}$	Turbulence intensity
α	Angle of defect, degrees
ρ_a	Density of air
ρ_H	Density of mercury

METEOROLOGICAL-TOWER INDUCED
WIND-FIELD PERTURBATIONS

1. INTRODUCTION

The purpose of this study was to determine how the presence of a typical meteorological tower disturbs the local wind pattern. Modifications found in the local winds, especially in the downstream wake (tower shadow), are studied but the significance of these perturbations to meteorological measurements is not elaborated upon. However, results obtained from this study yield correlation factors which will permit corrections to be made for actual anemometer sensings. Phenomena isolated by this study are receiving further study in the Fluid Dynamics and Diffusion Laboratory at Colorado State University.

Investigations reported in this paper are not the first to probe wind-field disturbances produced by a tower wake. Moses and Daubek (3), stated that "the air flow on the lee side of the tower may be reduced to nearly one-half its true value for light winds and nearly 25% for speeds of 10 to 14 mph." The conclusions reached by Moses and Daubek are valid, but insufficient data were obtained to allow practical use of their findings.

Experimental results reported in this paper are based on data taken upstream of, around, and downstream from a 1:4 scale model of a 20 ft segment of the prototype tower - the White Sands Missile Range 500 ft meteorological tower. Throughout this study the tower model is referred to as a "clean tower" or a "modified tower". These two tower structures are the same, the only difference being that the "clean tower" shown in Fig. 1 is the basic structure without the mechanism box, boom, ducts, and ladder. This model was used to find the effect of the tower structure on the wind velocity without the influence of accessories. The "modified tower" shown in Fig. 2 is the same basic structure with the aforementioned accessories mounted in their proper locations.

Using a 1:4 scale model, air for the modeling fluid, and a wind speed approximately the same as prototype wind speeds (30 fps), the model's Reynolds number was approximately one quarter that for the prototype. To determine if the difference in Reynolds number might influence the wind distribution, velocity measurements were made over a selected profile for three wind speeds (10, 30 and 60 fps). The distributions of wind speed appeared to be similar in all cases; therefore, it is concluded that the model wind data are not influenced by Reynolds number variation and are similar to the prototype wind field.

The following wind-field characteristics were found for both the clean and modified models:

1. The mean velocity profiles appearing around both of the models developed a downstream velocity defect angle which can be predicted.
2. Transverse velocity profiles taken at one height will differ from the same profile taken at another height at the same distance downstream from the tower.

The following major differences in wind disturbance around the clean and modified towers were found:

1. The maximum wind defect is 24% of the free-stream speed for the clean tower while it is about 40% for the modified tower.
2. The maximum wind augmentation is 5% of the free-stream speed for the clean tower while it is about 9% for the modified tower.

2. EXPERIMENTAL APPROACH

In order to achieve an accurate model of the disturbed wind pattern, several types of similarity must be satisfied. For this study, the following types of similitude were considered to be necessary and sufficient:

a. Geometric Similarity

b. Kinematic Similarity

c. Dynamic Similarity

These similarities were approximately achieved by the proper selection of scales and operating conditions.

a. Geometric similarity was assured by use of a reduced scale model on a ratio of 1:4 with the prototype. A 20 ft length of tower was considered to be adequate since air flow is ordinarily normal to the tower axis and not parallel to it.

b. Kinematic and dynamic similarity were assured by maintaining wind tunnel conditions that are approximately similar to those found in the atmosphere. This similarity was assured by:

   i. Maintaining a zero pressure gradient along the longitudinal axis of the wind tunnel.

   ii. Operating at a Reynolds number nearly equal to that for the prototype.

   iii. Taking all data measurements outside the boundary layers that are present at the floor, ceiling and walls of the wind tunnel because these boundary layers are very thin compared to the atmospheric boundary layer.

The following simplifications pertaining to practical aspects of this study were made:

a. Both the clean tower and the modified tower were subjected to a constant free-stream velocity of 30 fps. This velocity gave a sufficiently high Reynolds number to minimize viscous effects. However, the uniform velocity over the tower section made determination of effects due to actual wind shear, if there are any, impossible.

b. The natural ambient turbulence intensity of 0.1% was not altered for this study; therefore, the effects of higher turbulence intensities, up to 10% encountered in the prototype, on the wind distortion has been neglected.

c. It is assumed that the prototype segment, duplicated by the model, is located far enough above the ground to moderate influences exerted by the earth's terrain.

3. EXPERIMENTAL EQUIPMENT

3.1 Low-Speed Wind Tunnel (See Fig. 5)

The low-speed wind tunnel is of the recirculating type with a 6 x 6 ft test section. It is 32 ft in length and is powered by a constant-speed, variable-pitch fan rated at 75 hp. The mean-velocity range is from 3 to 90 fps and the ambient turbulence intensity is about 0.1%.

3.2 The Model Meteorological Tower

The model, constructed on a 1:4 ratio, duplicates that portion of the prorotype which begins at a level of 80 ft and ends at the 100 ft level. A detailed structural drawing of the prototype is shown in Fig. 3.

The model was constructed from three sizes of brass tubing which were in proportion to the three sizes of tubing used in the construction of the prototype. Testing accuracy required that the model be kept outside of the boundary layer created at the ceiling and floor of the wind tunnel. This requirement was fulfilled by attaching 6 in. supports to the top and bottom of the model.

3.3 Model-Positioning Mechanism

Winds striking the prototype from various directions created different wakes. This required installation of a positioning mechanism capable of rotating the model about its vertical axis. Once the model was mounted on this mechanism it could be rotated in the fixed direction free-stream of the tunnel thus simulating the flow produced by different wind directions.

The positioning mechanism and the model were installed in the tunnel in the following manner:

a. The circular base was placed on the tunnel floor. Its center was attached on the tunnel centerline 69 in. from the test-section entrance.

b. The ball bearing was inserted into the base-plate bearing seat.

c. The bottom 6 in. extension was attached to the bottom support.

d. The top 6 in. extension was attached to the top support.

e. The extension on the bottom support was fitted to the bearing, and the stabilizing pin was run through a hole in the tunnel ceiling and inserted into the tubing of the top support.

It should be noted that holes drilled in the bottom support facilitated the pinning of the model in its desired position.

3.4 Instrumentation

The instrumentation necessary for determining the model wind field consisted of the following:

a. Mean velocity instrumentation.

b. Turbulence instrumentation.

3.41 Mean Velocity Measurements

The following equipment was used to take mean-velocity measurements:

a. Prandtl tube. This tube, 1/4 inch in diameter, was mounted on a positioner which could be attached to an instrument carriage which runs on tracks attached to the tunnel walls. The positioner was moved either vertically or horizontally by an electric motor mounted on the instrument carriage. Motor operation is controlled by a switch located outside the wind tunnel.

b. Trans-sonic Pressure Meter -- second instrument from left in Fig. 4. This meter was connected to the Prandtl tube by flexible plastic tubing 1/4 in. in diameter.

All velocity measurements were read from the pressure meter and converted to the standard condition by a standardization chart. The data were then substituted in the following equation to find the true stream velocity:

$$U = \sqrt{\frac{2 \Delta p}{\rho_a}} = \sqrt{\frac{2 \rho_H g \Delta h}{\rho_a}} \approx 54 \sqrt{\Delta h} \quad \text{fps.}$$

ρ_a = density of air; ρ_H = density of mercury

Δh = mm of mercury; and g = gravitational acceleration, ft/sec^2.

3.42 Turbulence Measurements

The following equipment was used to measure turbulence:

a. Hot-Wire Probe. The hot-wire probe was a single platinum wire which was 0.0001 in. in diameter, 0.1 in. long, and had a resistance of 5 ohms.

b. Constant Temperature Servo Amplifier (Hubbard 3A) -- first instrument on left in Fig. 4.

c. RMS-Meter (Bruel and Kjaer 2409) -- third instrument from left in Fig. 4. This meter was modified to give an output voltage which is proportional to the rms-meter.

Voltage fluctuations from the bridge containing the hot-wire probe formed the input to the servo amplifier. The amplified AC output was fed to the rms-meter from which the rms-voltage was determined. The output voltage of the Hubbard amplifier is a linear function of the velocity. This function is determined by calibrating the amplifier output as measured by a DC meter against the Prandtl-tube-determined velocity when the hot-wire and Prandtl tube are placed together in the wind-tunnel air stream.

4. CALIBRATION PROCEDURES

4.1 Wind Tunnel Calibration

Calibration of the wind tunnel requires verification of two factors:

a. Pressure Gradient. Measuring the pressure along the center line of the wind tunnel must yield a zero pressure gradient.

b. Wind-Tunnel Velocity Distribution. To obtain results easily interpretable, the air stream approaching the model should be uniform.

Measurements of the velocity distribution across the tunnel indicated a spatial variation of less than 1 % excepting in the boundary-layer regions which were approximately 8 in. thick.

4.2 Instrument Calibration

All instruments with the exception of the hot-wire probe were calibrated by the manufacturer. Instruments were checked for proper null each time they were used.

4.21 Hot-Wire Probe Calibration

The probe was calibrated in conjunction with the Prandtl tube in the following manner:

a. The probe and tube were mounted in close proximity to each other at the center of the tunnel cross-section, and subjected to the same free-stream velocity.

b. The Prandtl-tube sensings, when taken from the transonics transducer, were converted to the corrected free-stream velocity by the following formula:

$$U \approx 54 \sqrt{\Delta h}$$

where $U =$ the local velocity, fps

and $\Delta h =$ reading from transonic pressure meter.

c. Hot-wire probe measurements were made simultaneously with the Prandtl-tube measurements so that the hot-wire voltage readings could be directly related to the free-stream velocity.

d. Voltages obtained from steps b and c were plotted on a graph to form a calibration curve.

5. TESTING PROCEDURES

Velocity measurements were made at all or some portion of the eight test stations listed in the following table:

Test-Station Number	Location	Remarks
-1	15 in. upstream from center of model	
0	69 in. from the tunnel entrance	This station is at center of model.
1	15 in. downstream from center of model	
2	30 in. downstream from center of model	
A	35 in. downstream from center of model	This is the location of boom tip in the modified model for an orientation of 0^0 position.
3	60 in. downstream from center of model	
4	120 in. downstream from center of model	
5	300 in. downstream from center of model	This point is equivalent to a point 33 m from the prototype where field measurements of wind velocity were made atop poles 20 m high.

Unless otherwise noted the free-stream velocity was 30 fps and the tower was oriented in the position shown in Fig. 1.

5.1 Procedure for Obtaining Velocity Contours (Isotachs)

Isotachs were obtained at test stations A and 2 only. All measurements were taken with the Prandtl tube attached to the positioner which was mounted on the instrument carriage.

5.11 Clean Tower

a. The Prandtl tube was set at the tower center-line, 25.5 in. above the tunnel floor, and the first reading of the transverse profile taken.

b. Maintaining the 25.5 in. height, the Prandtl tube was moved 1/2 in. in a westward direction and a second reading taken.

c. Step b was repeated until the Prandtl tube had covered a distance of 14 in. in the westward direction.

d. The Prandtl tube was returned to the tower center line and the initial measurement was verified.

e. Maintaining the 25.5 in. height, the Prandtl tube was moved 1/2 in. in an eastward direction and a transverse profile reading taken.

f. Step e was repeated until the Prandtl tube had covered a distance of 14 in. in the eastward direction.

g. Repeat steps a through f for each 1/2 in. interval of height from 25.5 in. to 35.5 in.

h. To complete the isotach, all readings were plotted on a graph and all points of equal velocity were connected.

5.12 Modified Tower

The procedure for obtaining isotachs for the modified tower is identical to procedure 5.11 excepting that the isotachs ran from a height of 9.5 in to 26.5 in. Measurements were taken at 1 in. intervals.

5.2 <u>Procedure for Taking Transverse Velocity Profiles</u>

Transverse velocity profiles were taken at test stations -1, 0, 1, 2, 3, 4, and 5. All measurements were taken with the Prandtl tube attached to the positioner which was mounted on the instrument carriage.

5.21 Clean Tower

This procedure is identical to steps a through f of procedure 5.11, except the initial height was 20.5 in. The procedure was repeated at all test stations and all readings were plotted on a velocity-distance graph in the dimensionless form. The characteristic velocity for this case is the ambient velocity of 30 fps, and the characteristic length is the width of one side of the tower; i.e., one foot.

5.22 Modified Tower

This procedure is identical to 5.21. It should be noted that the boom and mechanism box were not included in this procedure.

5.3 Procedure for Taking Circular Velocity Profiles

5.31 Clean Tower

Circular profiles generated by the clean tower were measured at the outside perimeter of two circles, one having a 15 in. radius and the other a 30 in. radius.

a. The two circles were drawn on the tunnel floor using the model center as the center of each circle.

b. The Prandtl tube, attached to its positioner, was placed on the tunnel floor 20.5 in. above the outside perimeter of the circle and parallel to the free-stream velocity.

c. Data were taken at each 30^0 position around the upstream portion of the circle (240^0).

d. Data were taken at each 15^0 position around the downstream portion of the circle (60^0) not including the wake sector.

e. In the wake sector data were taken at 7.5^0 segments on the circle.

5.32 Modified Tower

Circular profiles generated by the modified tower were measured on the outside perimeter of a figure constructed in the following manner. A circle with a 35 in. radius, corresponding to the boom-tip distance, was drawn on the tunnel floor. To avoid the boundary layers that exist along the walls of the wind tunnel, a line parallel to each wall 24.8 in. from the center of the circle was drawn. Each line was long enough to bisect the circle in two places. The final figure is an area whose upstream and downstream boundaries are circular curves. The following procedure was followed when collecting data along a contour having the shape of this figure:

a. The Prandtl tube, attached to its positioner, was placed on the tunnel floor 20.5 in. above the floor, over a point on the perimeter of the area defined in the previous paragraph, and parallel to the tunnel free-stream velocity.

b. Data were taken on the two parallel lines at the following points:

   i. Where the lines intersect the circle.

   ii. At the center point of each straight line. This point is found by drawing a line from the center of the circle perpendicular to the parallel line. The point where these two lines intersect is the center point of the parallel line.

   iii. Two points, one on either side of the center point, 28 in. from the center of the circle.

c. Data were taken at each 15^0 position along the upstream curve.

d. Data were taken at each 15^0 position along the downstream curve excųlding the wake sector.

e. Within the wake sector data were taken at 7.5^0 intervals.

5.4 Procedure for Taking Vertical Velocity Profiles (clean tower only)

Vertical velocity profiles were taken at test stations 2, 3 and 5.

5.41 The Prandtl tube, attached to its positioner, was placed at a height of 16.5 in. at the center line of the tower.

5.42 Data were taken at 1/2 in. intervals up to a height of 55.5 in.

5.5 Procedure for Taking Transverse Velocity Profiles at Different Ambient Velocities (clean tower only)

Transverse velocity profiles were taken at test station 1 only. The procedure at this station is identical to procedure 5.21, excepting that the tower was subjected to wind velocities of 10, 30 and 60 fps.

5.6 Procedure for Taking Transverse Velocity Profiles While Rotating the Tower (clean tower only)

These transverse profiles were taken at test stations 1, 2 and 3. At stations 1 and 2 the tower was rotated in increments of 15^0 in a counter-clockwise direction, while at station 3 the tower was rotated at 30^0 increments in the same direction. All measurements were taken with the Prandtl tube attached to the positioner which was mounted on the instrument carriage.

5.61 The Prandtl tube was set at the center line of the tower, 20.5 in. above the tunnel floor, and the first reading taken.

5.62 Maintaining the 20.5 in. height, the Prandtl tube was moved 1/2 in. in a westward direction and a second reading taken.

5.63 Step 5.62 was repeated until the Prandtl tube had covered a distance of 14 in. in the westward direction.

5.64 The Prandtl tube was returned to the center line of the tower and the initial measurement was verified.

5.65 Maintaining the 20.5 in. height, the Prandtl tube was moved 1/2 in. in an eastward direction and a reading taken.

5.66 Step 5.65 was repeated until the Prandtl tube had covered a distance of 14 in. in the eastward direction.

5.67 Upon completion of step 5.66 the tower was rotated the desired number of degrees (depending on the test station) and steps 5.61 through 5.66 were repeated.

5.7 Procedure for Making Turbulence-Intensity Measurements.

Turbulence intensity was measured at test stations -1, 0, 1, 2, 3 and 5. The procedure at these stations was identical to 5.6 excepting that the Prandtl tube and the hot-wire probe were both used.

6. DATA ANALYSIS

Foregoing procedures revealed many significant phenomena for both the clean and modified towers. The purpose of this section is to present the phenomena found by each testing procedure. For the sake of convenience, phenomena are presented under basically the same title and in the same sequence as the foregoing procedures.

6.1 Velocity Contours (Isotachs)

6.11 Clean Tower (see Fig. 6)

Procedure 5.11 revealed the following phenomena:

a. The lowest dimensionless velocity, 0.825, appeared at test station 2.

b. There are various paths through the tower where the free-stream velocity is changed only slightly. Fig. 6 shows several wind peaks which are the result of these paths, the highest being the same as the ambient velocity. This particular path was observed at test station 2 when the Prandtl tube was at the center line of the tower, 27 to 27.5 in. above the tunnel floor.

6.12 Modified Tower (see Fig. 7)

Procedure 5.12 revealed the following phenomena:

a. The lowest dimensionless velocity, 0.600, appeared at test station A.

b. The accessories of the modified tower changed the circular peaks generated by the clean tower to zig-zag contour lines.

c. At test station "A" the ambient velocity near the vertical tower center line was reduced a maximum of 40%, while at station 2 the maximum reduction was 37.5%.

d. For practical purposes one may say that the field wind velocity is reduced by 25 to 40% if the wind passes through the tower before it reaches the anemometer.

e. The front view of the tower seen in Fig. 7 does not indicate any restricted flow paths through the tower wake, but this does not mean that these paths do not exist. This figure only indicates that accessories on the tower dominate the wind distribution.

6.13 General Phenomena

Figs. 6 and 7 represent two different segments of the tower model. Fig. 7 depicts the lower half of the model while Fig. 6 illustrates the upper portion. To perform a comparison of data the two figures may be placed with Fig. 6 on top of Fig. 7. This comparison reveals the following phenomena:

a. For the clean tower, the minimum velocity reduction occurs downstream from the tower axis. Whereas for the modified tower the maximum reduction occurs at this location. This maximum reduction gradually decreases with increased lateral distance from the center.

b. The diagonal members of the clean tower divide its overall area into several small open spaces. These spaces are obvious when viewing the model from the frontal position. The smallest amount of velocity reduction occurs at the geometric center of these spaces, and increases as it moves towards the members outlining these spaces. These spaces are responsible for the circular contours seen in Fig. 6 .

6.2 <u>Transverse Velocity Profiles at Different Test Stations</u>

6.21 Clean Tower (see Fig. 8)

Procedure 5.21 revealed the following phenomena:

a. At station -1 the tower reduced the free-stream velocity 0.5%.

b. Mean velocities with the tower at station 0 could not be accurately determined because of large disturbances.

c. Three wakes, formed by the tower legs, were obvious at stations 1 and 2. At station 3 the wakes had diffused to two and at station 5 had coalesced into a single wake.

d. Eddy shedding was observed around the tower legs during this testing procedure, but the Karman vortex trail was not distinct because of the intense mixing produced by flow through the tower.

e. The maximum wind defect, 24%, was recorded at station 1, while a 4% reduction was still present at station 5 (see Fig. 8).

f. To maintain conservation of mass, the wind velocity increased above the ambient around the sides of the tower.

g. The point of minimum reduction at stations 1 and 2 is the point of maximum reduction at station 3 and the point of minimum reduction at station 5. These paths of reduction more or less follow the center line of wind-tunnel flow.

6.22 Modified Tower (see Fig. 9)

Procedure 5.22 revealed the following phenomena:

a. The accessories mounted on the modified tower changed the characteristics of the model to the point that it behaved almost as a solid prism.

b. As can be seen in Fig. 9, there was a 37.5% wind defect at station 2. At station 5 this defect had been reduced to 10%.

c. At station -1 the tower reduced the free-stream velocity 0.5%.

d. The accessories attached to the tower increased the flow speed around the tower sides to about double that for the clean tower.

e. The wake consisted of a large central wake with a small wake on each side which disappeared at station 3.

6.23 General Phenomena

The difference in maximum reduction for the clean and modified tower is 13.5%. This difference is 6% at station 5.

6.3 <u>Circular Velocity Profiles</u>

6.31 Clean Tower (see Figs. 10 and 11)

Procedure 5.31 revealed the following phenomena:

The wake sector varied from 60^0 to 40^0 at the two different radii. The wake sector is defined as that region where the wind defect can be observed. The nature of this angle can be seen in Figs. 10 and 11.

6.32 Modified Tower (see Fig. 12)

Procedure 5.32 revealed the following phenomena:

a. For the horizontal circle 1 ft. above the boom position a maximum velocity defect of 0.4 U_a is formed.

b. At station "A" the wake sector is 30 degrees.

6.4 <u>Vertical Velocity Profiles (clean tower only)</u>

Procedure 5.4 revealed the following phenomena (Figs. 13, 14 and 15 refer to test stations 2, 3 and 5 respectively, and all figures refer to the illustration seen in Fig. 13):

a. It was found at station 2 that there was a spot in every tower section where the local velocity was equal to the free-stream velocity.

b. A uniform velocity profile with a wind defect of 4% was found at station 5.

6.5 <u>Comparison of Transverse Velocity Profiles at Different Ambient Velocities (clean tower only)</u>

Procedure 5.5 revealed that (see Figs. 16, 17 and 18) changing the free-stream velocity did not have a qualitative effect on wind-profile shape, but it did have a 5% increase on wind defect at the low speed of 10 fps. However, an insignificant difference was found at 30 and 60 fps.

6.6 <u>Transverse Velocity Profiles Taken While Rotating the Model (clean tower only)</u>

The phenomena revealed by procedure 5.6 will be discussed in relation to the following four tower orientations--the vertex referred to in these positions is that tower corner which is opposite the side containing the two mounting racks (see Fig. 1):

a. 0^0 position - tower vertex facing upstream.

b. 180^0 position - tower vertex facing downstream.

c. 90^0 position - side containing the racks parallel to the west wall of tunnel.

d. 270^0 position - tower is rotated 180^0 from the 90^0 position.

6.61 Test Station 1 (see Figs. 18-41)

a. <u>0^0 position</u> - Three superimposed wakes were found at this position.

b. <u>180^0 position</u> - Three wakes with similar shapes were found at this position. The difference in maximum reduction when compared with the 0^0 position is 1.5%.

c. <u>90^0 position</u> - At this position the tower legs are in line with the free-stream velocity, thus increasing the amount of maximum reduction to 38%.

d. <u>270^0 position</u> - Phenomena found at this position is identical to that of the 90^0 position except the maximum reduction is 45%. The maximum reduction at the 90^0 and 270^0 position should be identical, but in this case they are not because of the overall error in measurement.

e. <u>General Phenomena</u> -

i. For the 24 investigated positions the number of wakes varied from two to five. These wakes at test station 1 could be ascribed to particular members of the structure.

ii. The maximum velocity reduction did not exceed 45% of the free-stream velocity at any orientation of the tower.

6.62 Test Station 2 (see Figs. 42-65)

a. <u>0^0 position</u> - Three wakes were found at this point with a maximum reduction of 19%.

b. <u>180° position</u> - Phenomena found at this point is identical but reversed with respect to wake configuration in the 0° position.

c. <u>90° position</u> - Maximum reduction at this position was 26%.

d. <u>270° position</u> - Phenomena found at this point is identical but reversed with respect to the 90° position.

e. <u>General phenomena</u> - At this test station the three wakes were beginning to appear more as two wakes. In general, turbulent diffusion has reduced the spatial non-uniformities and the velocity deficiencies in the wakes.

6.63 Test Station 3 (see Figs. 66-77)

a. <u>0° position</u> - Two wakes, one strong and one weak, were found at this position with a maximum reduction of 12.7%.

b. <u>180° position</u> - Two wakes one strong and one weak, were found at this point with a maximum reduction of 11.5%.

c. <u>90° position</u> - Reduction at this position is 15.6%.

d. <u>270° position</u> - Reduction at this position is 17.5%.

e. <u>General phenomena</u> - One strong wake appeared at all positions and was always accompanied by a weak wake appearing on either side of it.

6.7 <u>Turbulence Intensity Measurements (see Fig. 78)</u>

Procedure 5.7 revealed the following phenomena while probing five turbulence intensity $\frac{\sqrt{\overline{u^2}}}{U_a}$ profiles:

a. Three wakes were found at stations 1, 2 and 3, but at station 5 these wakes had smoothed and combined so as to appear as a curved line.

b. An intensity of 3% was found at station 5.

c. An intensity of 1% was found at station -1.

7. CONCLUSIONS

Flow around a 1:4 scale model of a section of the White Sands Missile Range 500 ft meteorological tower using a wind speed of 30 fps was at a sufficiently large Reynolds number to be representative of atmospheric flow around the prototype. An attempt was not made to determine the effects (estimated to be small) of vertical wind shear, intensity of turbulence and the scale of turbulence relative to the tower width on the deficiency of velocity in the wake (shadow) and the decay of these deficiencies with distance downstream from the tower. Further refinements of the present findings, however, should include a determination of such effects.

Referring to points on an arc having a radius of 2.5 tower widths (approximately where meteorological instruments are usually mounted) with center at the axis of the clean tower, the velocity in a sector 90^0 either way from mean wind direction produces a maximum perturbation of only a few percent. The major effect is a velocity deficiency up to about 30% in a 40^0 sector directly downwind of the tower or in the tower wake. Sectors of 70^0 each on either side of the wake have perturbations up to about 10% above the ambient wind speed. Considering the structural arrangement of this typical tower, the foregoing results can be used as a reference to compare with wind perturbations produced around towers with various hardware appended.

Appending hardware such as vertical rails, ducts and wires and booms tend to increase the percentage of velocity increase found around the sides of the tower. However, this appears to be compensated by the wake occupying a smaller sector. Adding appendages such as those found on the meteorological tower being studied, yielded increases of velocity up to 18% of the ambient and the wake sector decreased to about 30^0 with a velocity decrement of 38%.

The dimensionless velocity ratios at different wind orientations can be used to correct anemometer readings made from a meteorological tower.

Such corrections would be especially useful for readings when the fixed anemometers fall within the tower wake. However, such corrections should be made with caution because of the rapid change in velocity defect with angle within and adjacent to the wake sector.

BIBLIOGRAPHY

1. Hinze, J. O. Turbulence. McGraw-Hill, New York, 1959.

2. Knudsen, J. G. and Katz, D. L. Fluid Dynamics and Heat Transfer. Eng. Res. Bull. No. 37, Ann Arbor, Mich., Eng. Res. Inst., Univ. Inst., Univ. Mich., 1954.

3. Moses, H. and Daubek, H. G. Errors in Wind Measurements Associated with Tower-Mounted Anemometers. Bulletin American Meteorological Society, April 1960.

4. Plate, E. J. and Cermak, J. E. Micrometeorological Wind Tunnel Facility. Final Report on Contract No. DA-36-039-SC-80371, U. S. Army, CER63EJP-JEC9, Colorado State University, Fort Collins, Colorado, 1963.

5. Sanuki, M., Kimura, S., and Toyama, S. Anemometer Reading in the Presence of Nearby Obstacle. Meteorology and Geophysics, Vol. VI, No. 2, 1955.

6. Sanuki, M. and Tsuda, M. What are We Measuring on Top of a Tower. Meteorology and Geophysics, Vol. VIII, No. 1, 1957.

7. Schlichting, H. Boundary Layer Theory. 4th edition, McGraw-Hill, 1962.

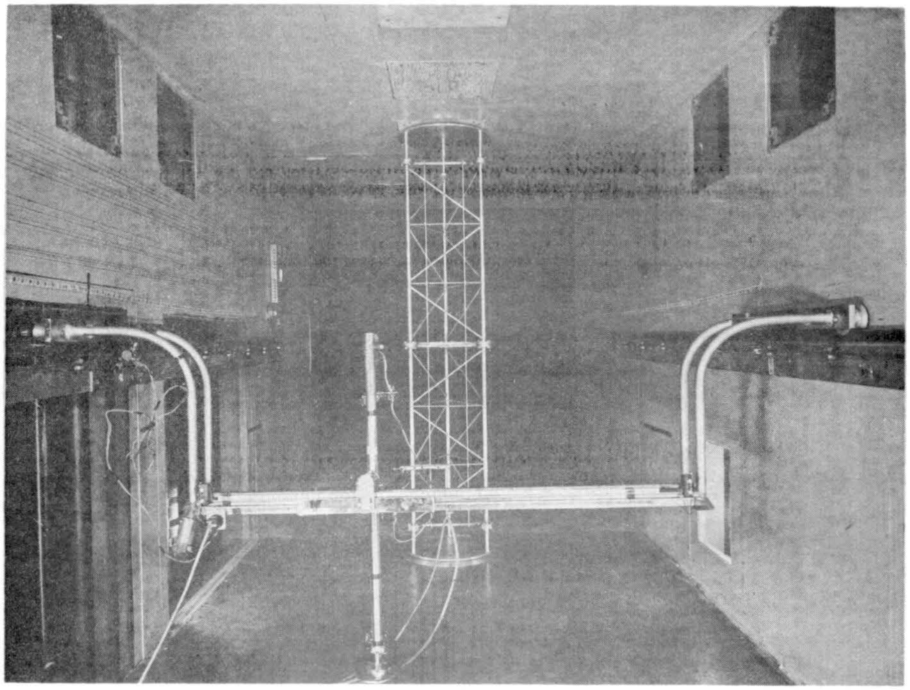

FIG. 1 CLEAN TOWER SET-UP

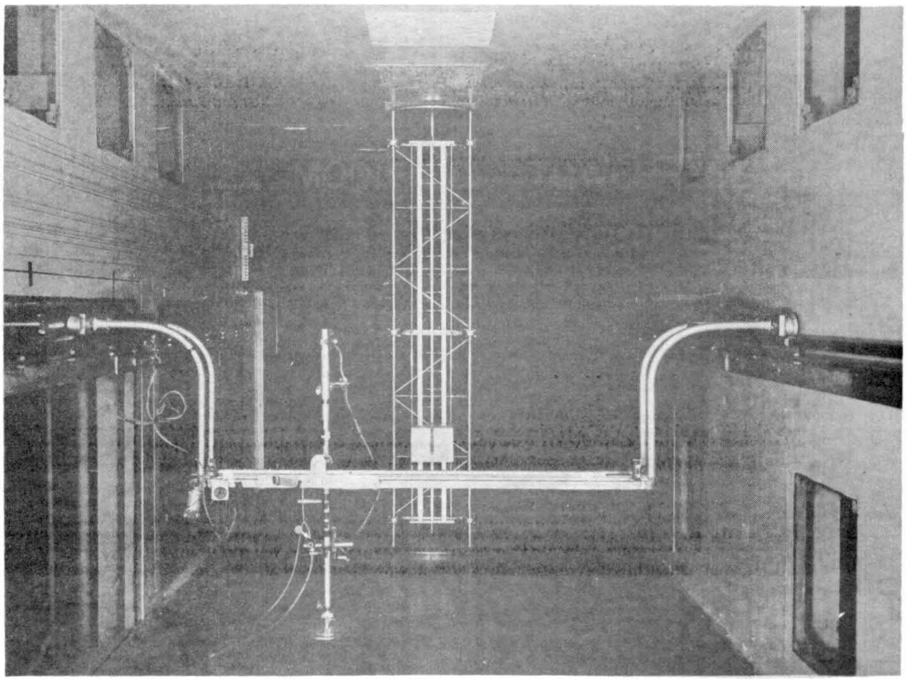

FIG. 2 MODIFIED TOWER SET-UP

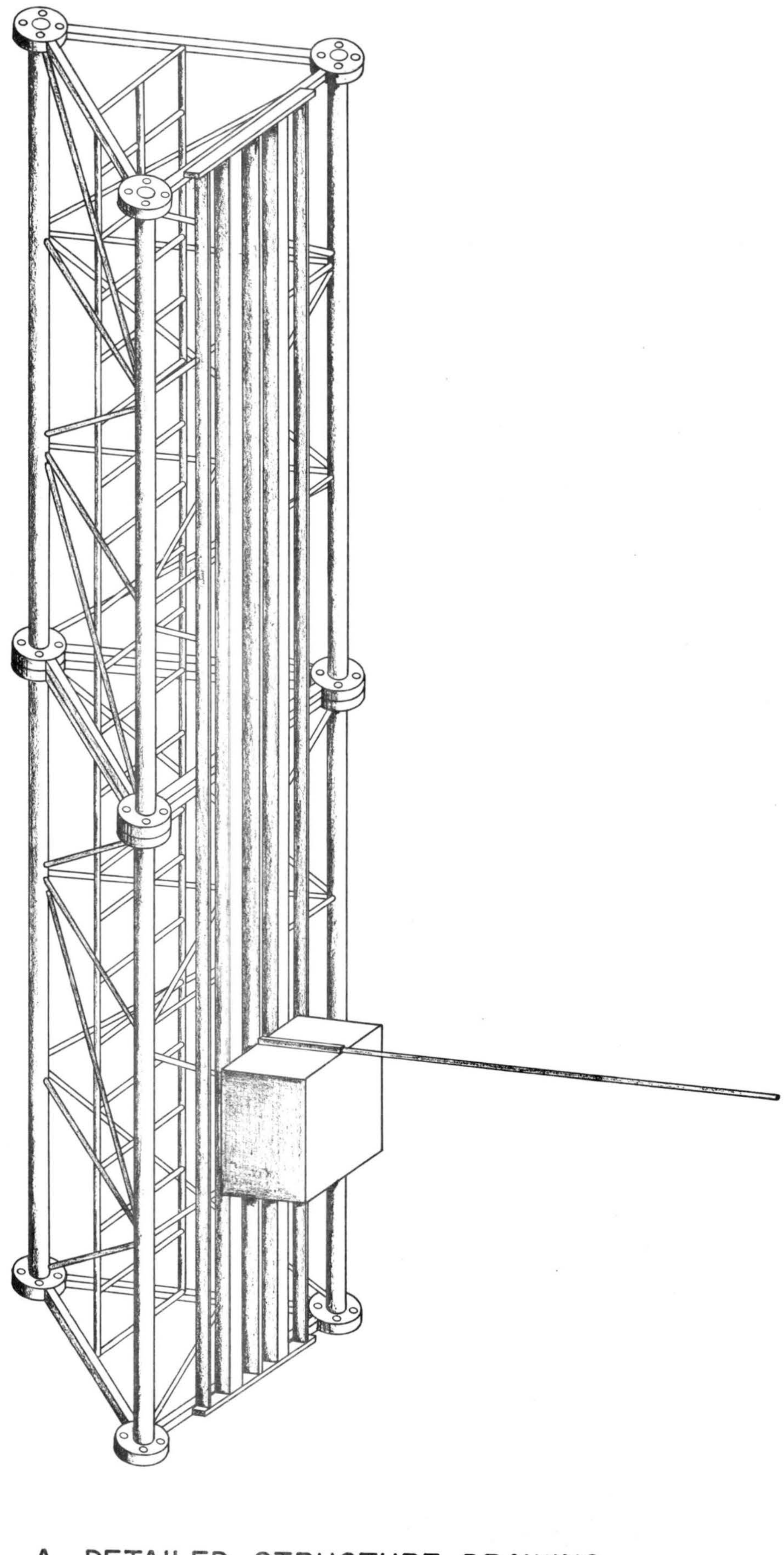

FIG. 3 A DETAILED STRUCTURE DRAWING OF THE PROTOTYPE

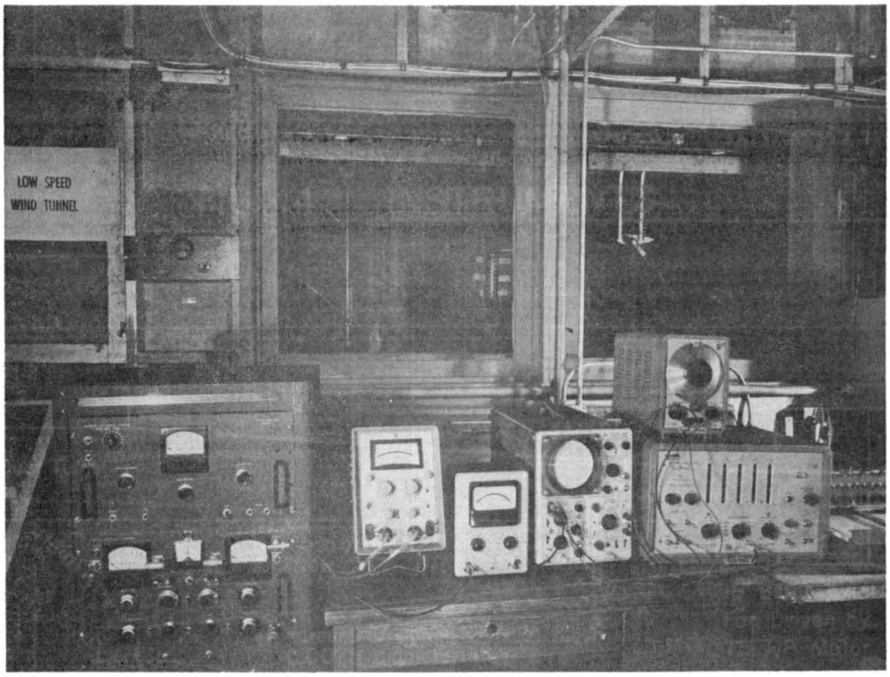

FIG. 4 INSTRUMENTS

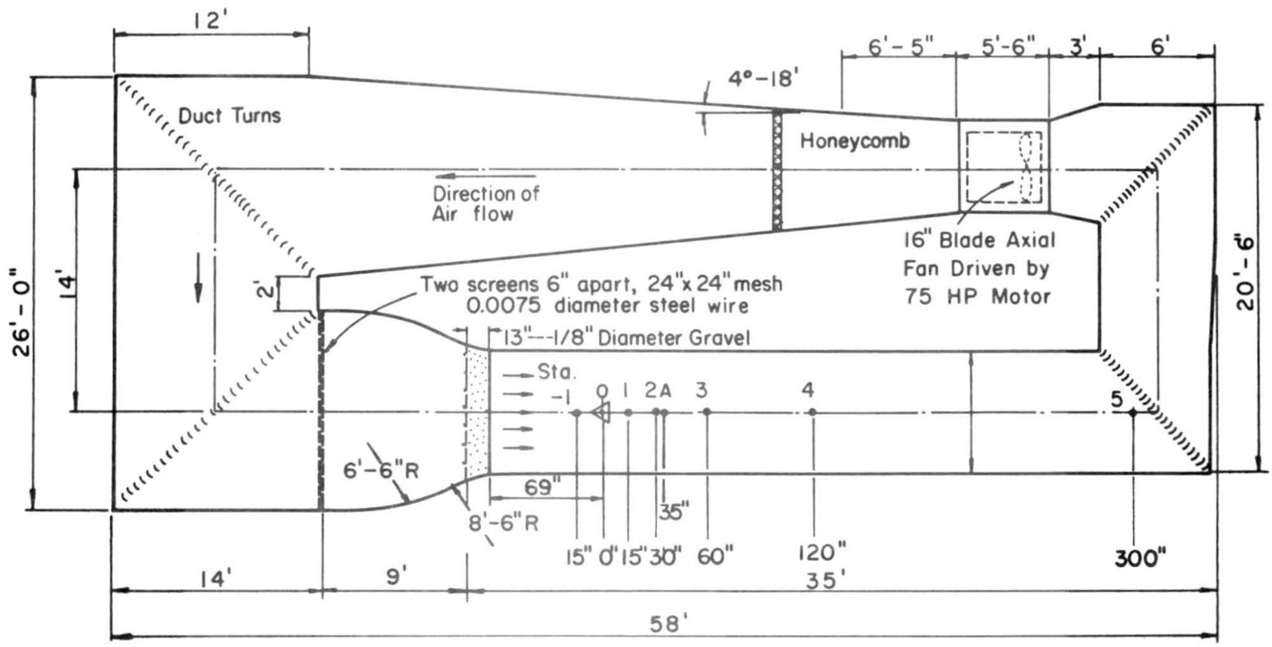

FIGURE 5 SMALL WIND TUNNEL & STATION INDICATION (Tower at zero degrees)

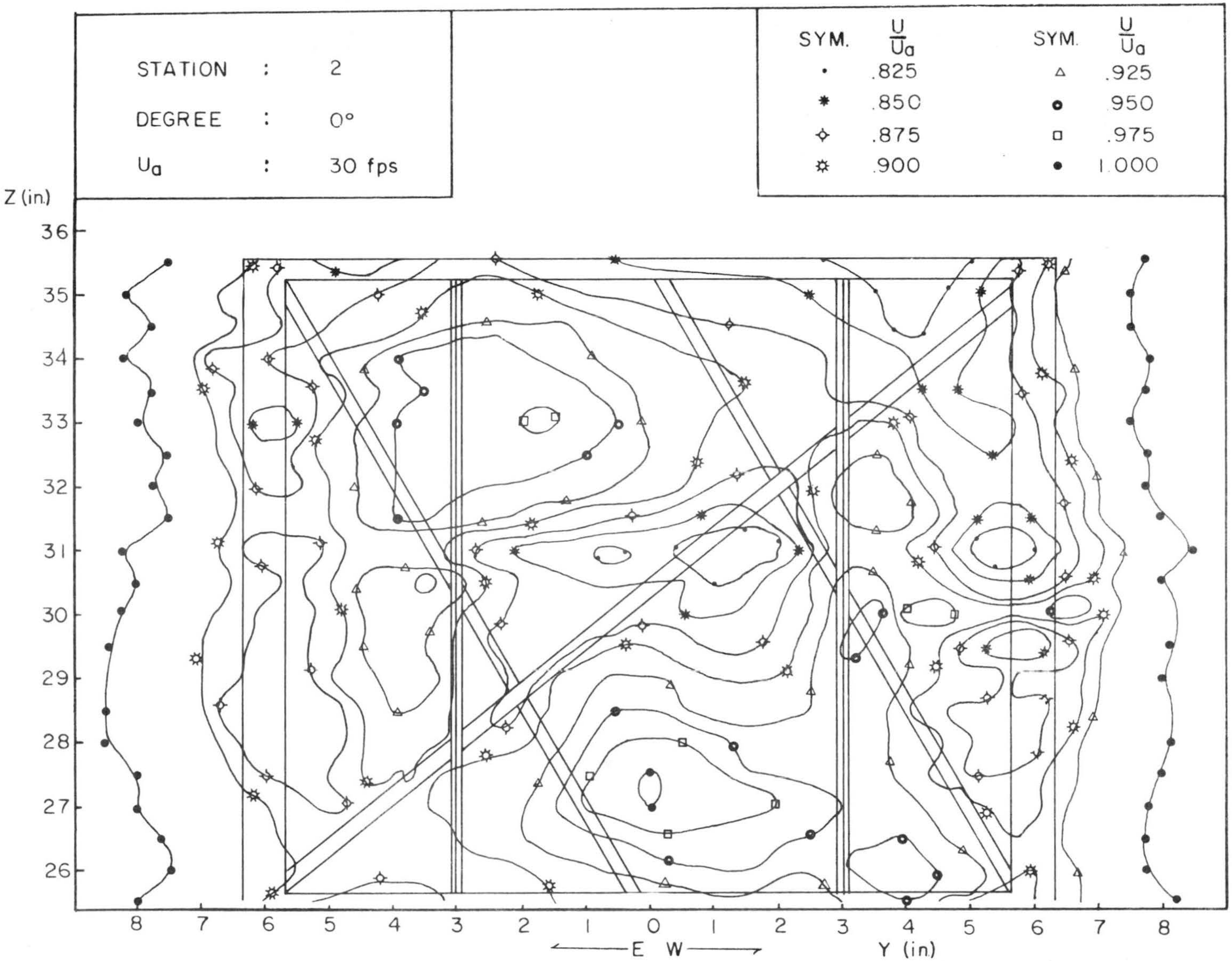

FIG. 6 ISOTACHS FOR ONE SECTION OF THE CLEAN TOWER

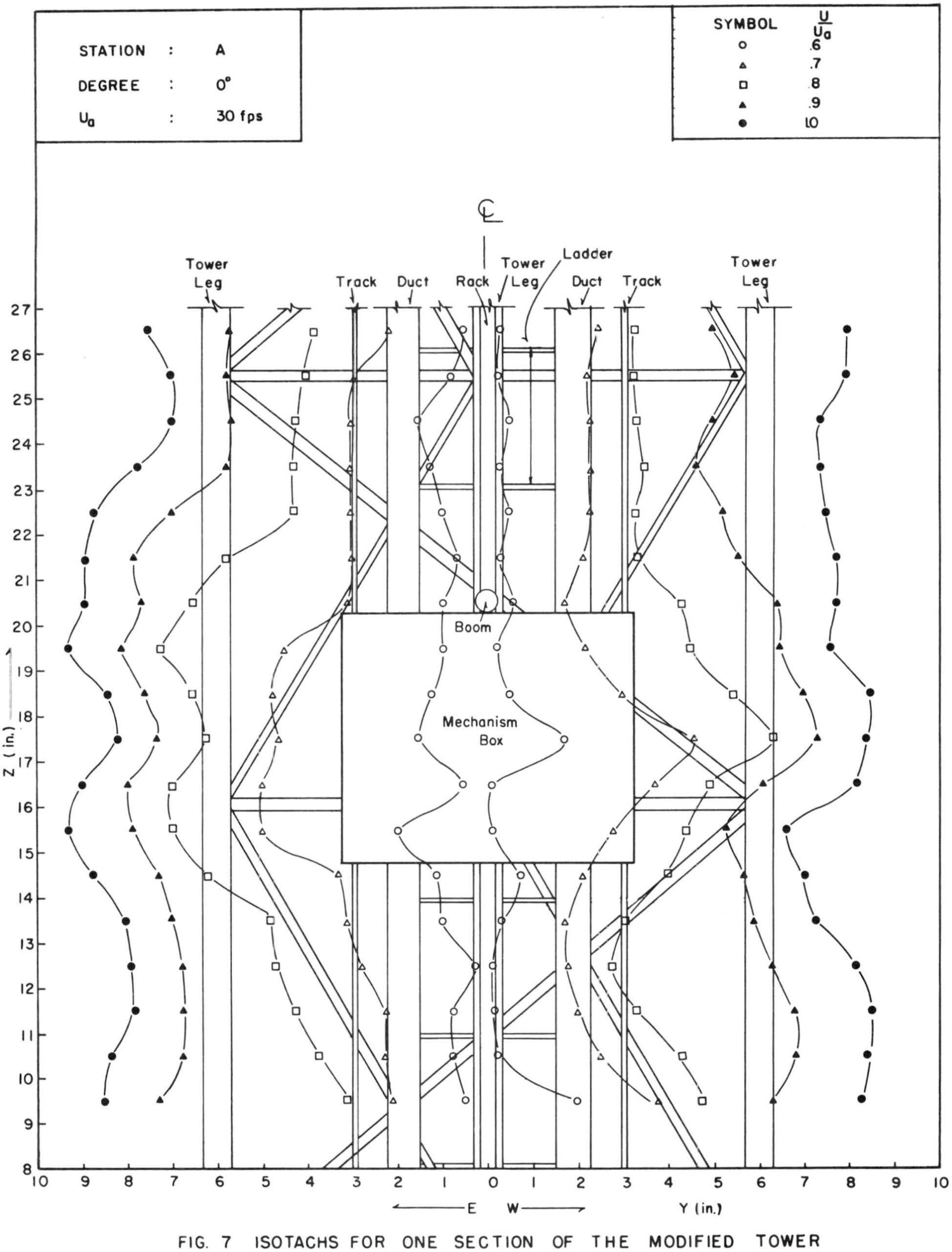

FIG. 7 ISOTACHS FOR ONE SECTION OF THE MODIFIED TOWER

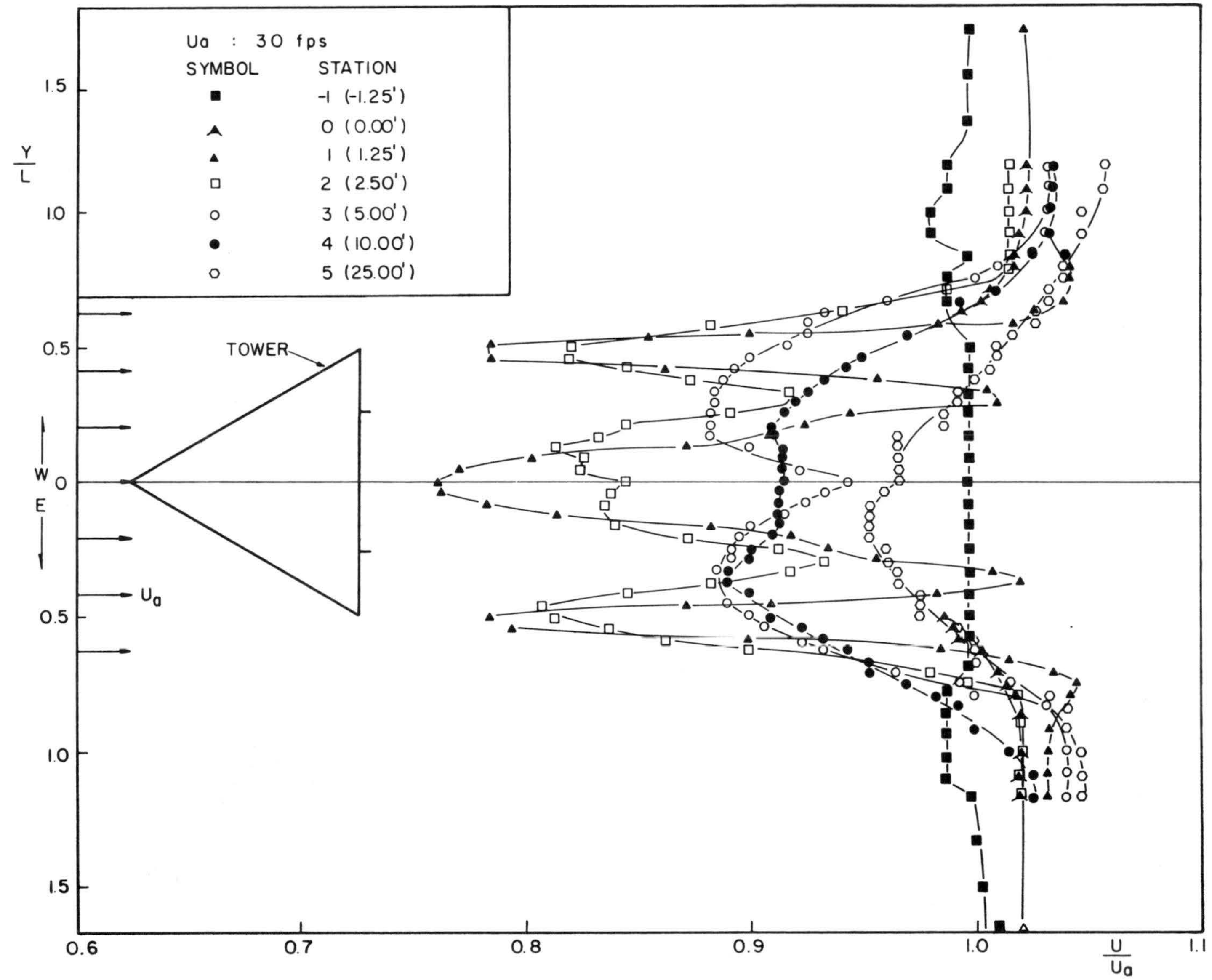

FIG. 8 TRANSVERSE VELOCITY PROFILE, CLEAN TOWER

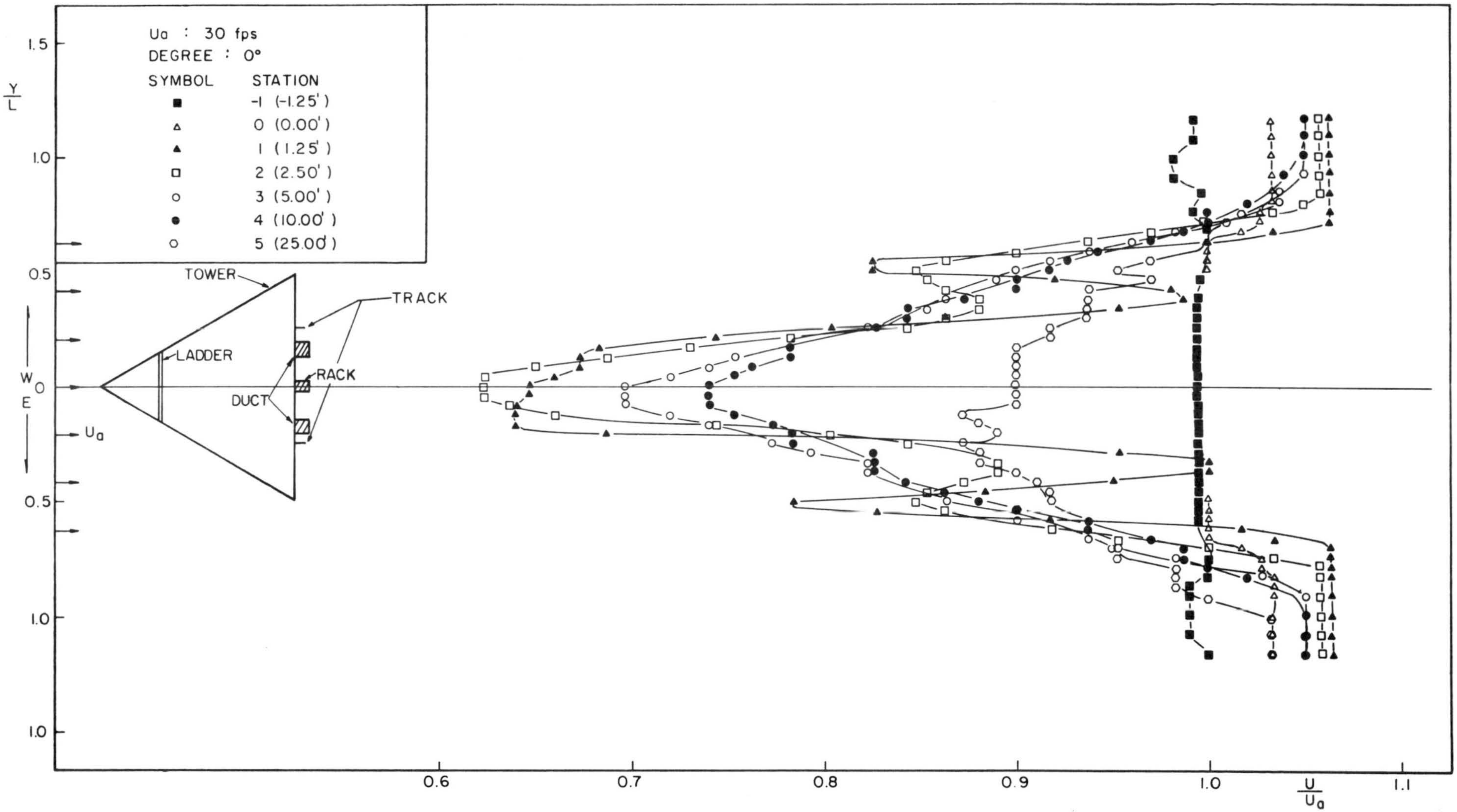

FIG. 9 TRANSVERSE VELOCITY PROFILE, MODIFIED TOWER

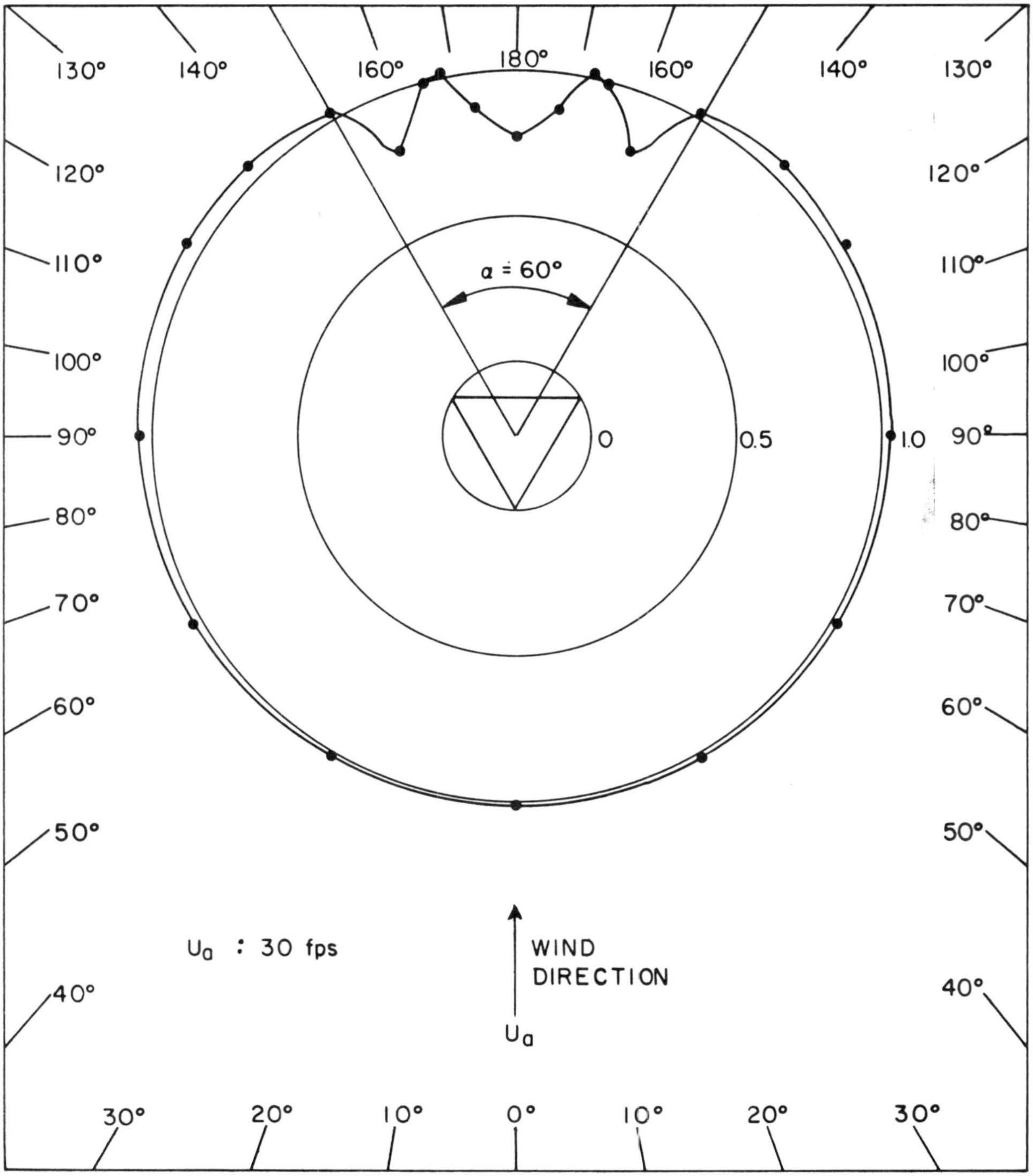

FIG. 10 MEAN VELOCITY PROFILE AROUND THE TOWER, 15" RADIUS CIRCLE

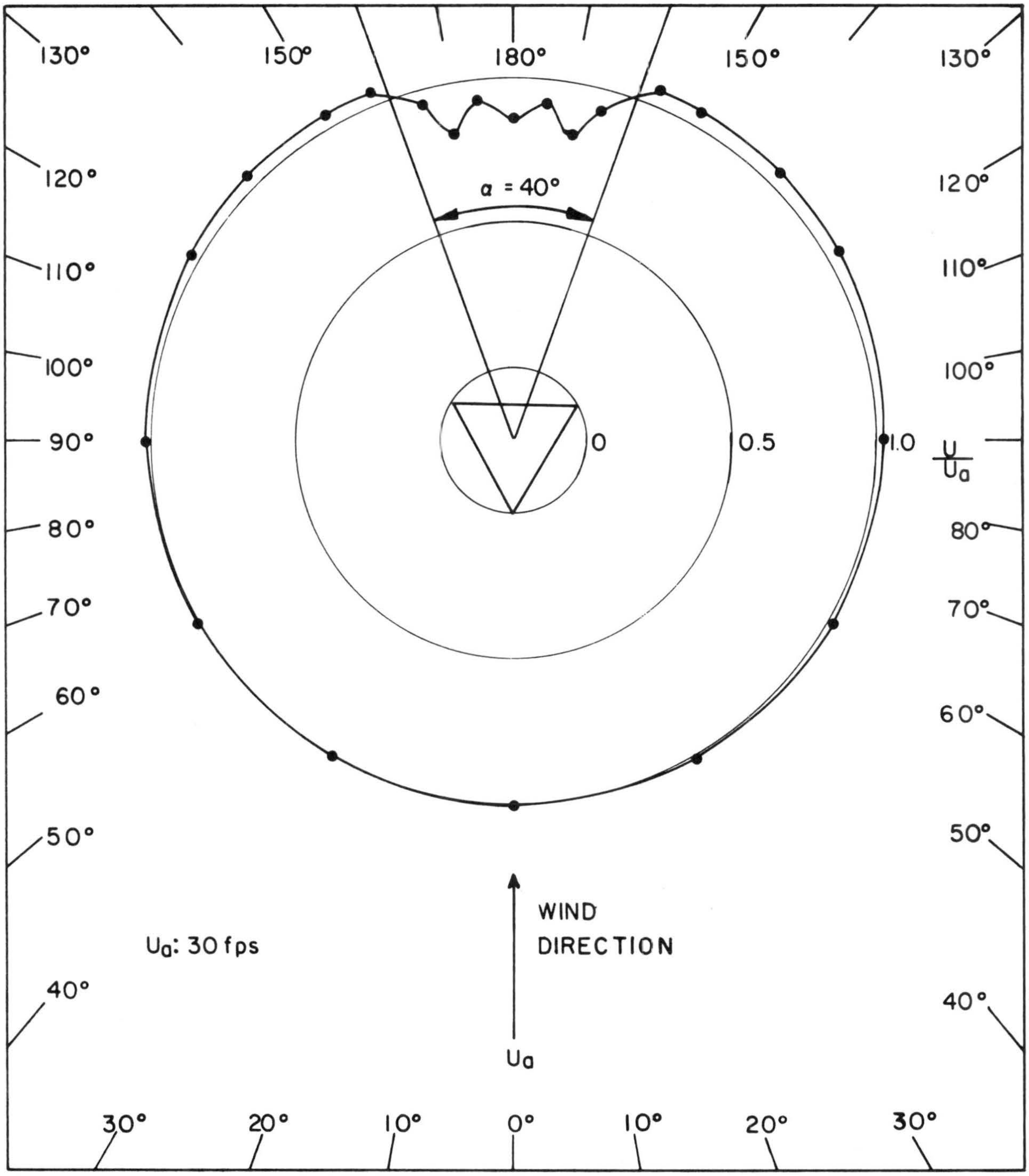

FIG. 11 MEAN VELOCITY PROFILE AROUND CLEAN TOWER, 30" RADIUS CIRCLE

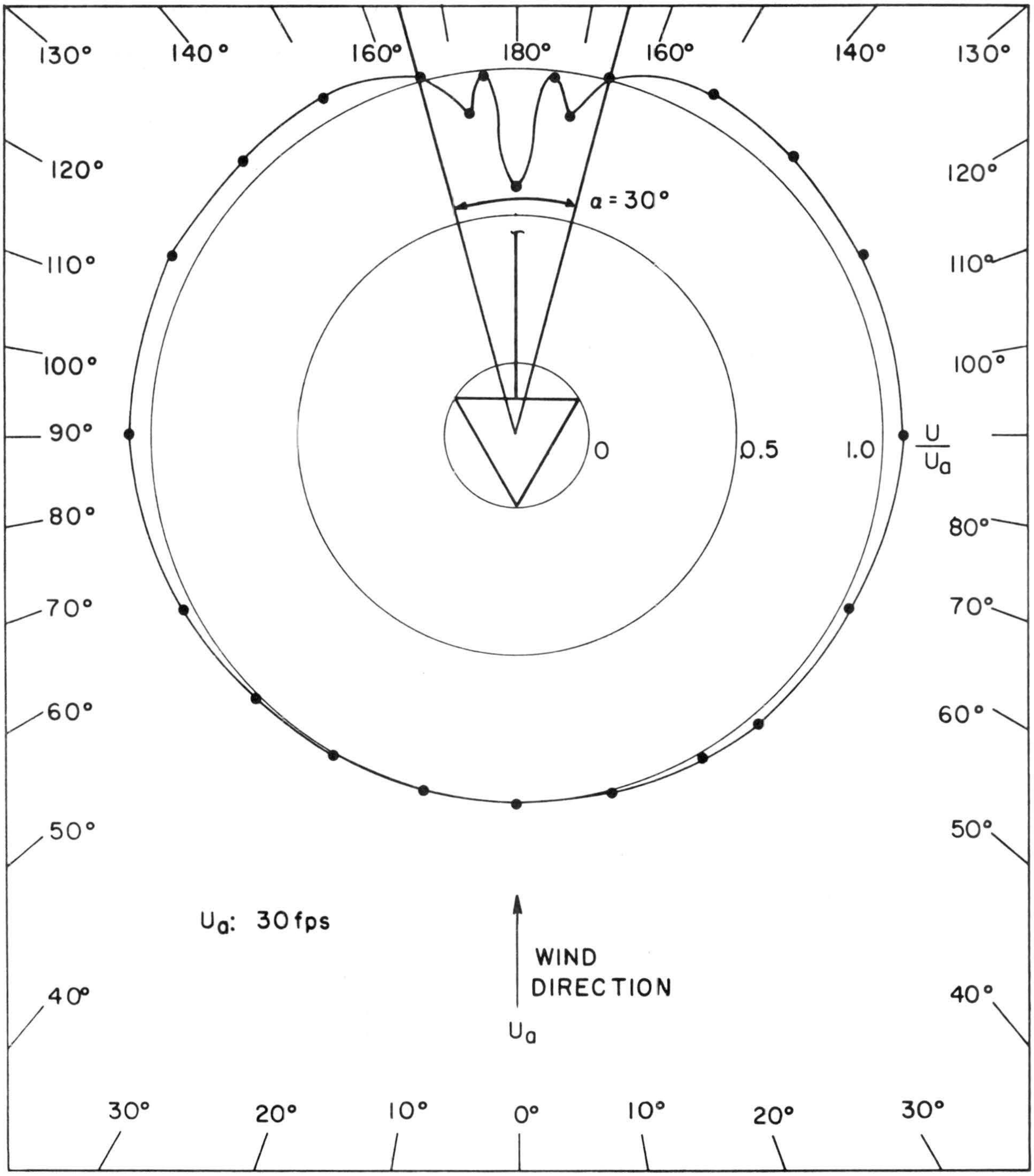

FIG. 12 MEAN VELOCITY PROFILE AROUND MODIFIED TOWER
35" RADIUS CIRCLE

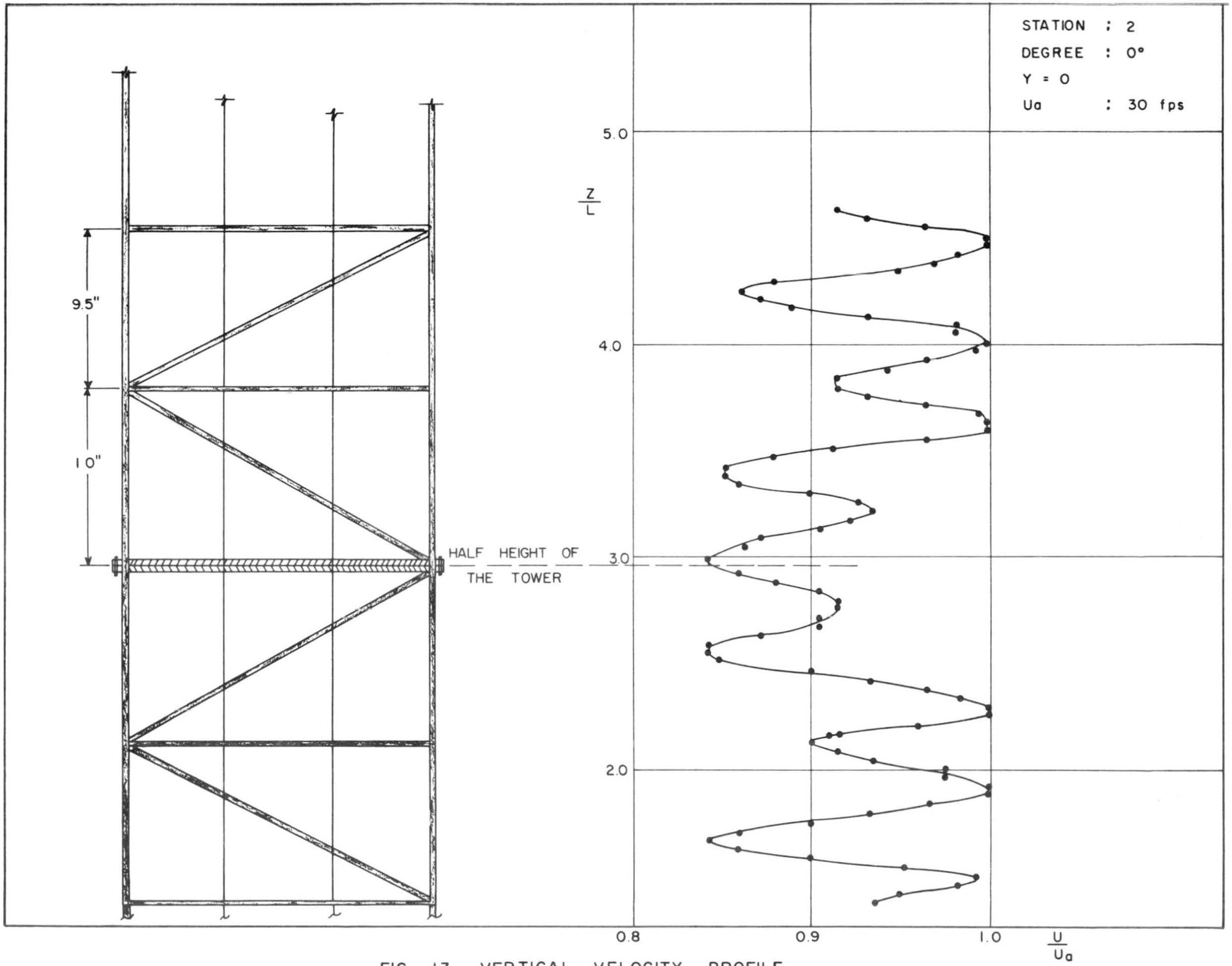

FIG. 13 VERTICAL VELOCITY PROFILE

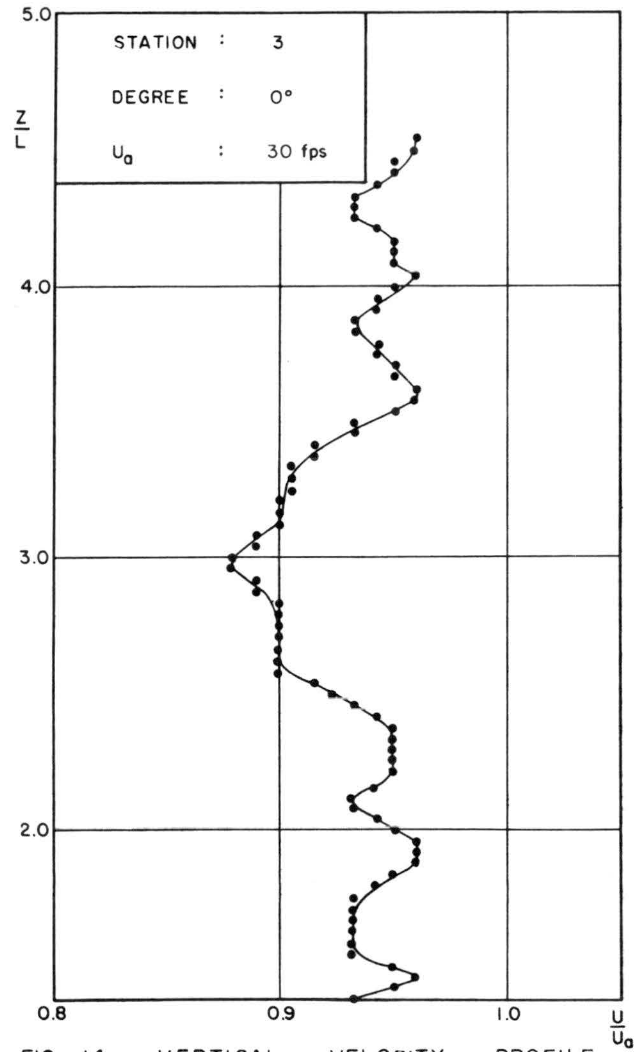

FIG. 14 VERTICAL VELOCITY PROFILE

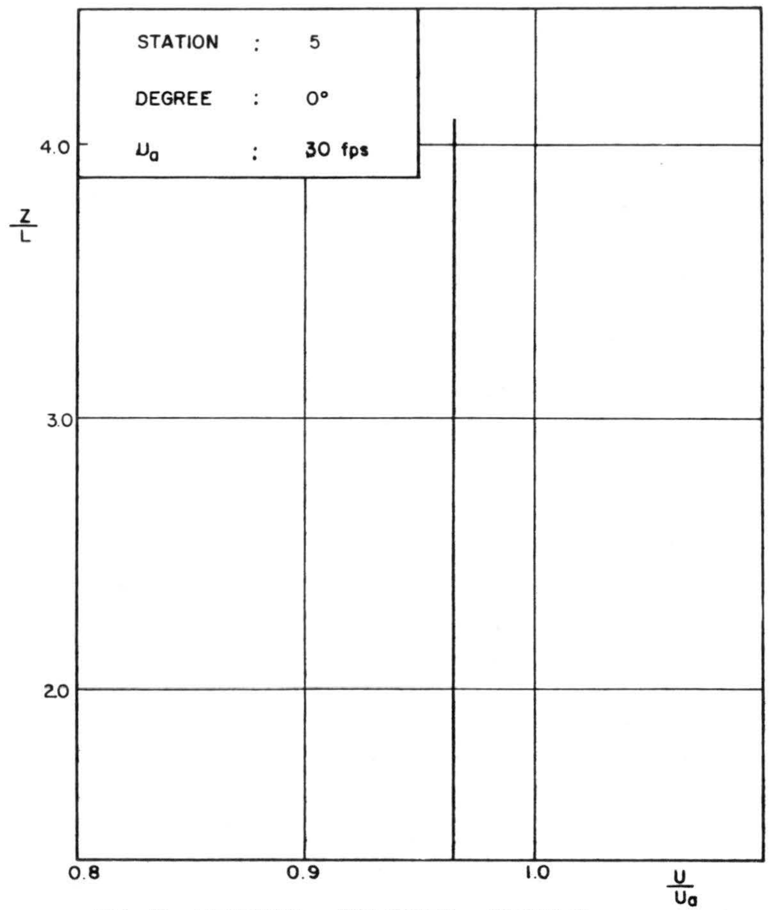

FIG. 15 VERTICAL VELOCITY PROFILE

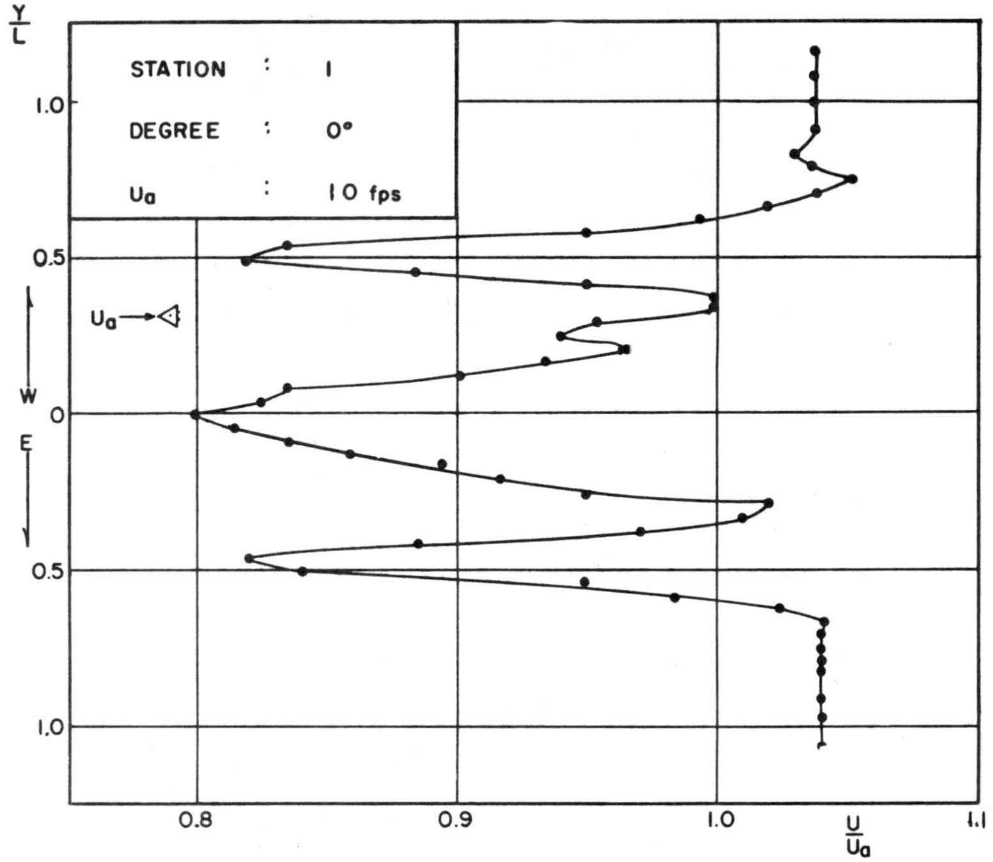

FIG. 16 TRANSVERSE VELOCITY PROFILE

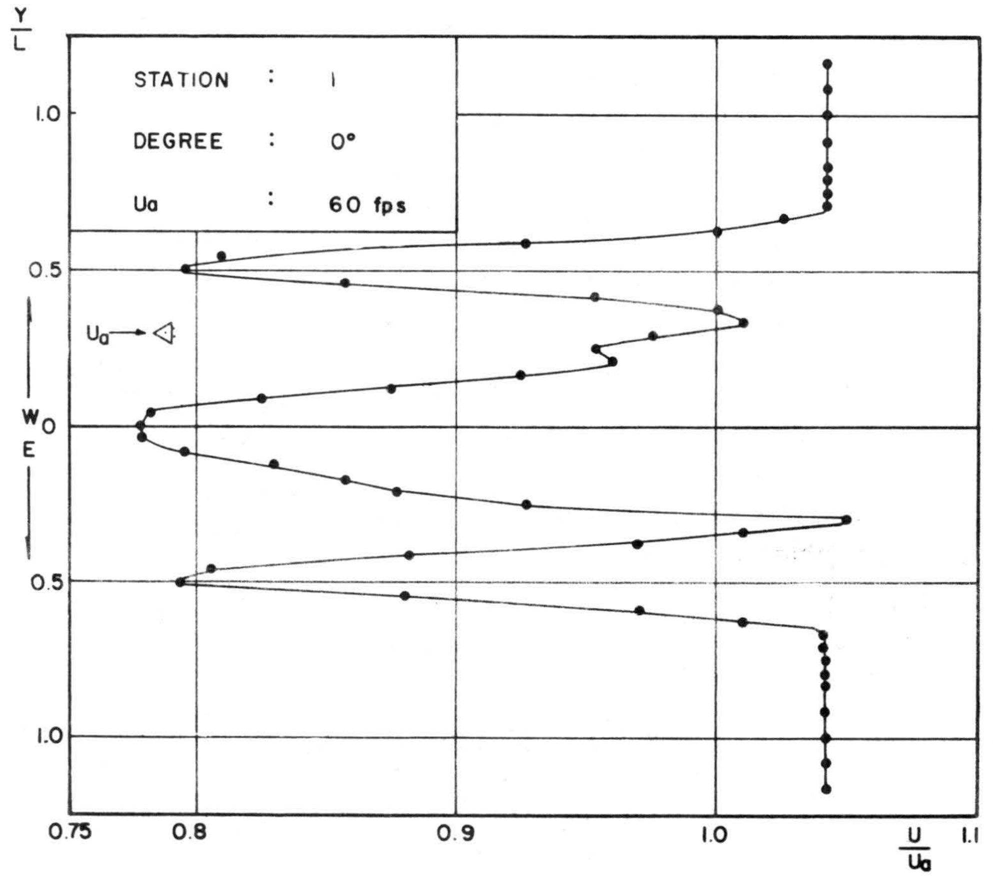

FIG. 17 TRANSVERSE VELOCITY PROFILE

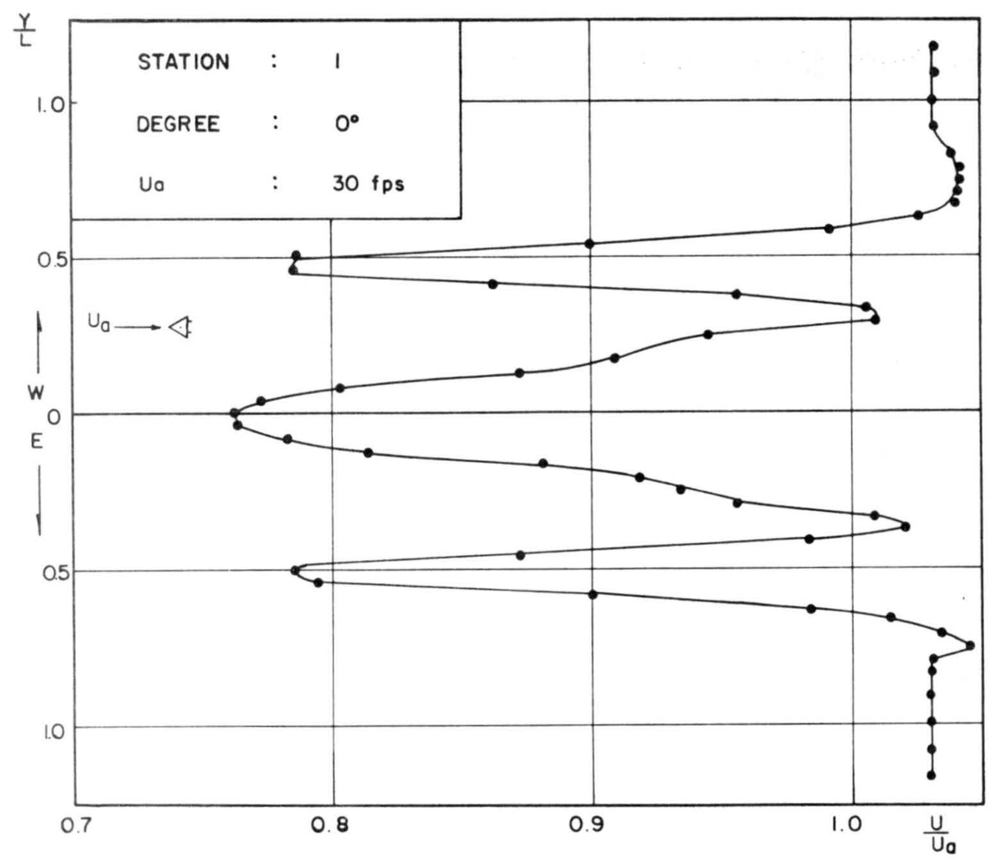

FIG. 18 TRANSVERSE VELOCITY PROFILE

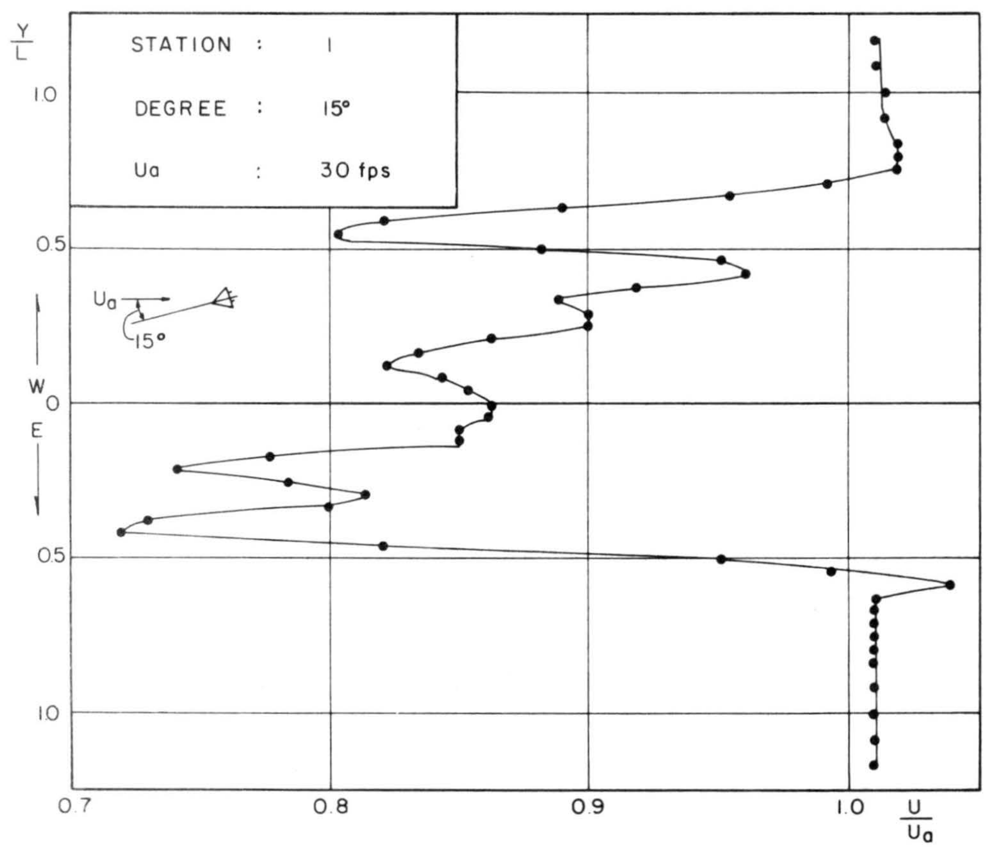

FIG. 19 TRANSVERSE VELOCITY PROFILE

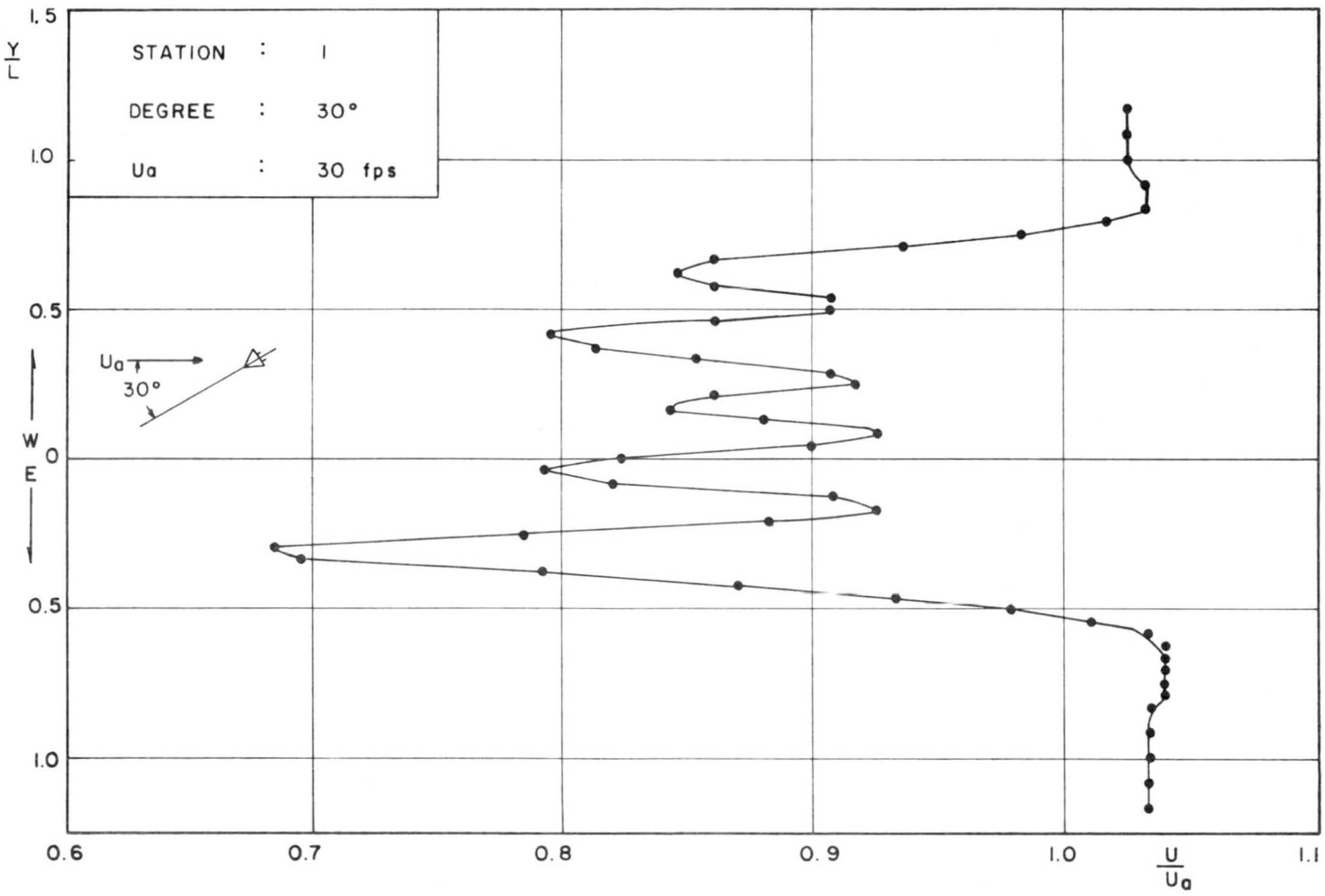

FIG. 20 TRANSVERSE VELOCITY PROFILE

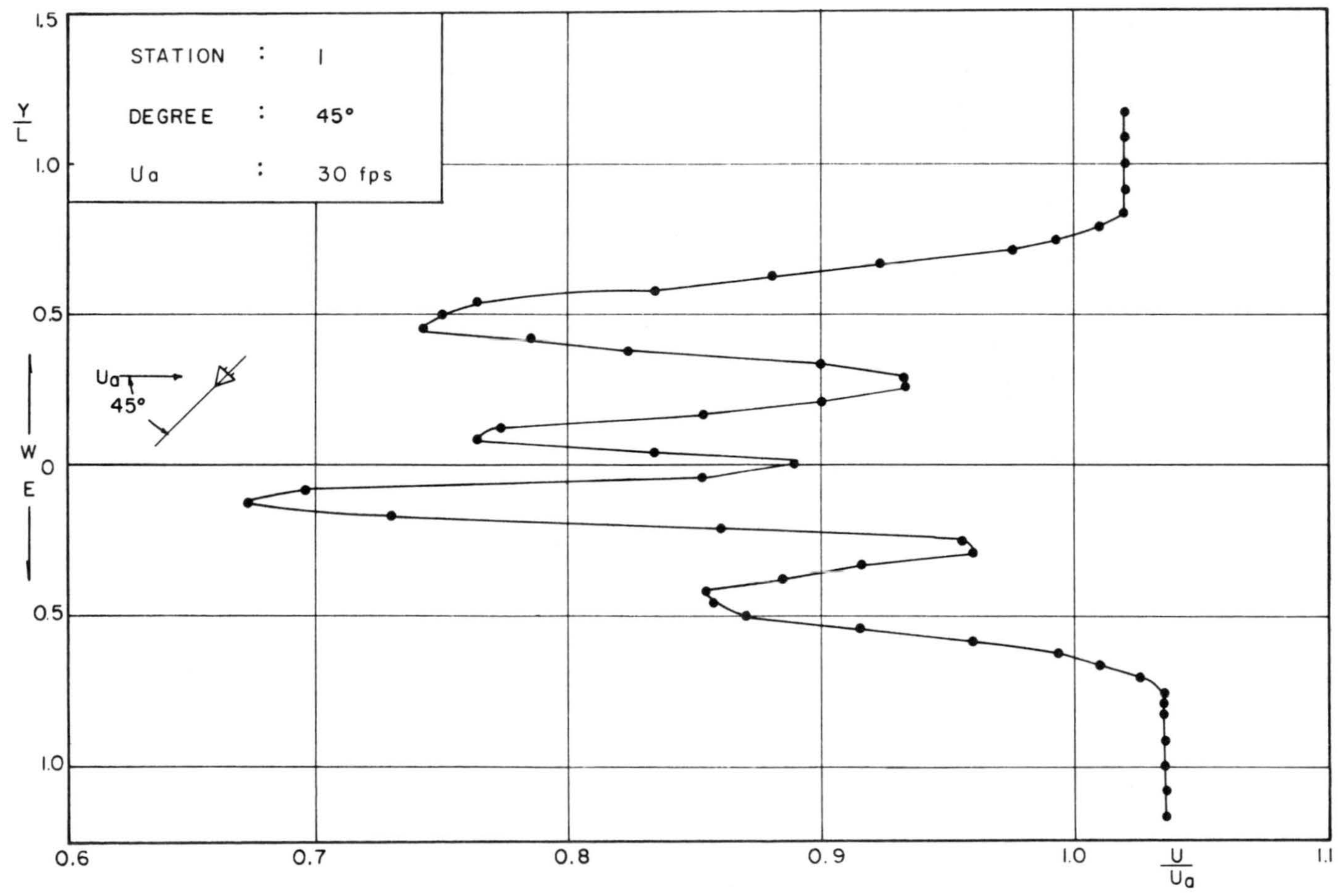

FIG. 21 TRANSVERSE VELOCITY PROFILE

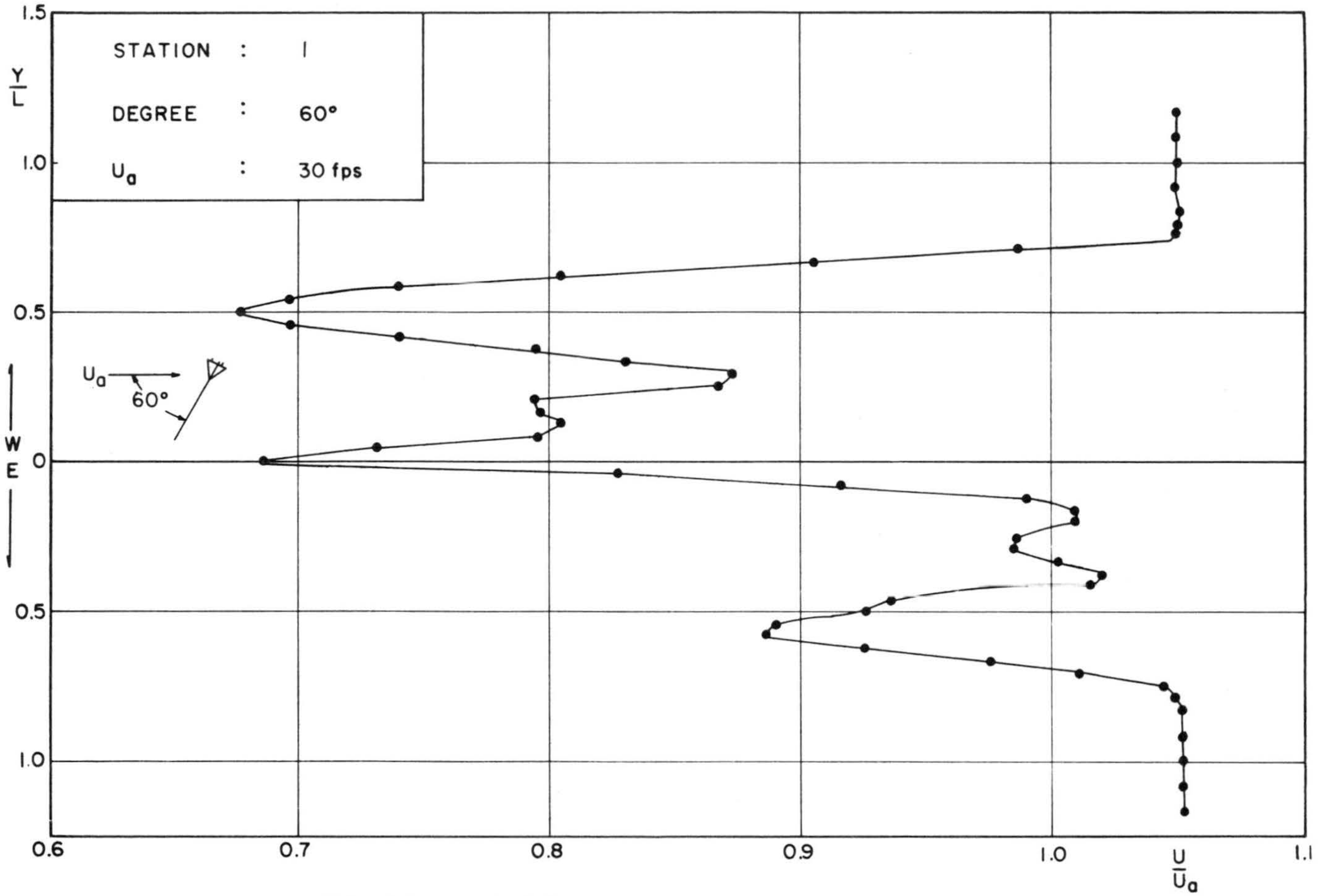

FIG. 22 TRANSVERSE VELOCITY PROFILE

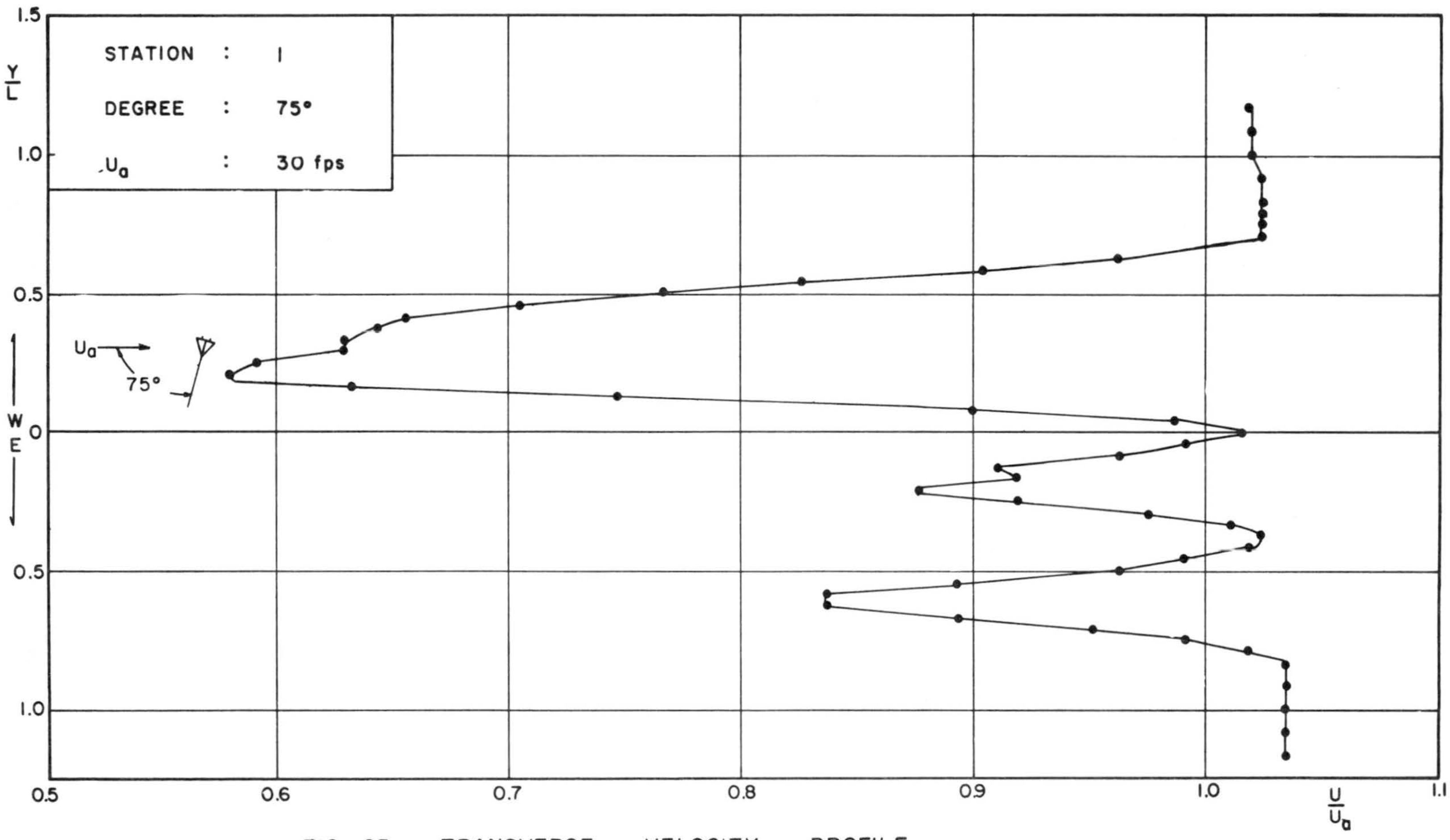

FIG. 23 TRANSVERSE VELOCITY PROFILE

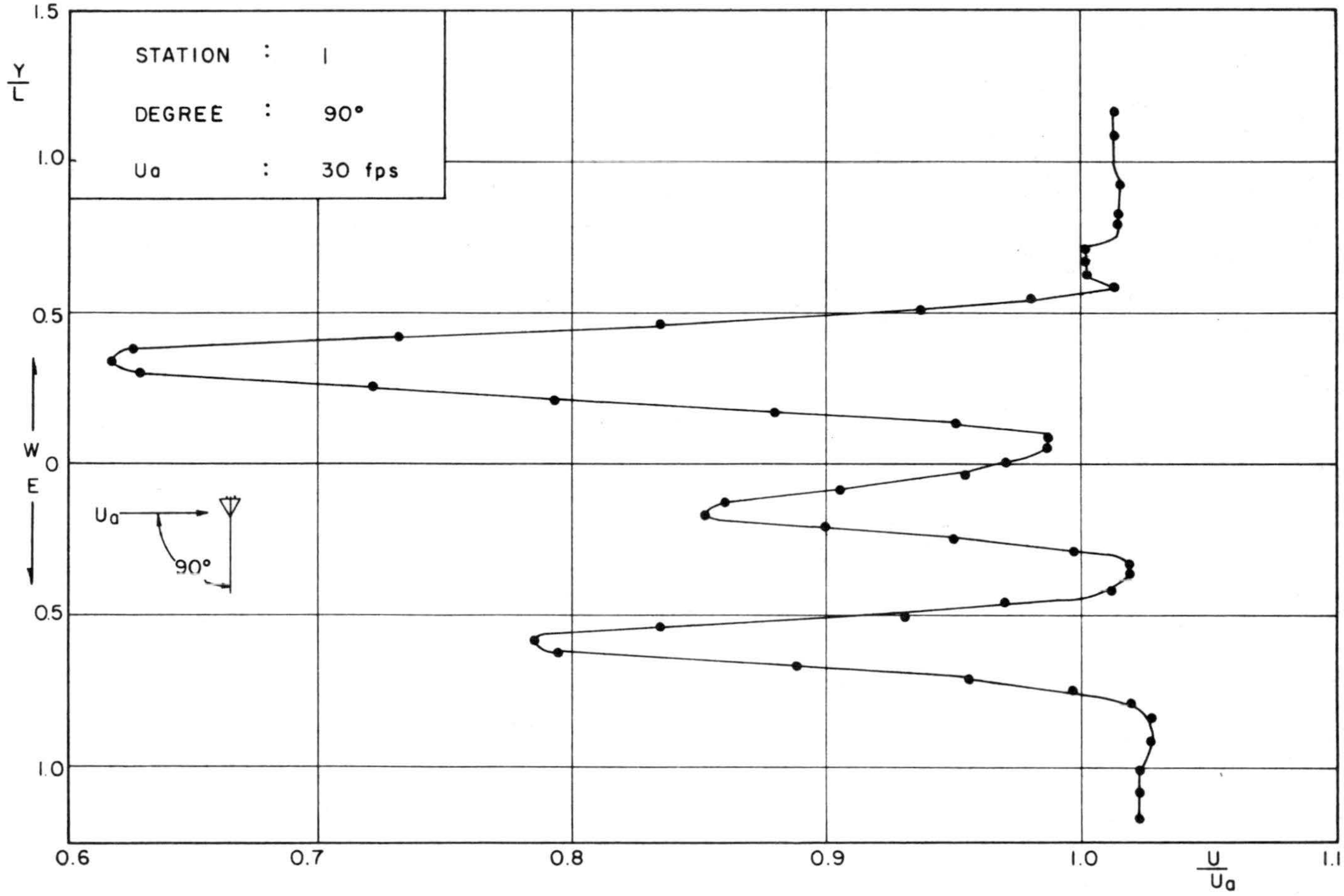

FIG. 24 TRANSVERSE VELOCITY PROFILE

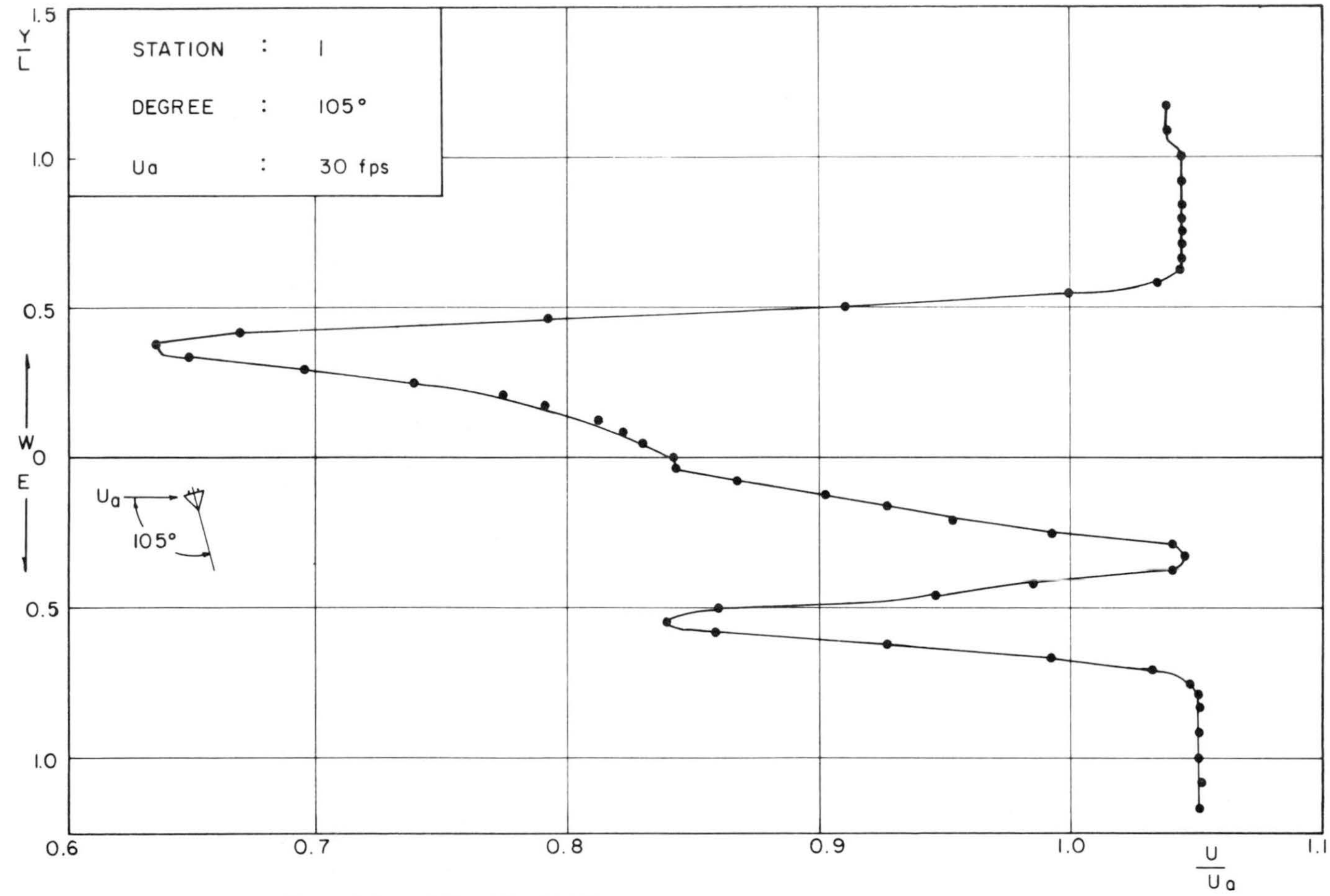

FIG. 25 TRANSVERSE VELOCITY PROFILE

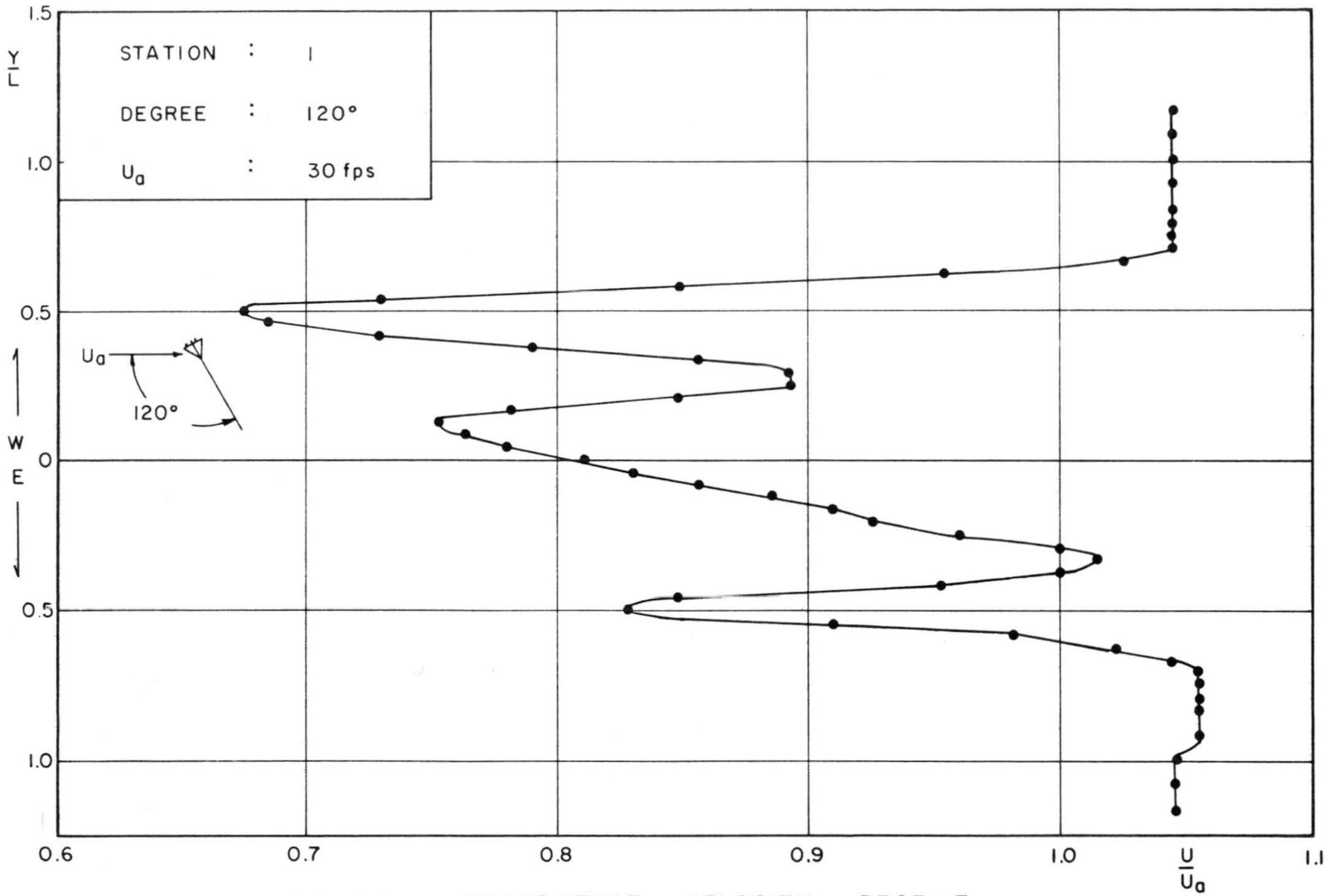

FIG. 26 TRANSVERSE VELOCITY PROFILE

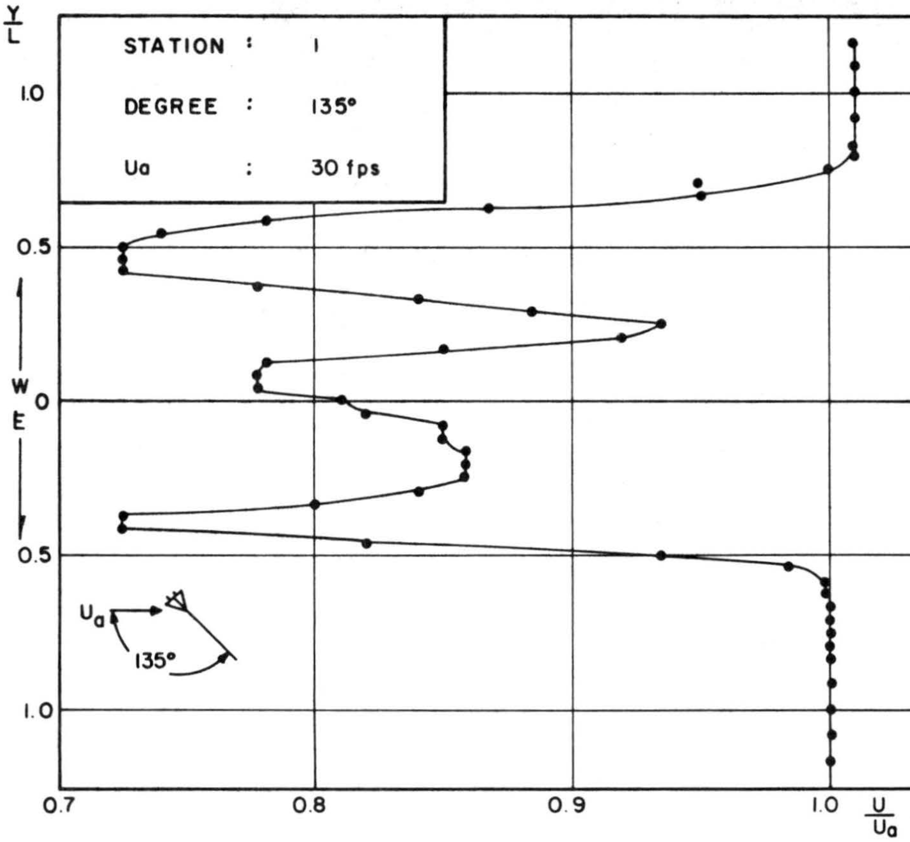

FIG. 27 TRANSVERSE VELOCITY PROFILE

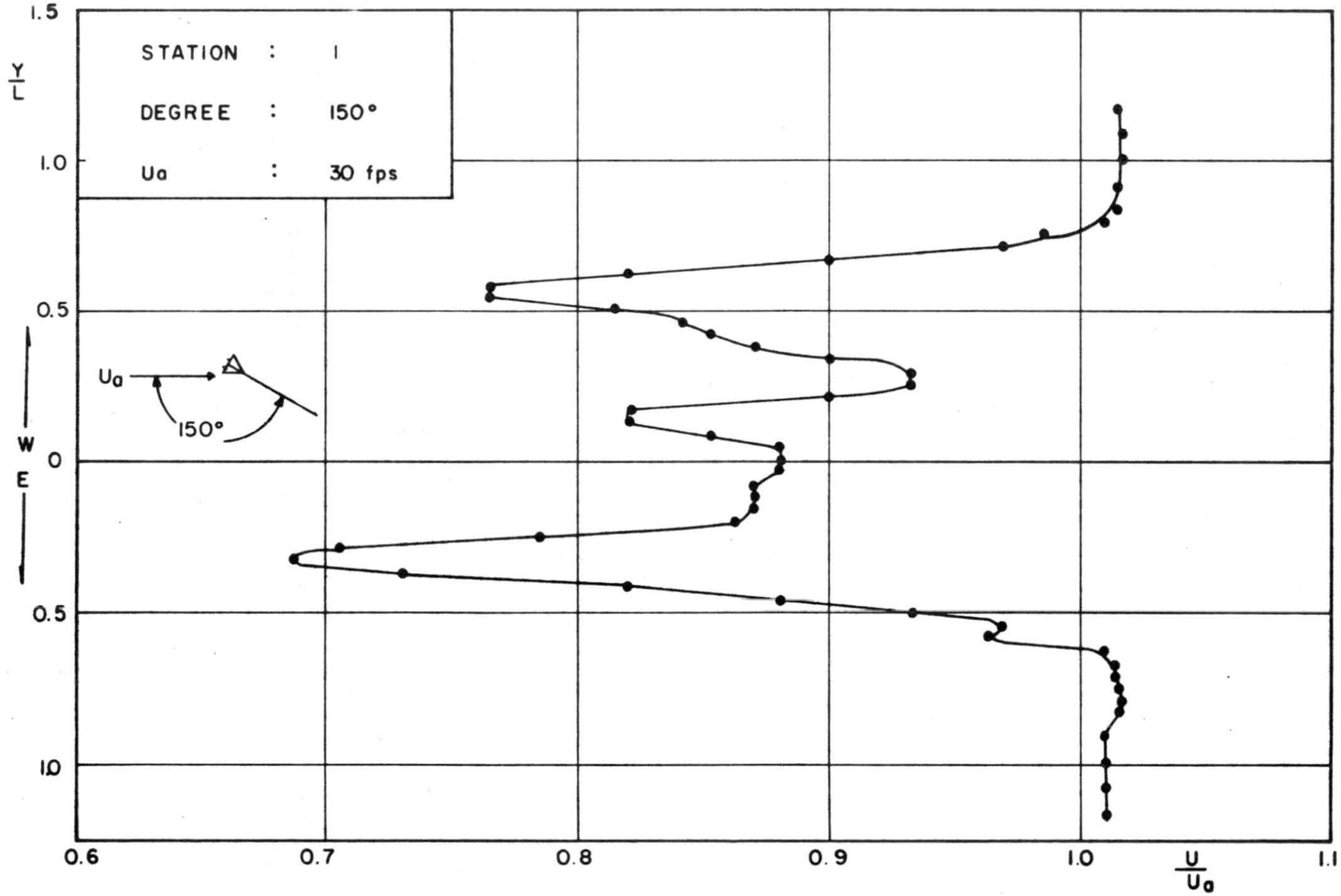

FIG. 28 TRANSVERSE VELOCITY PROFILE

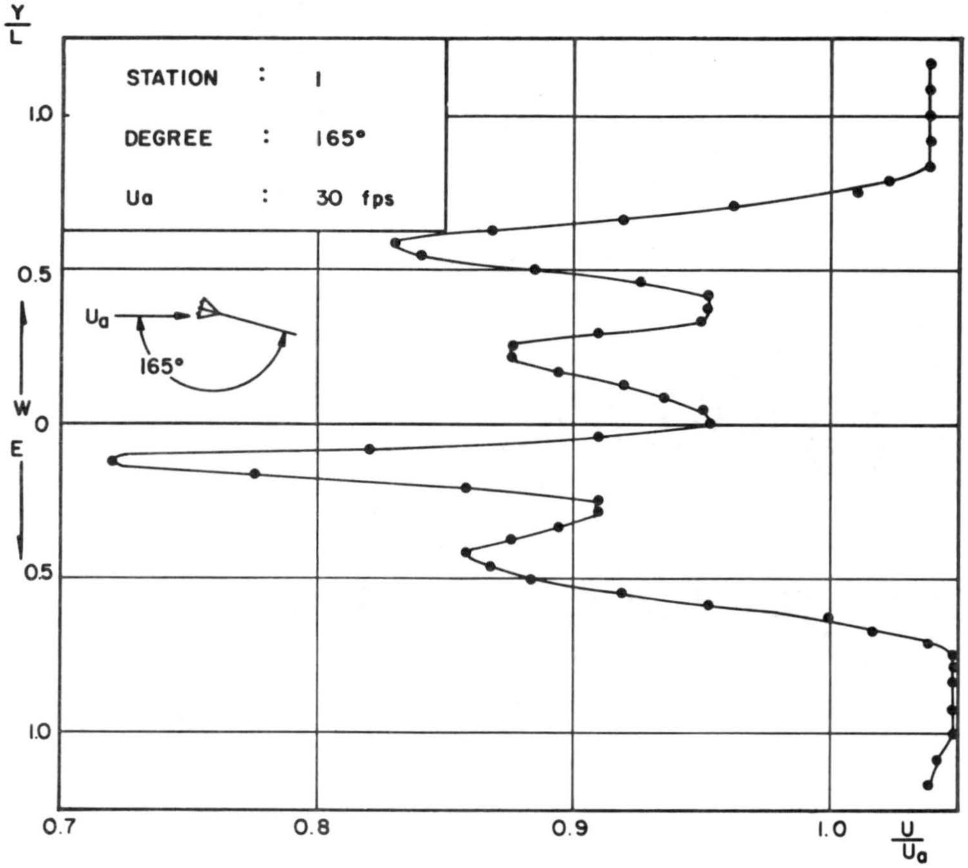

FIG. 29 TRANSVERSE VELOCITY PROFILE

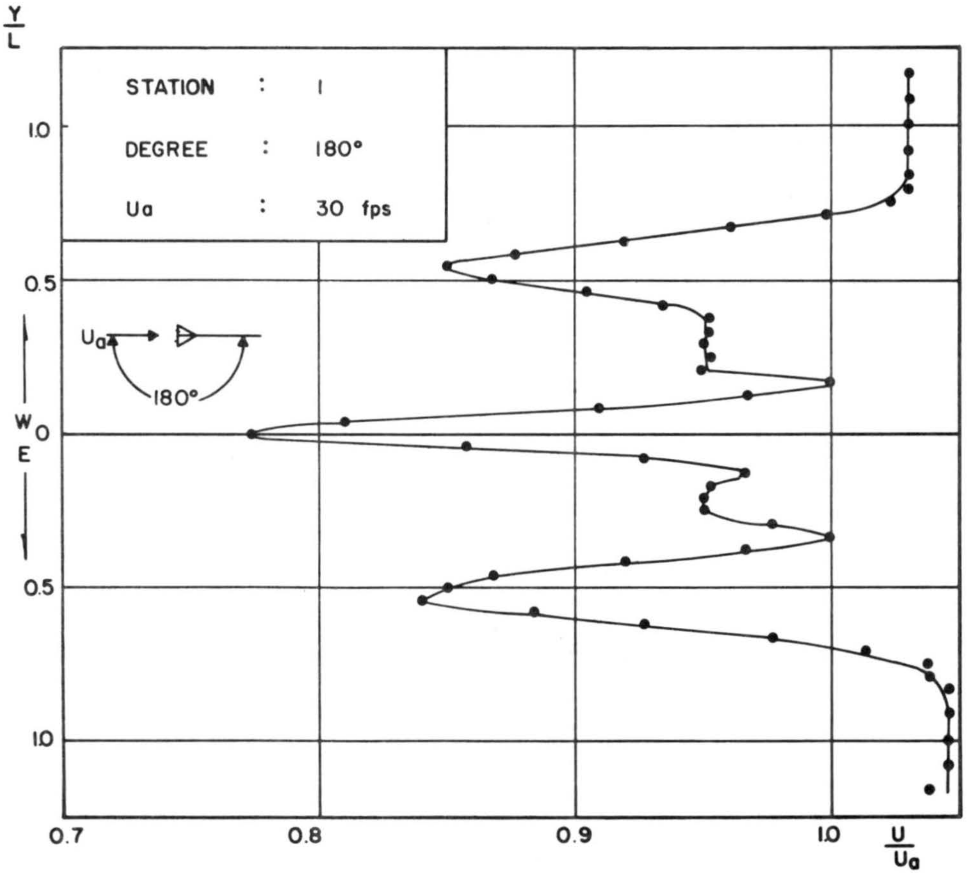

FIG. 30 TRANSVERSE VELOCITY PROFILE

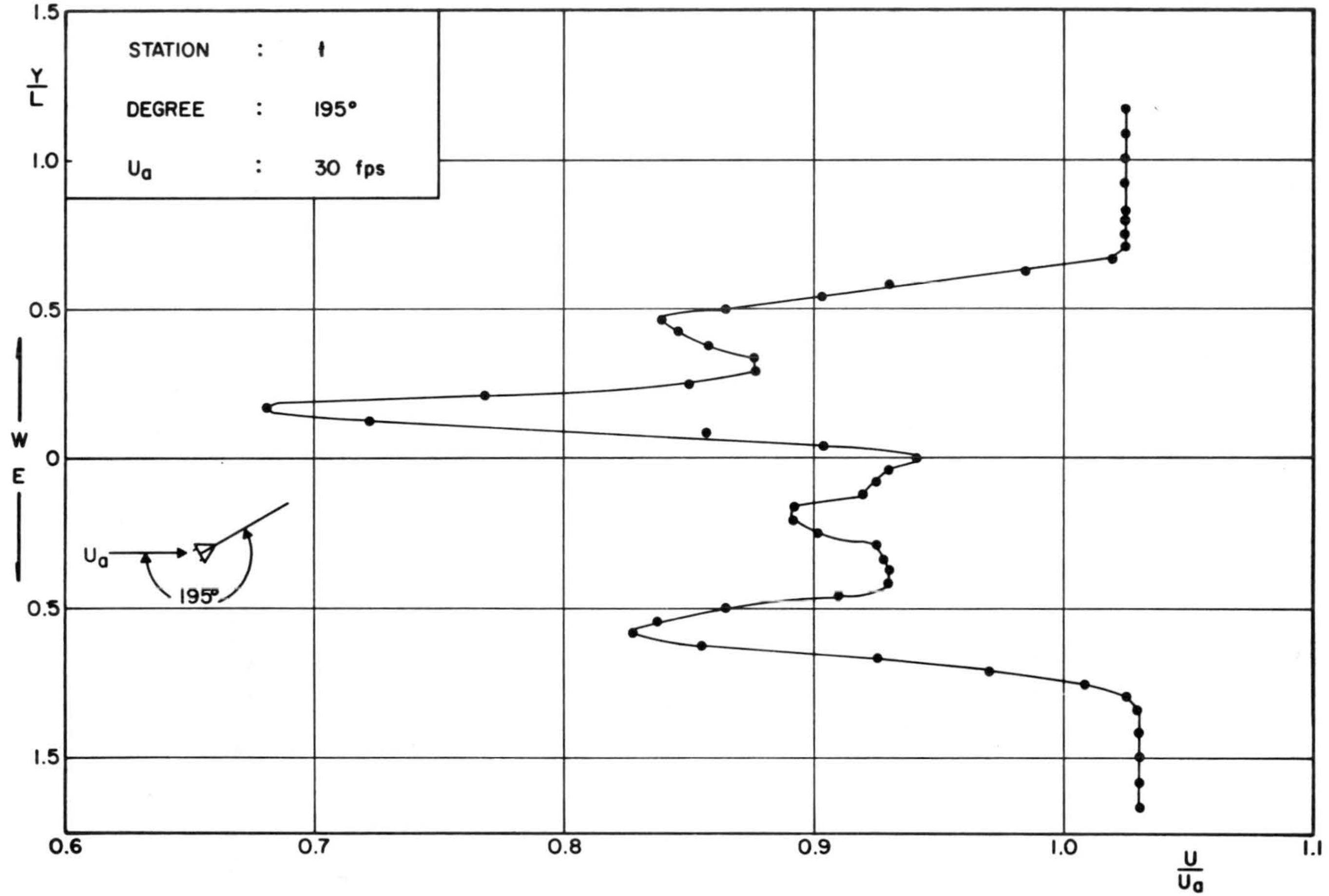

FIG. 31 TRANSVERSE VELOCITY PROFILE

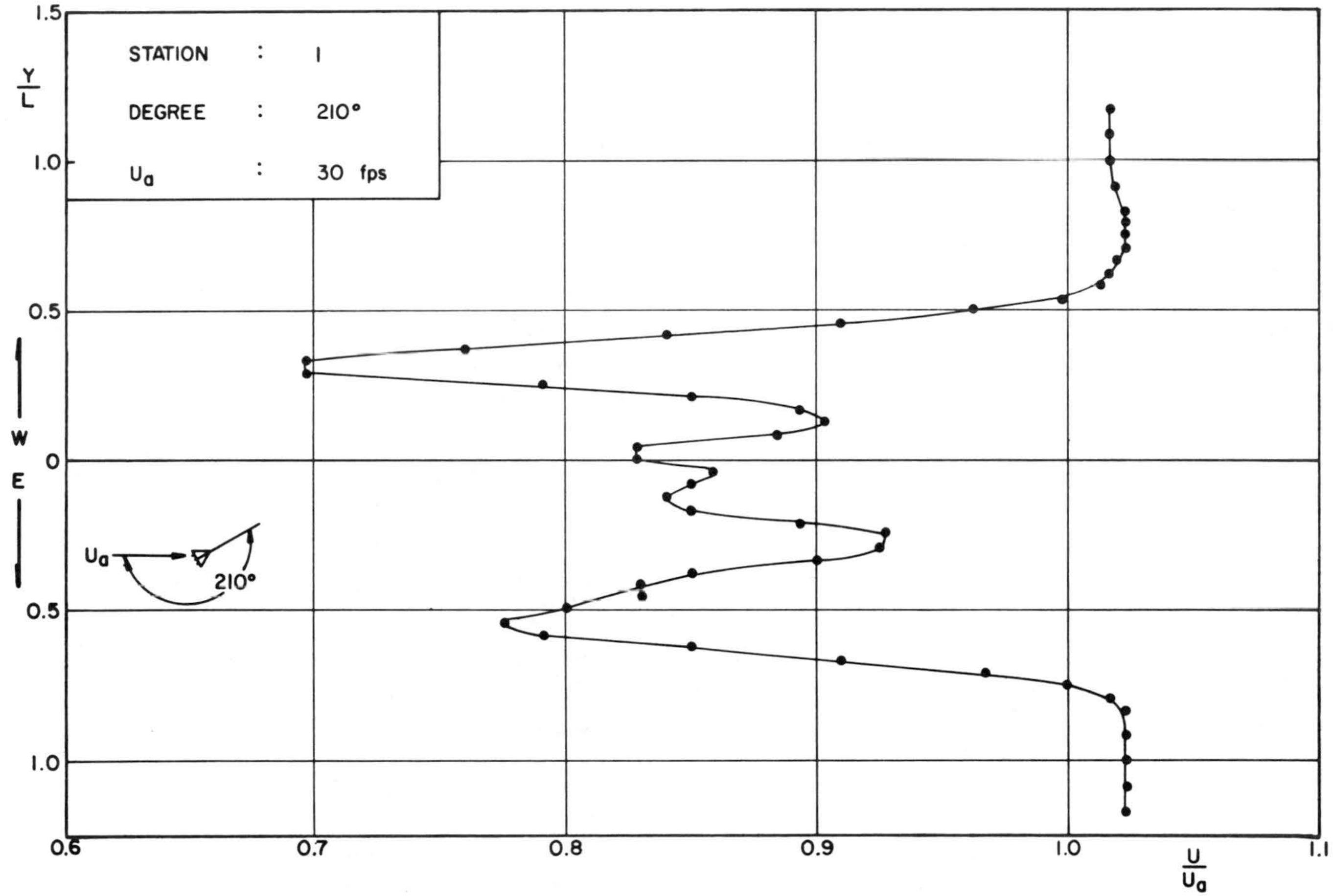

FIG. 32 TRANSVERSE VELOCITY PROFILE

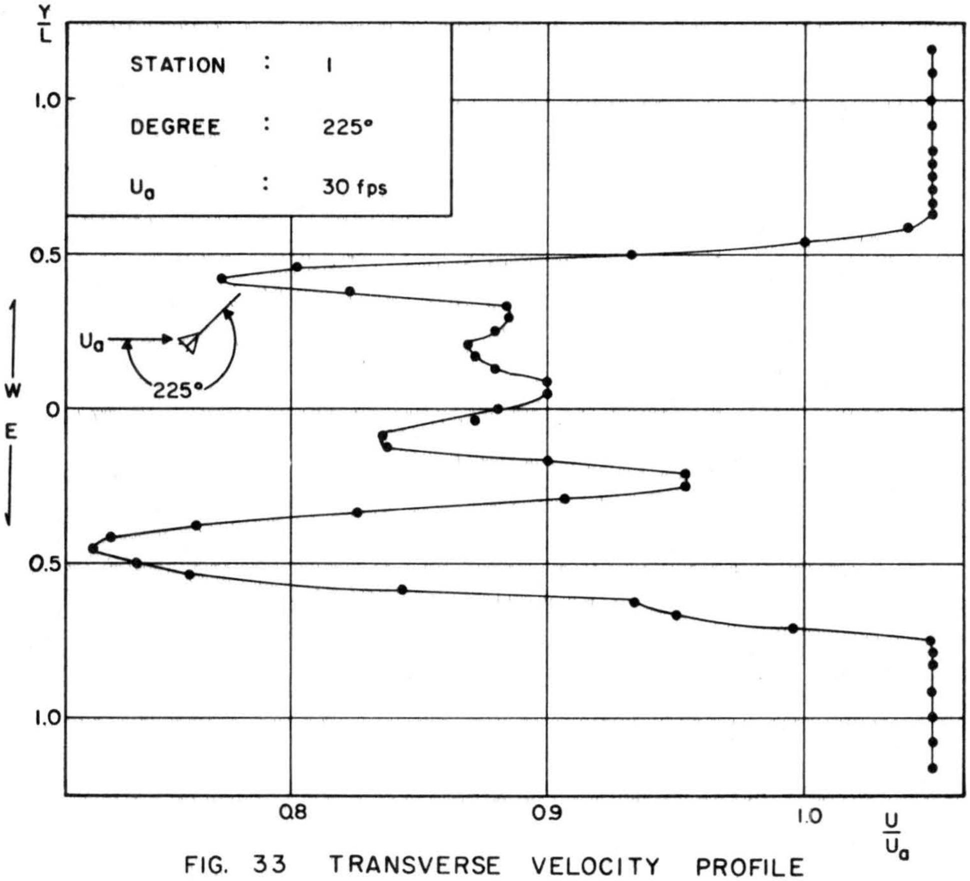

FIG. 33 TRANSVERSE VELOCITY PROFILE

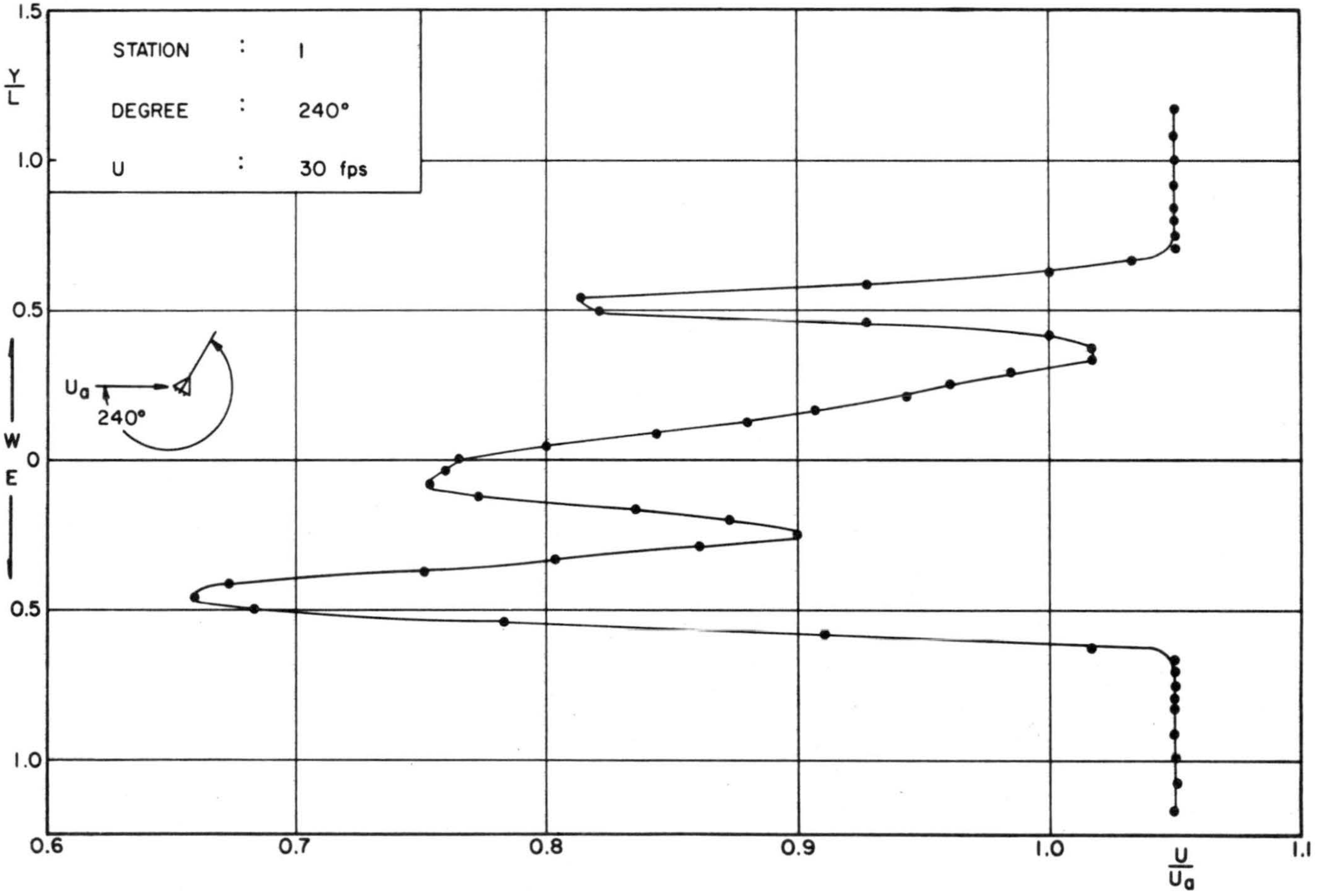

FIG. 34 TRANSVERSE VELOCITY PROFILE

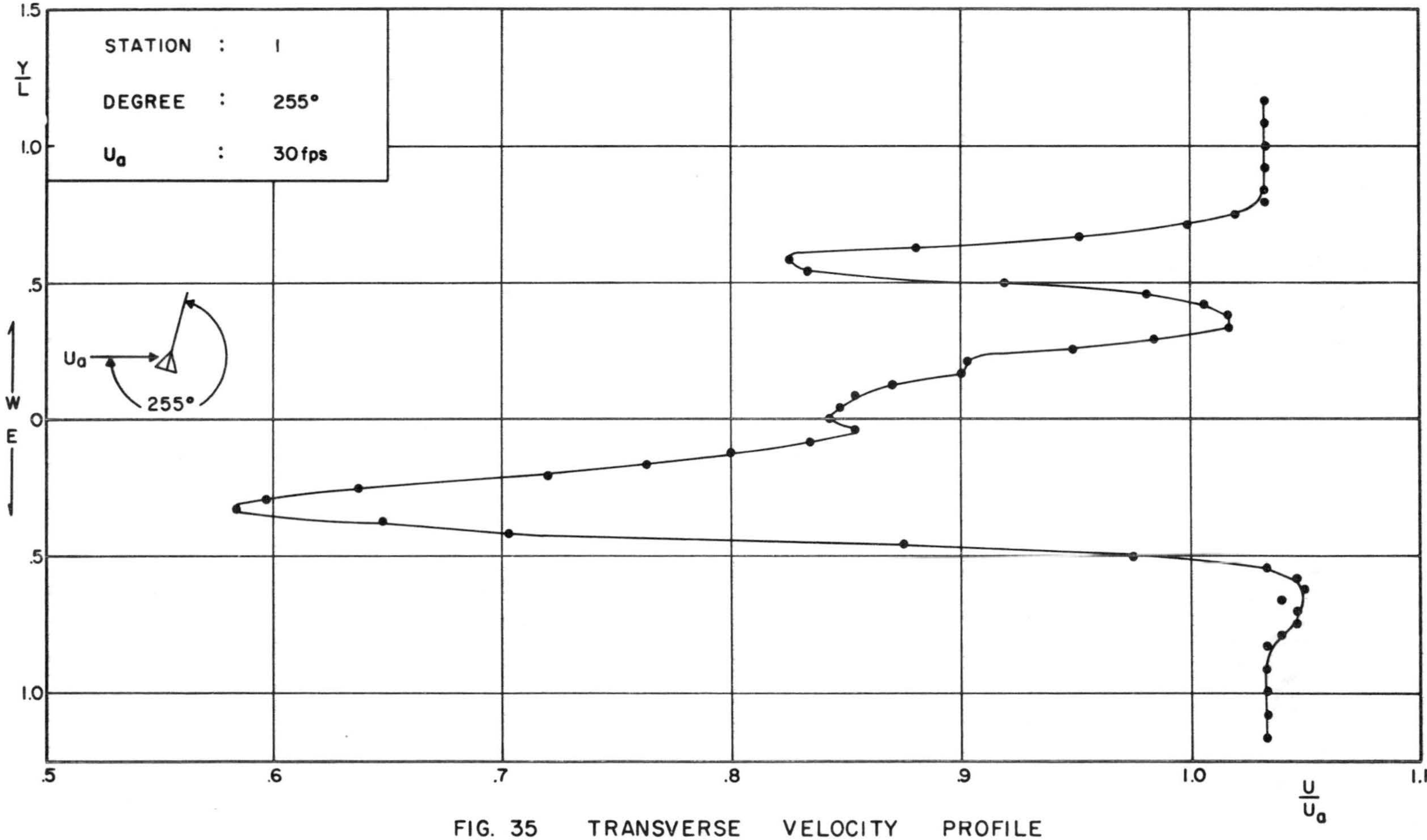

FIG. 35 TRANSVERSE VELOCITY PROFILE

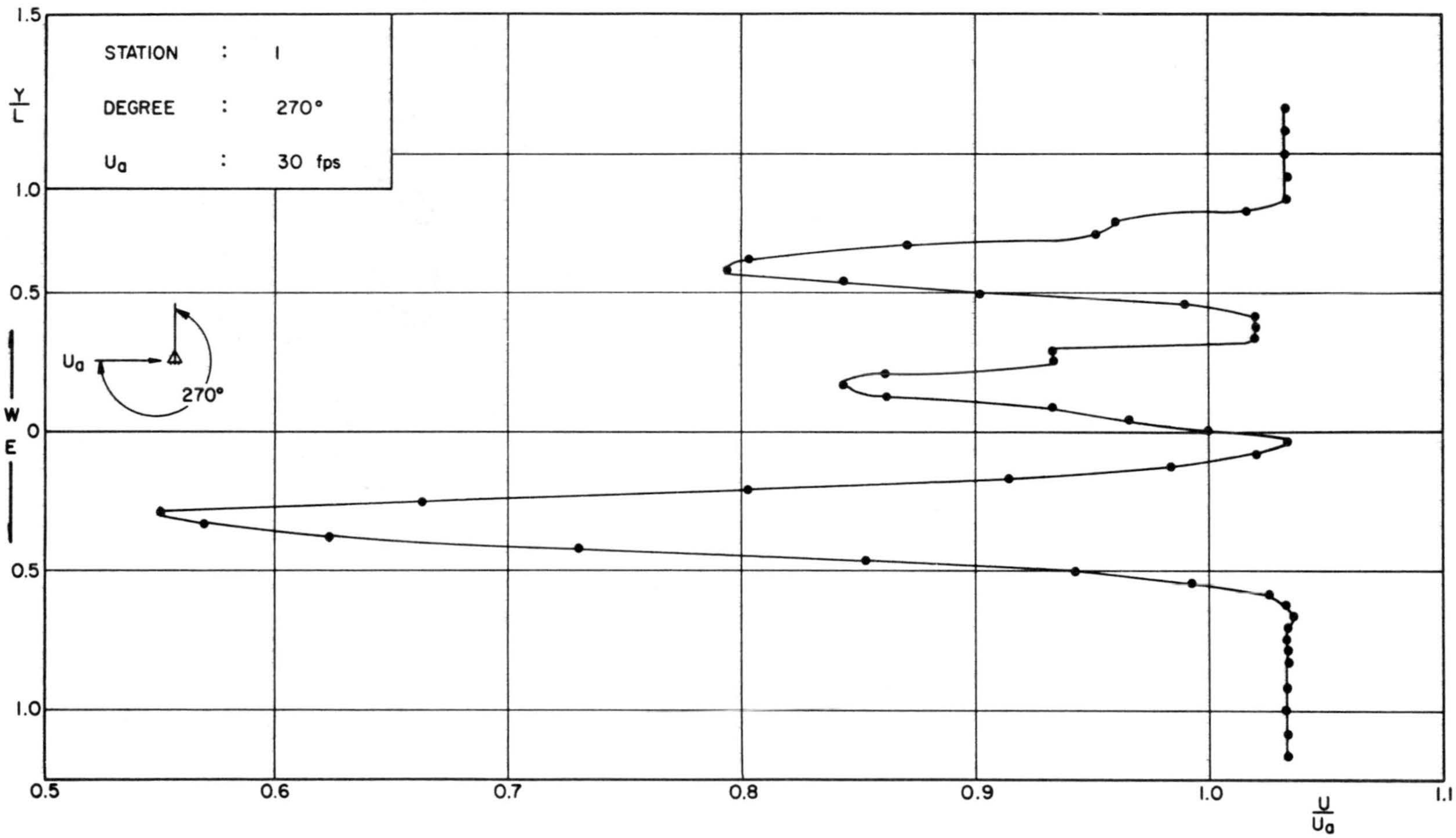

FIG. 36 TRANSVERSE VELOCITY PROFILE

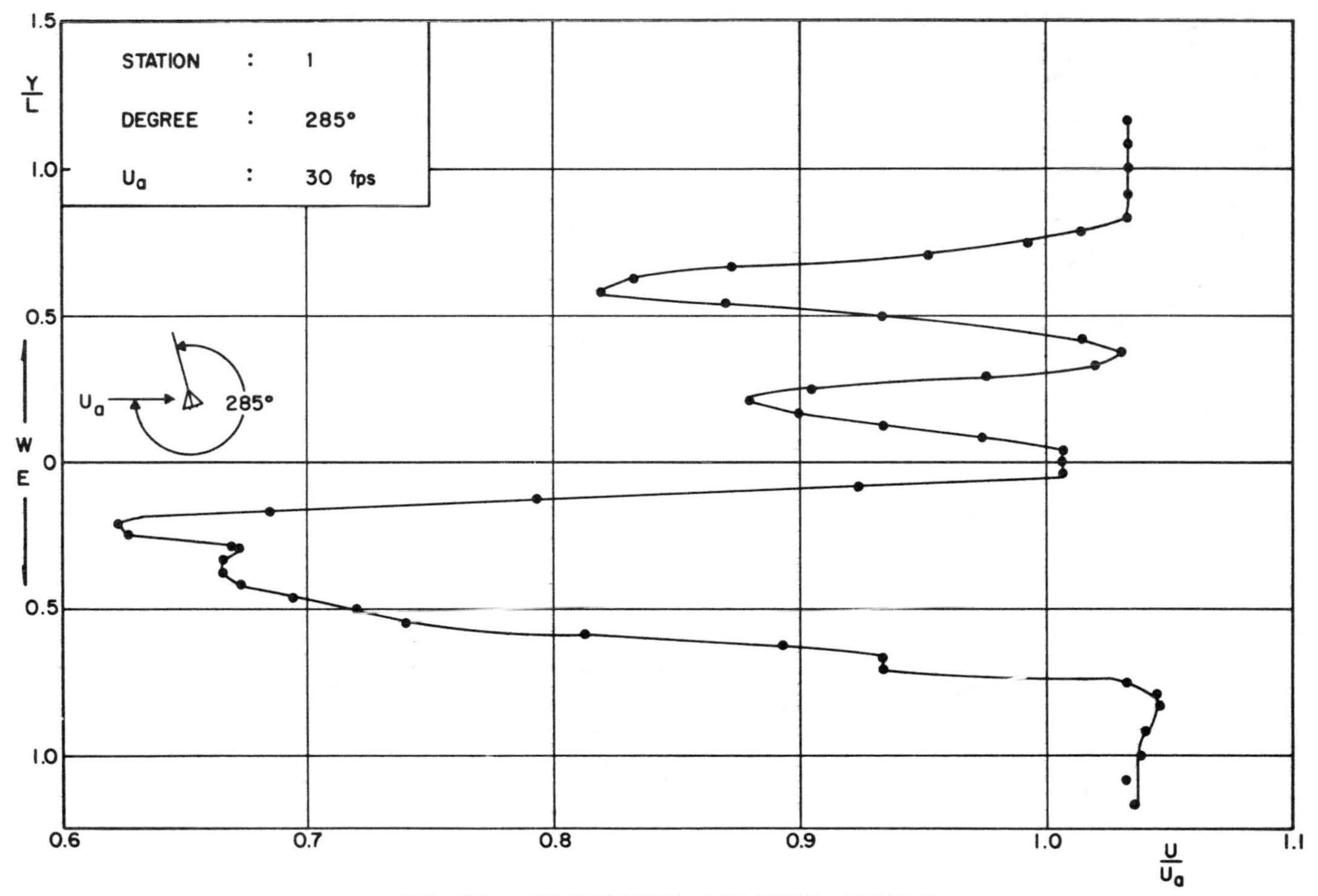

FIG. 37 TRANSVERSE VELOCITY PROFILE

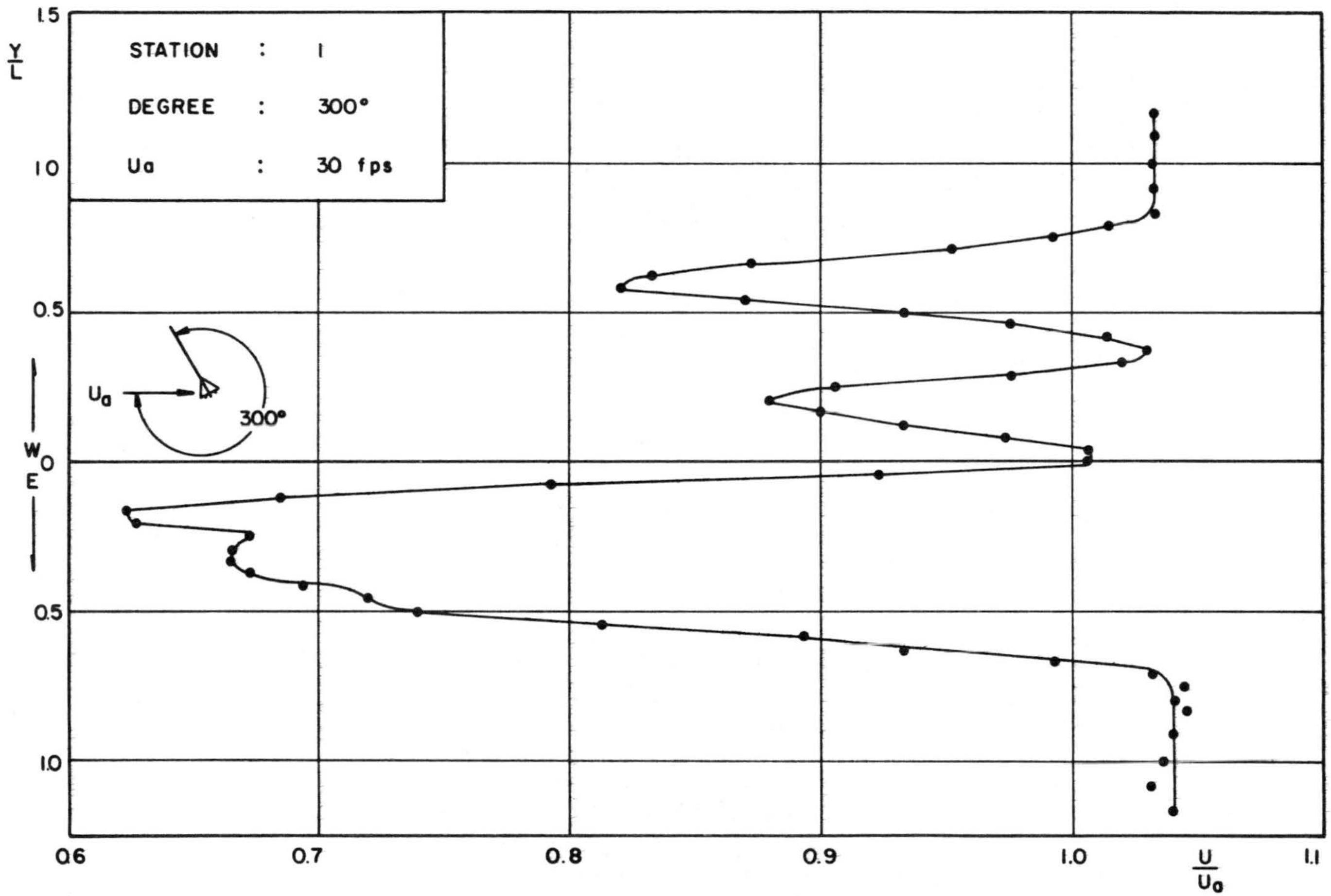

FIG. 38 TRANSVERSE VELOCITY PROFILE

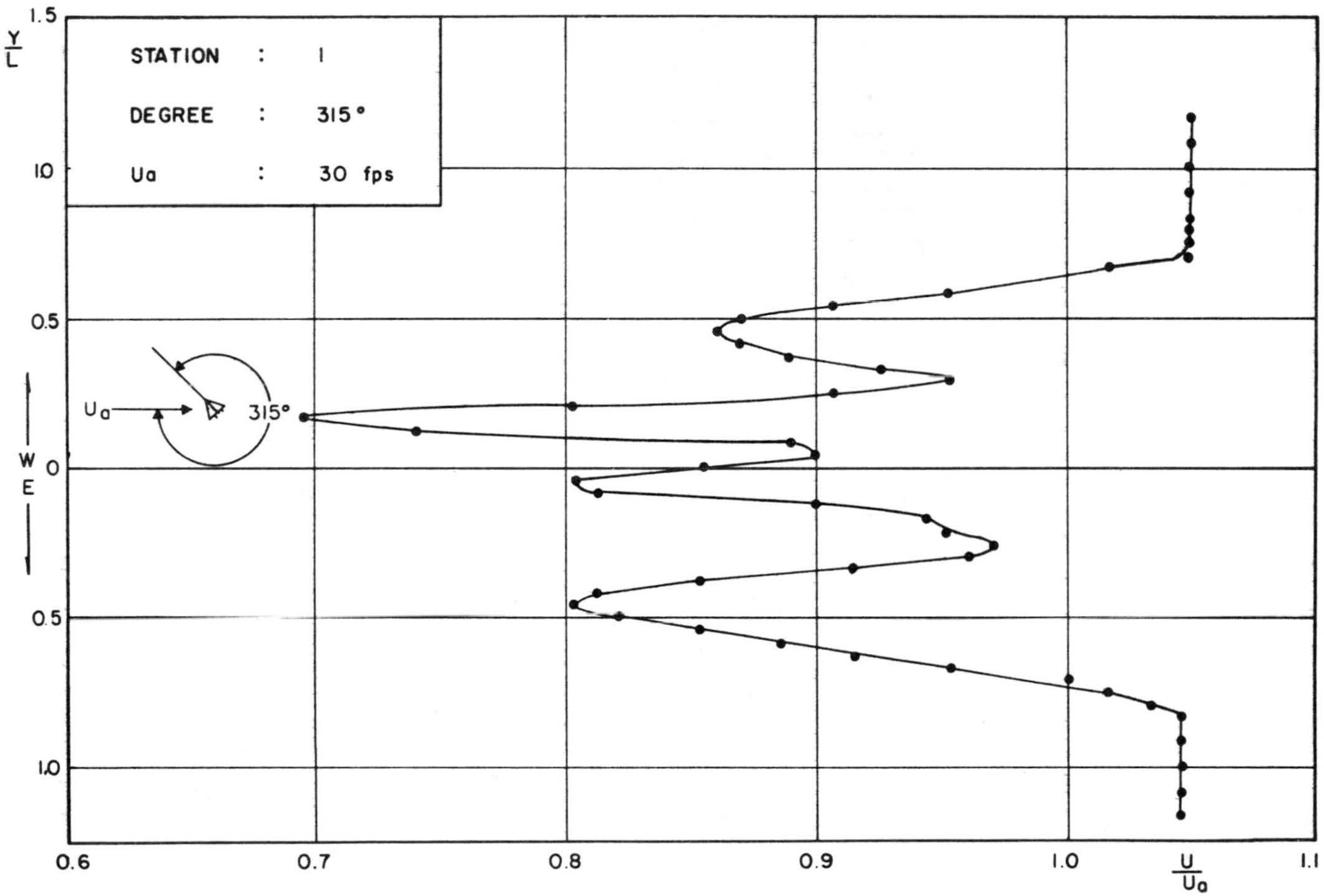

FIG. 39 TRANSVERSE VELOCITY PROFILE

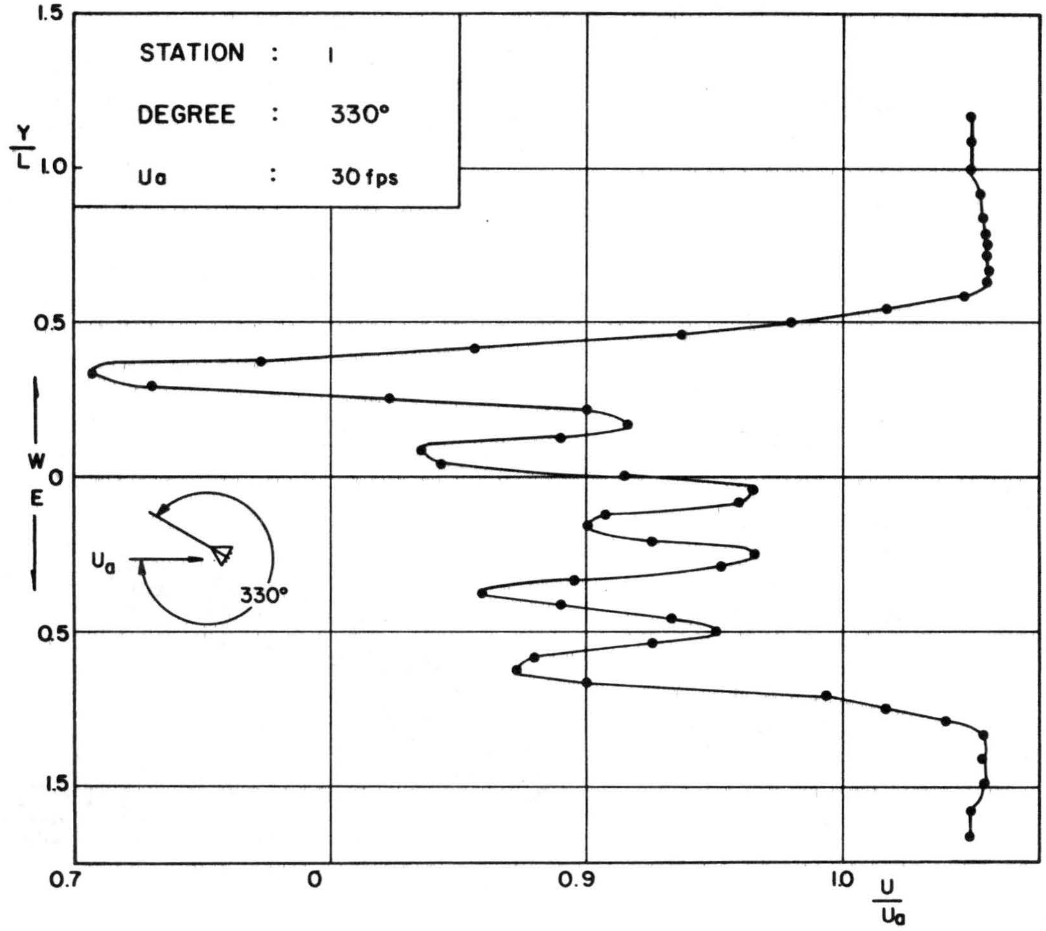

FIG. 40 TRANSVERSE VELOCITY PROFILE

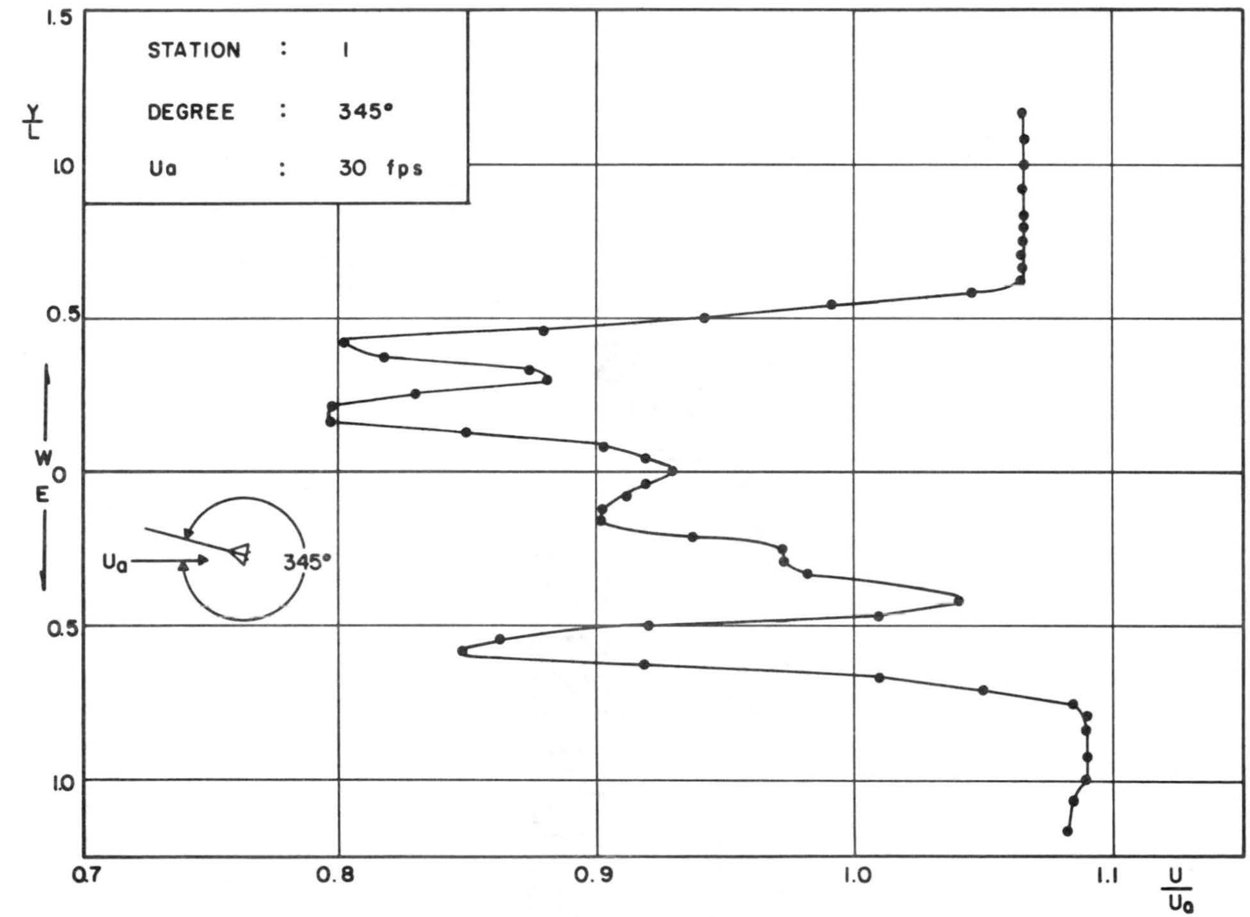

FIG. 41 TRANSVERSE VELOCITY PROFILE

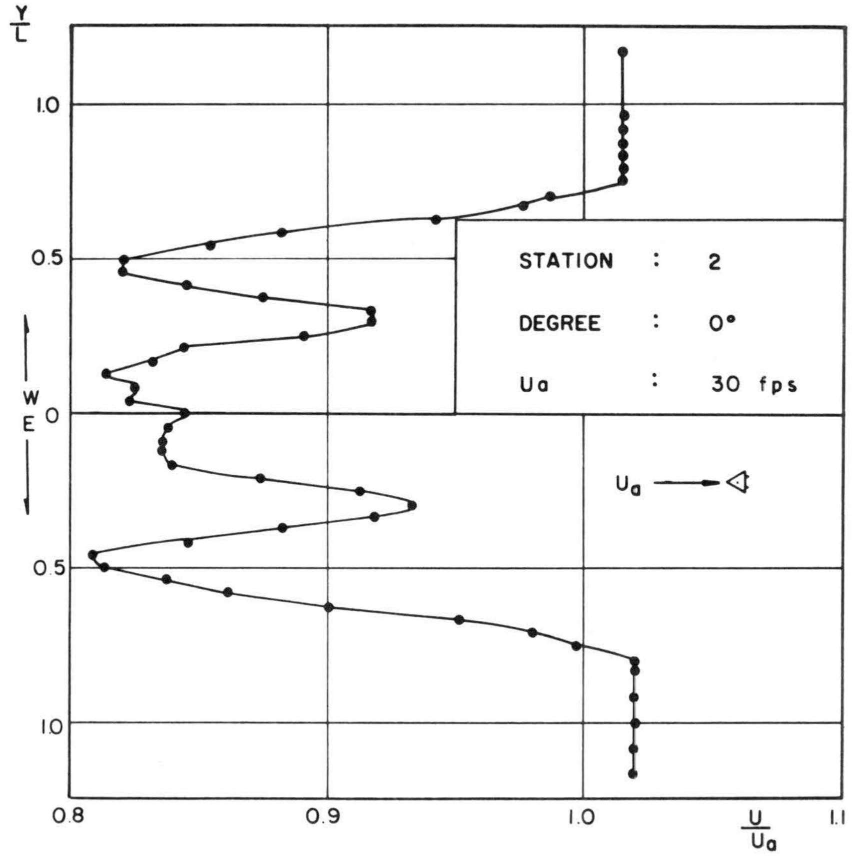

FIG. 42 TRANSVERSE VELOCITY PROFILE

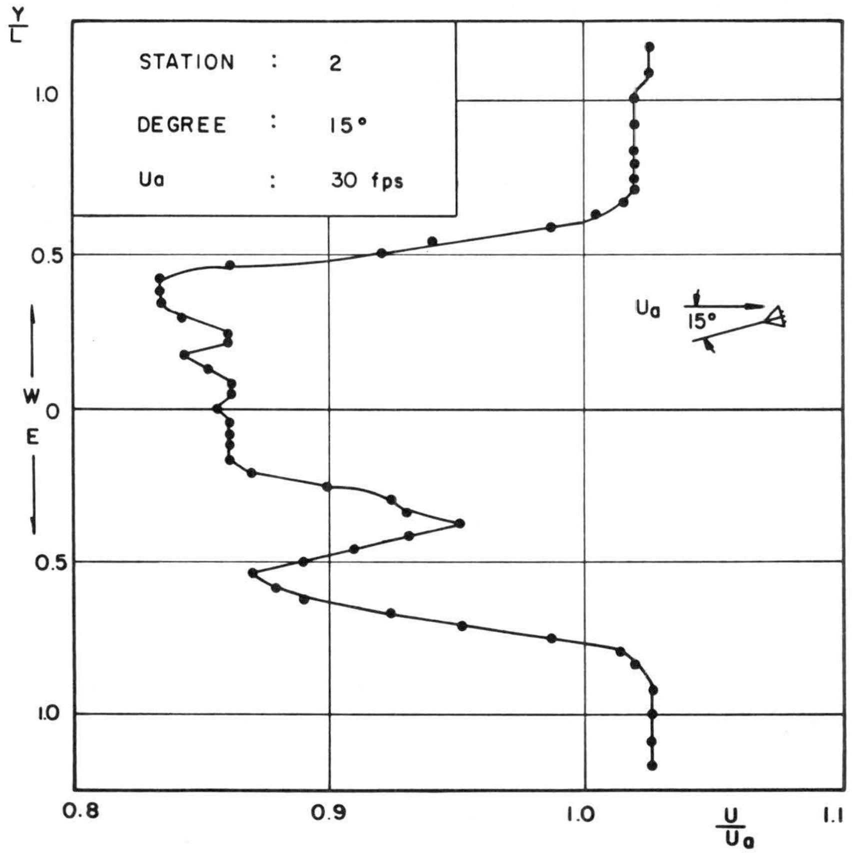

FIG. 43 TRANSVERSE VELOCITY PROFILE

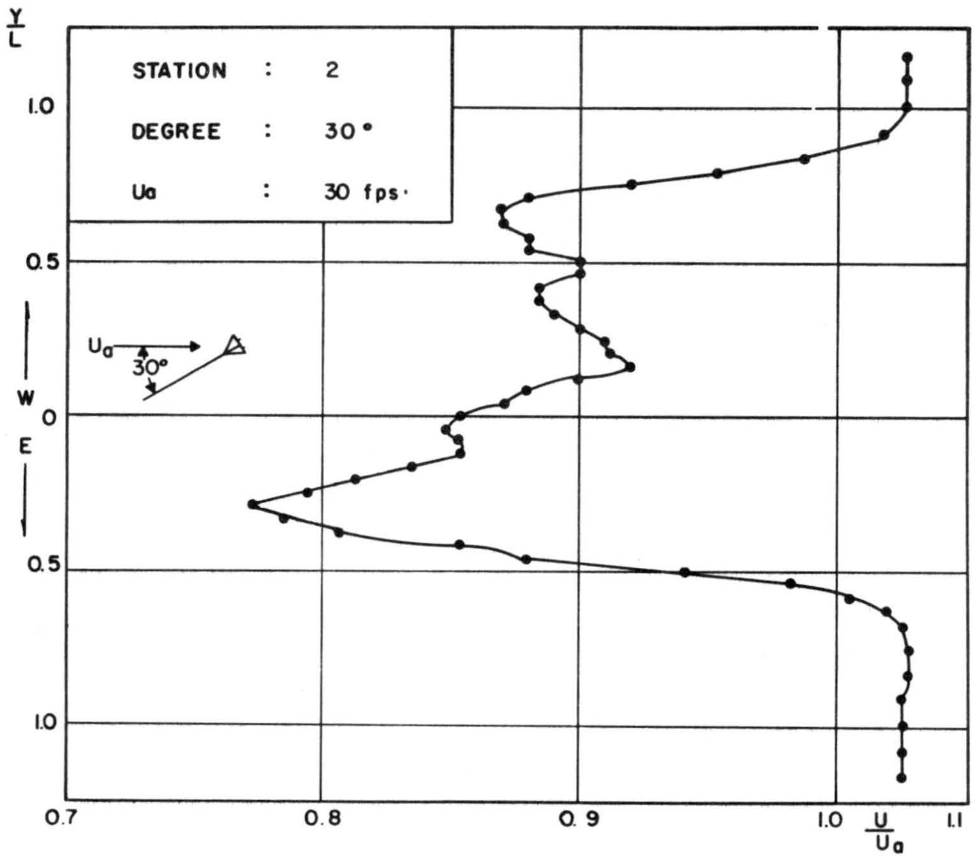

FIG. 44 TRANSVERSE VELOCITY PROFILE

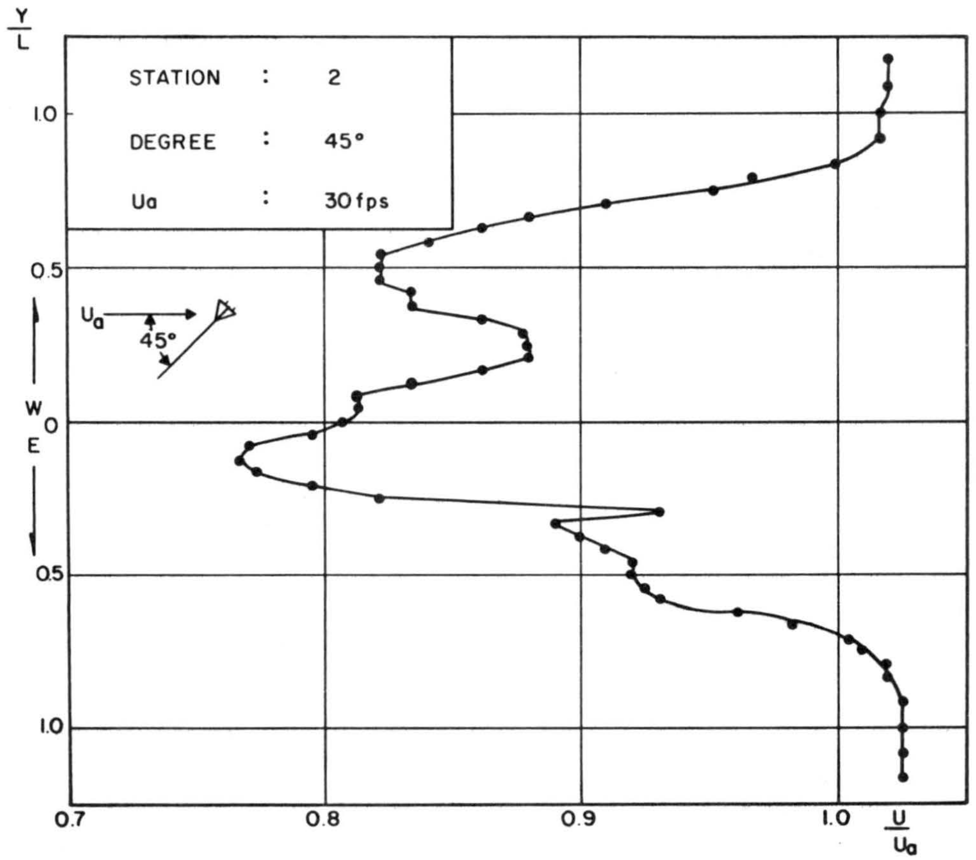

FIG. 45 TRANSVERSE VELOCITY PROFILE

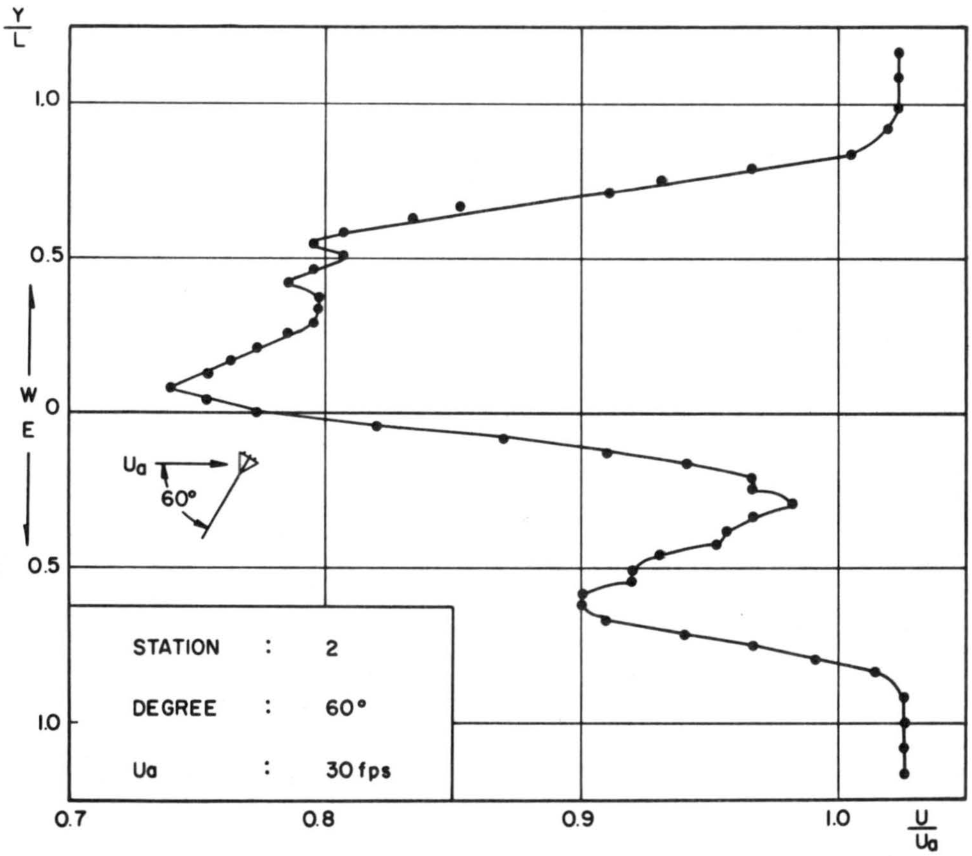

FIG. 46 TRANSVERSE VELOCITY PROFILE

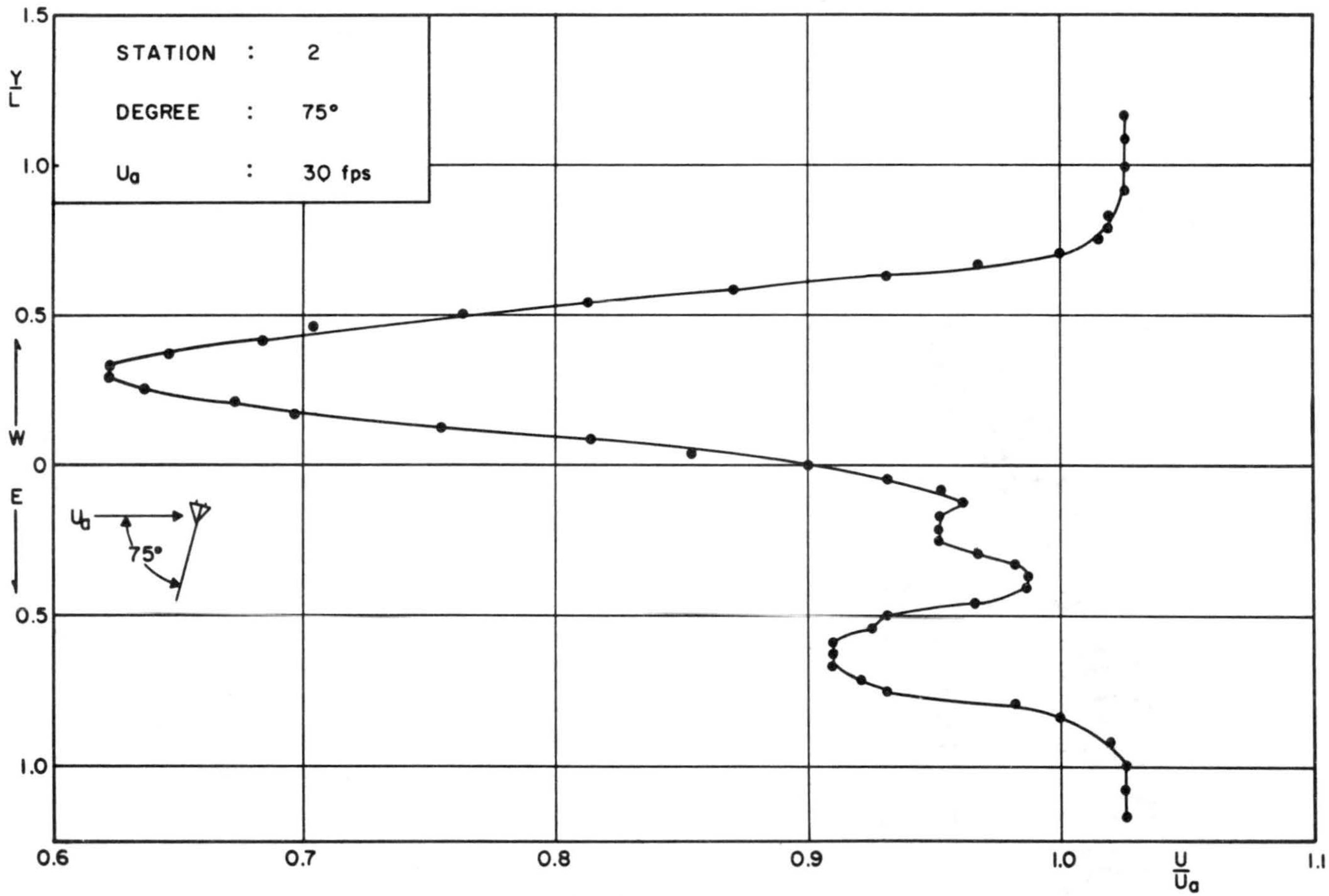

FIG. 47 TRANSVERSE VELOCITY PROFILE

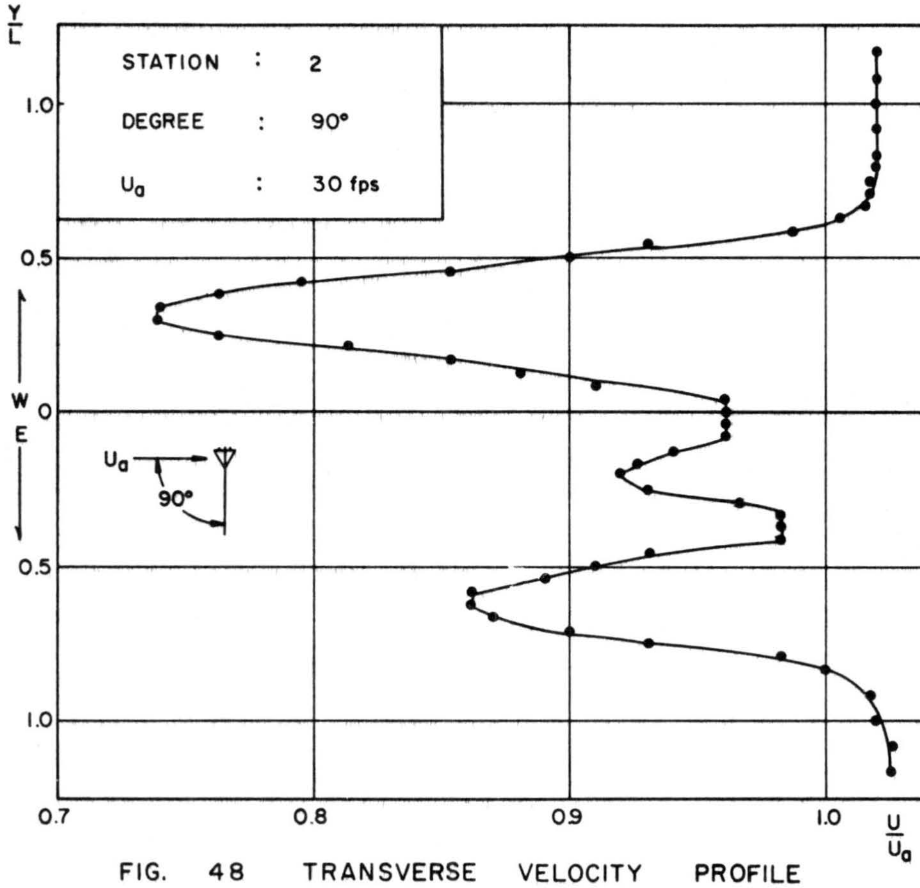

FIG. 48 TRANSVERSE VELOCITY PROFILE

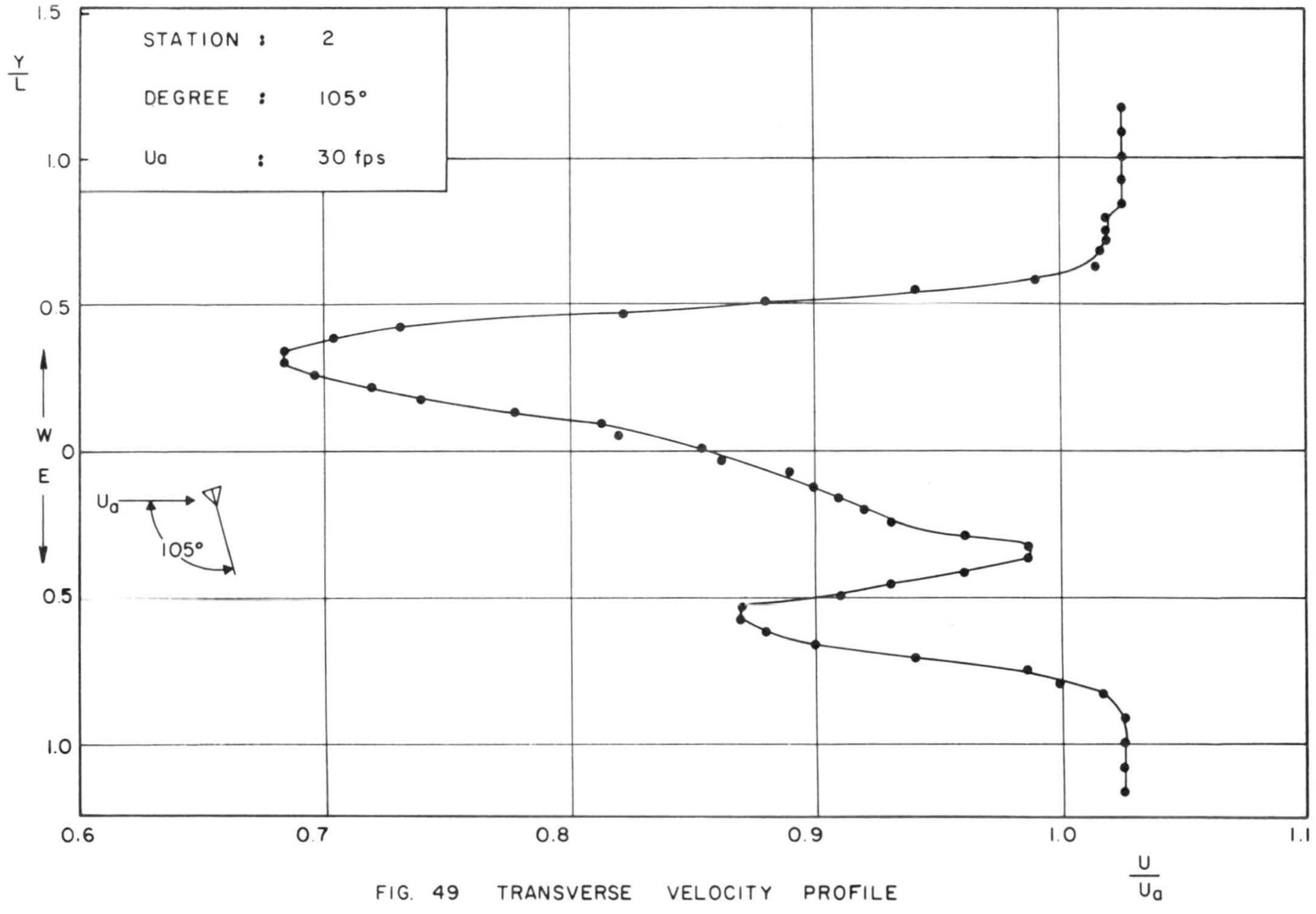

FIG. 49 TRANSVERSE VELOCITY PROFILE

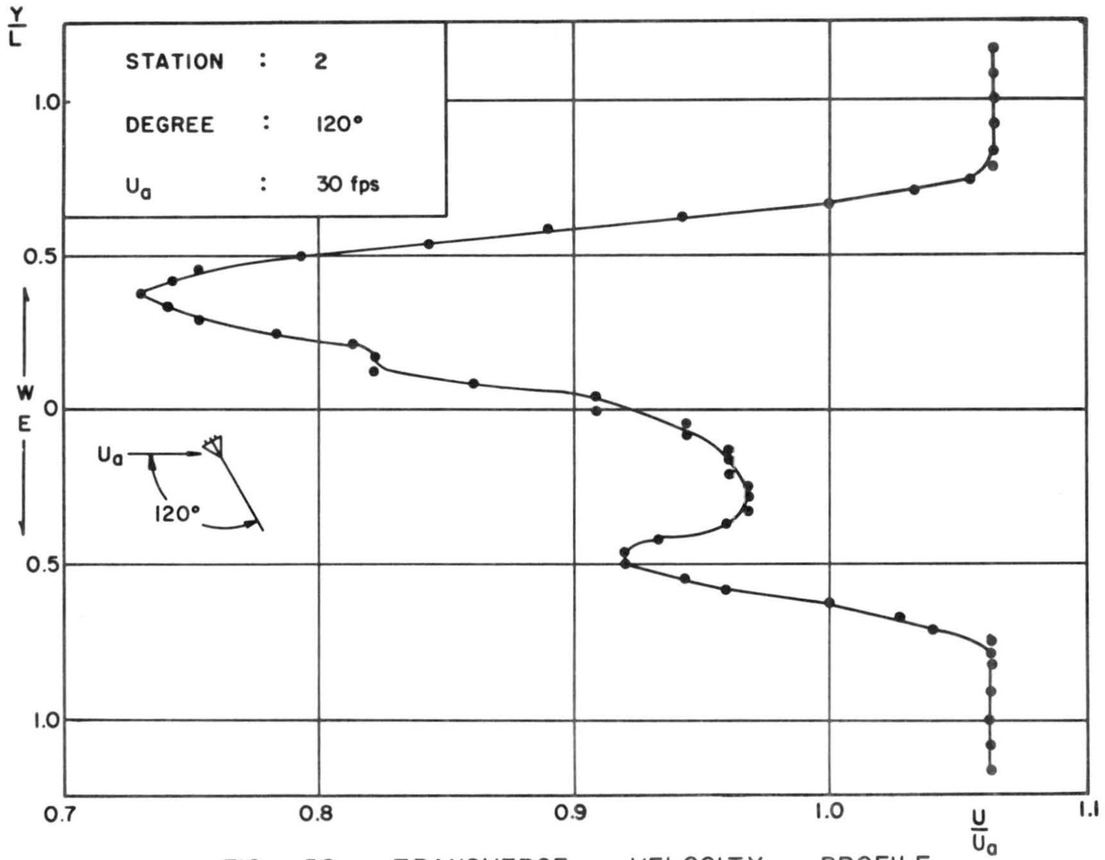

FIG. 50 TRANSVERSE VELOCITY PROFILE

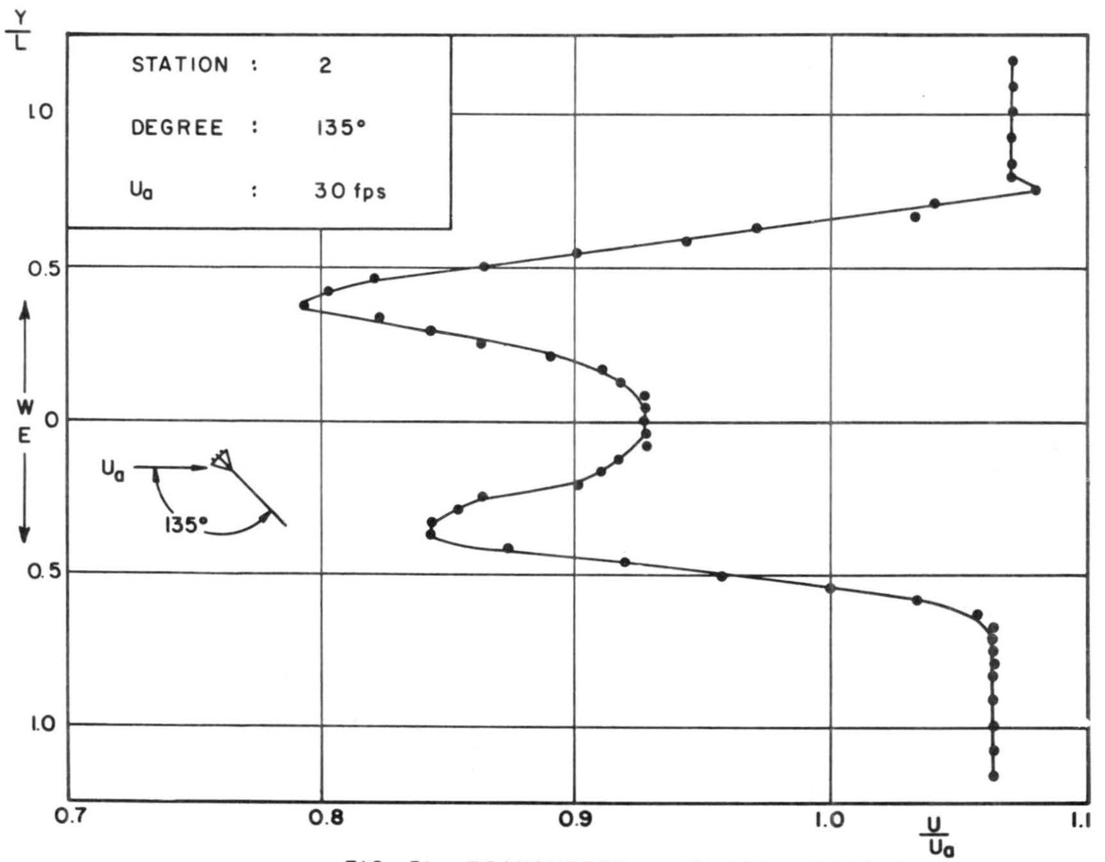

FIG. 51 TRANSVERSE VELOCITY PROFILE

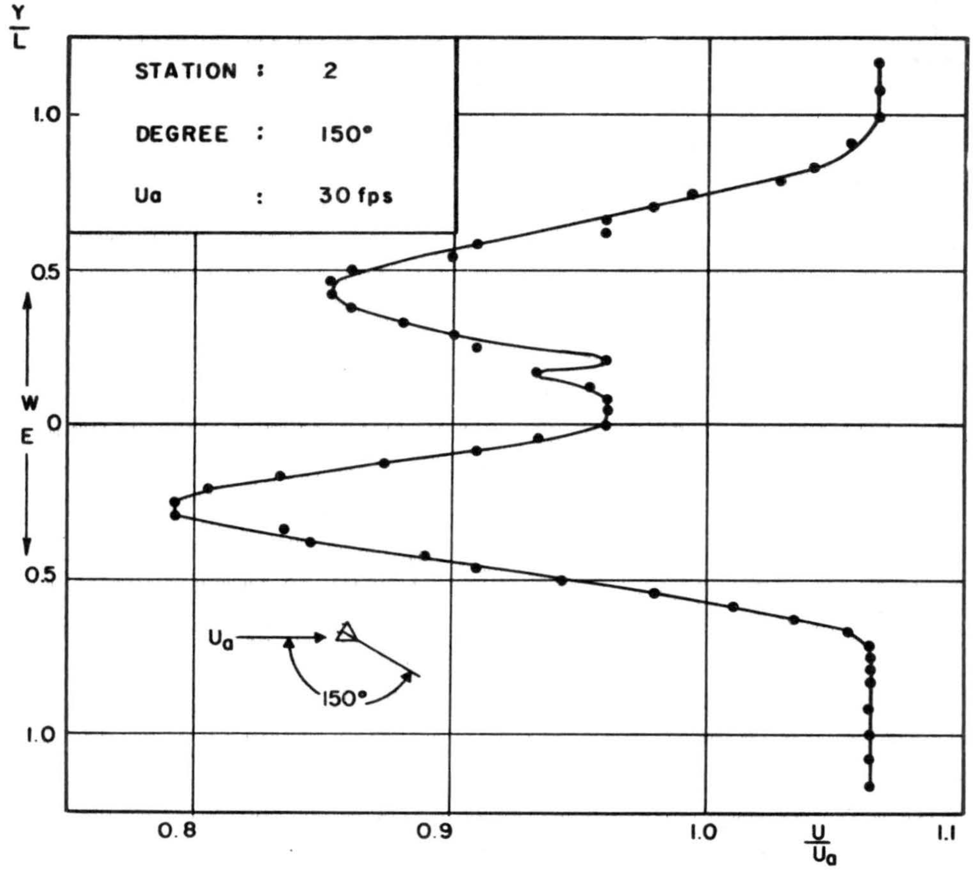

FIG. 52 TRANSVERSE VELOCITY PROFILE

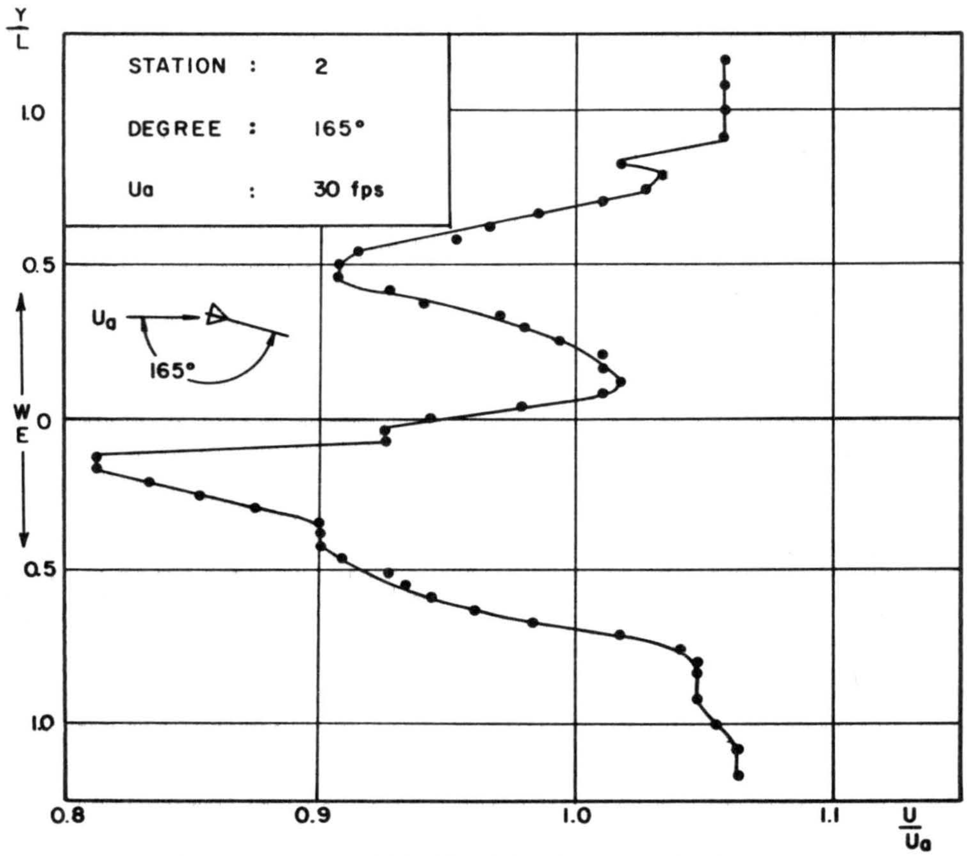

FIG. 53 TRANSVERSE VELOCITY PROFILE

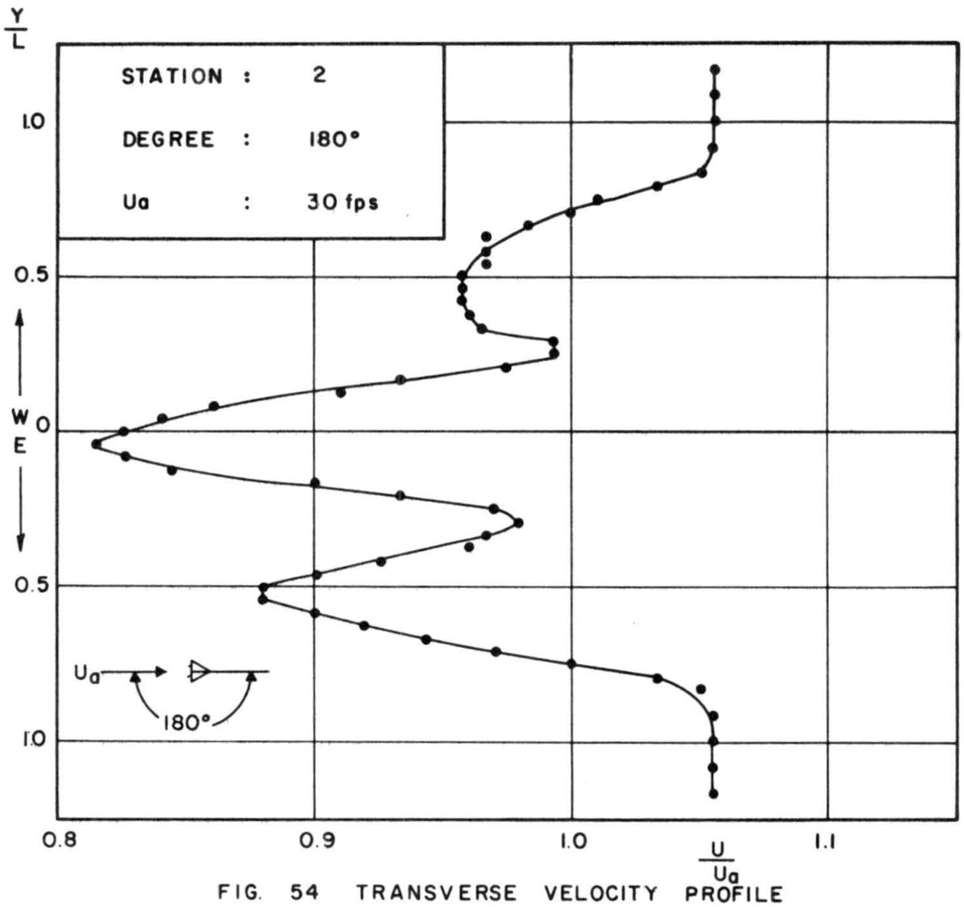

FIG. 54 TRANSVERSE VELOCITY PROFILE

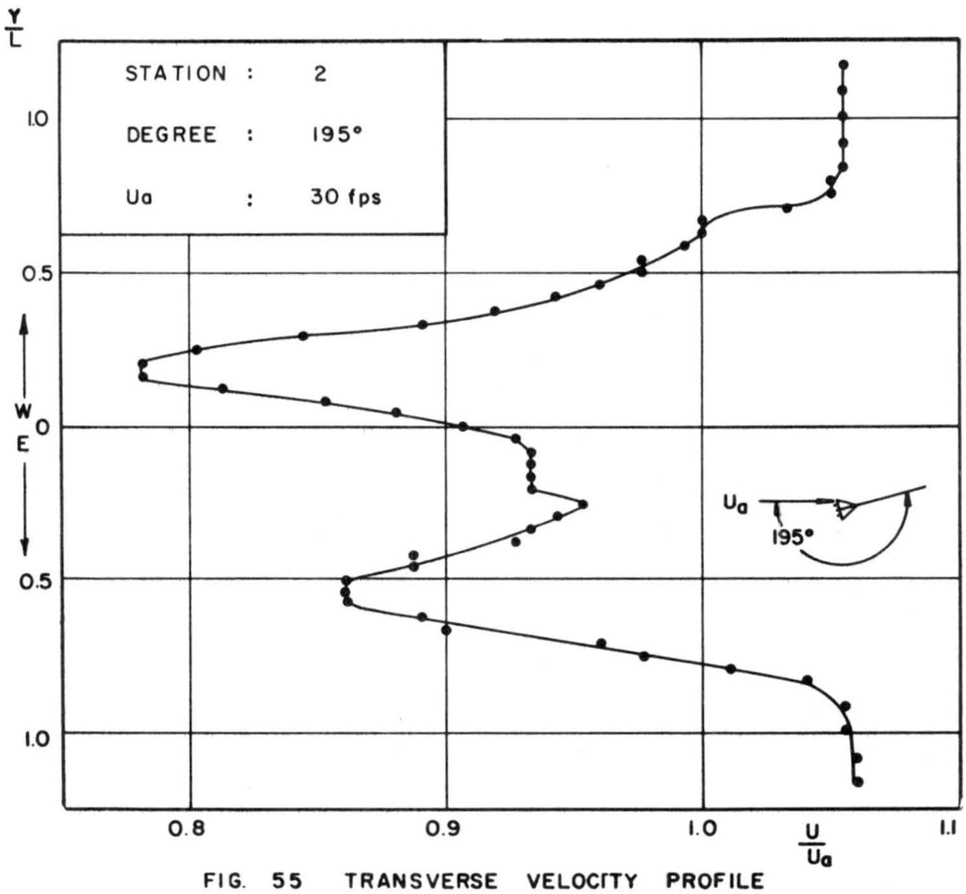

FIG. 55 TRANSVERSE VELOCITY PROFILE

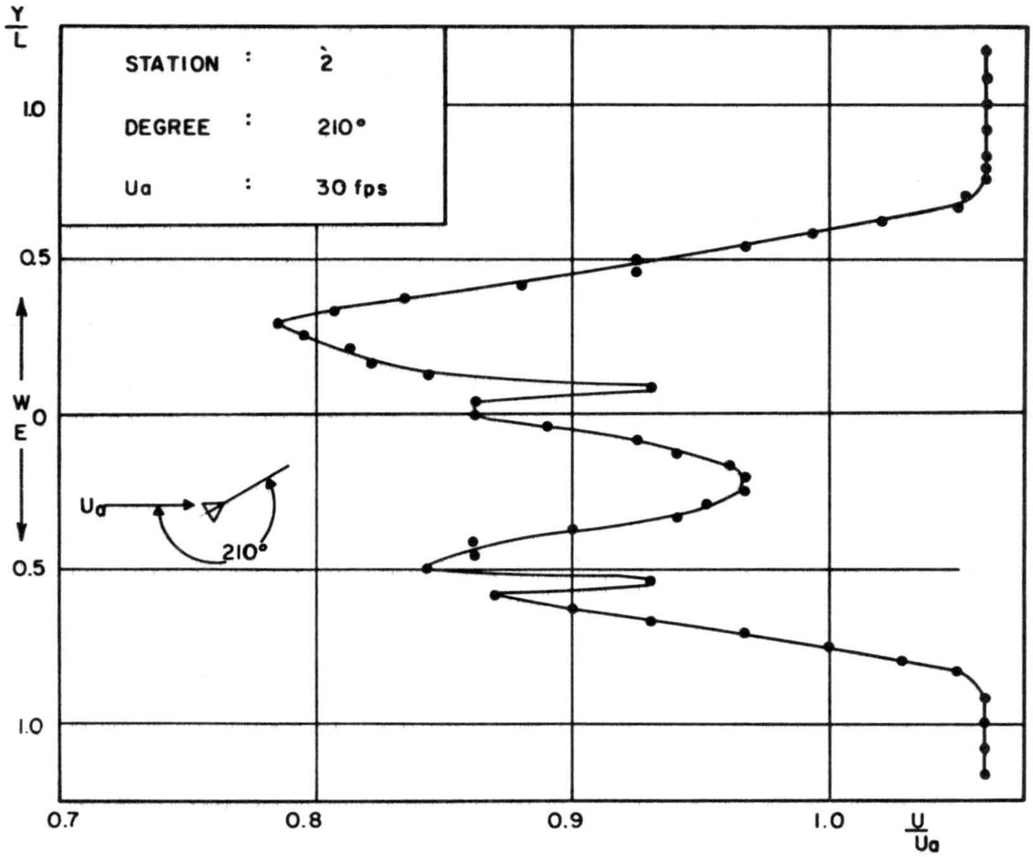

FIG. 56 TRANSVERSE VELOCITY PROFILE

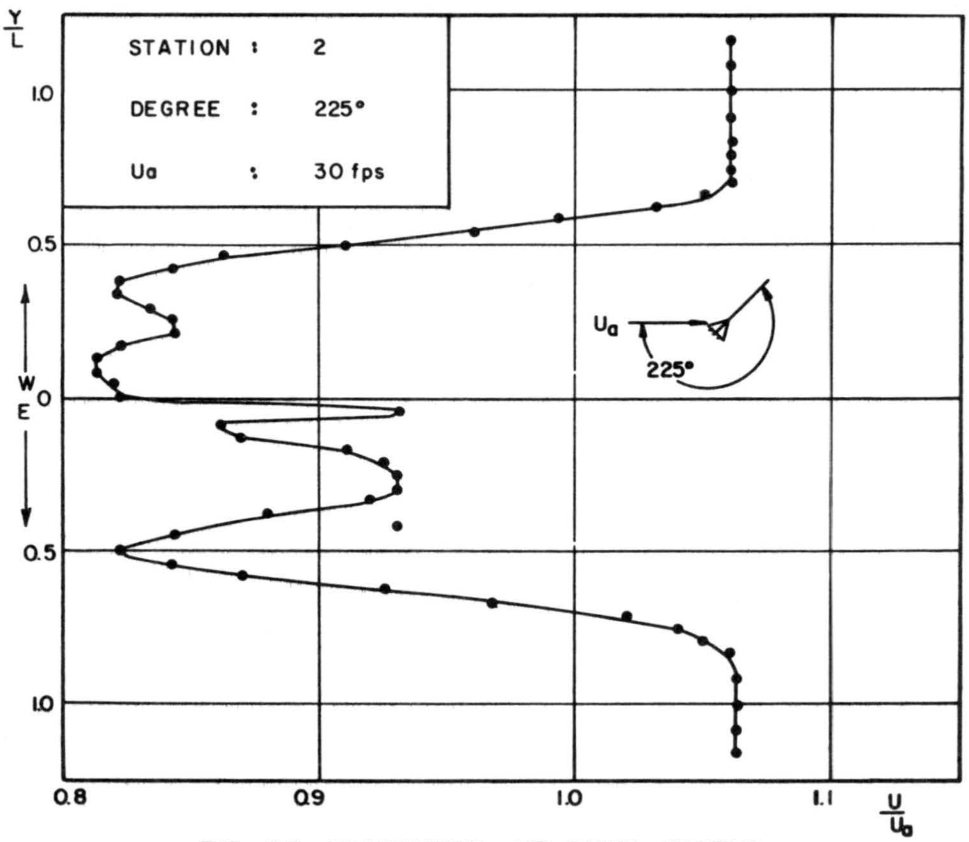

FIG. 57 TRANSVERSE VELOCITY PROFILE

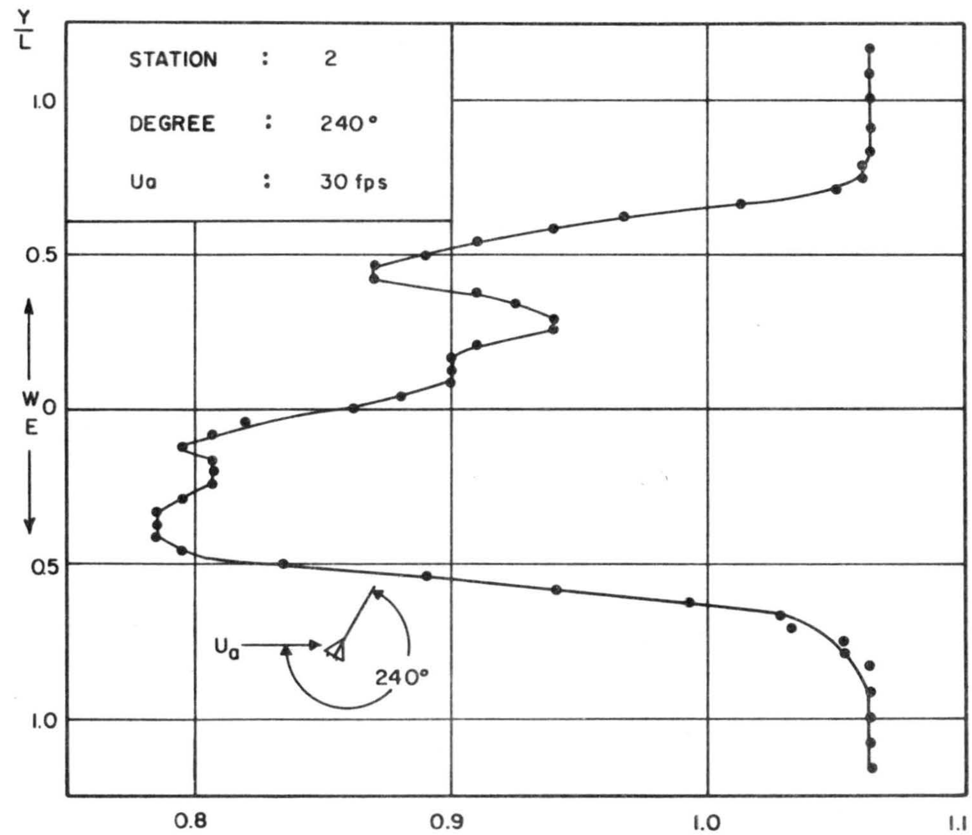

FIG. 58 TRANSVERSE VELOCITY PROFILE

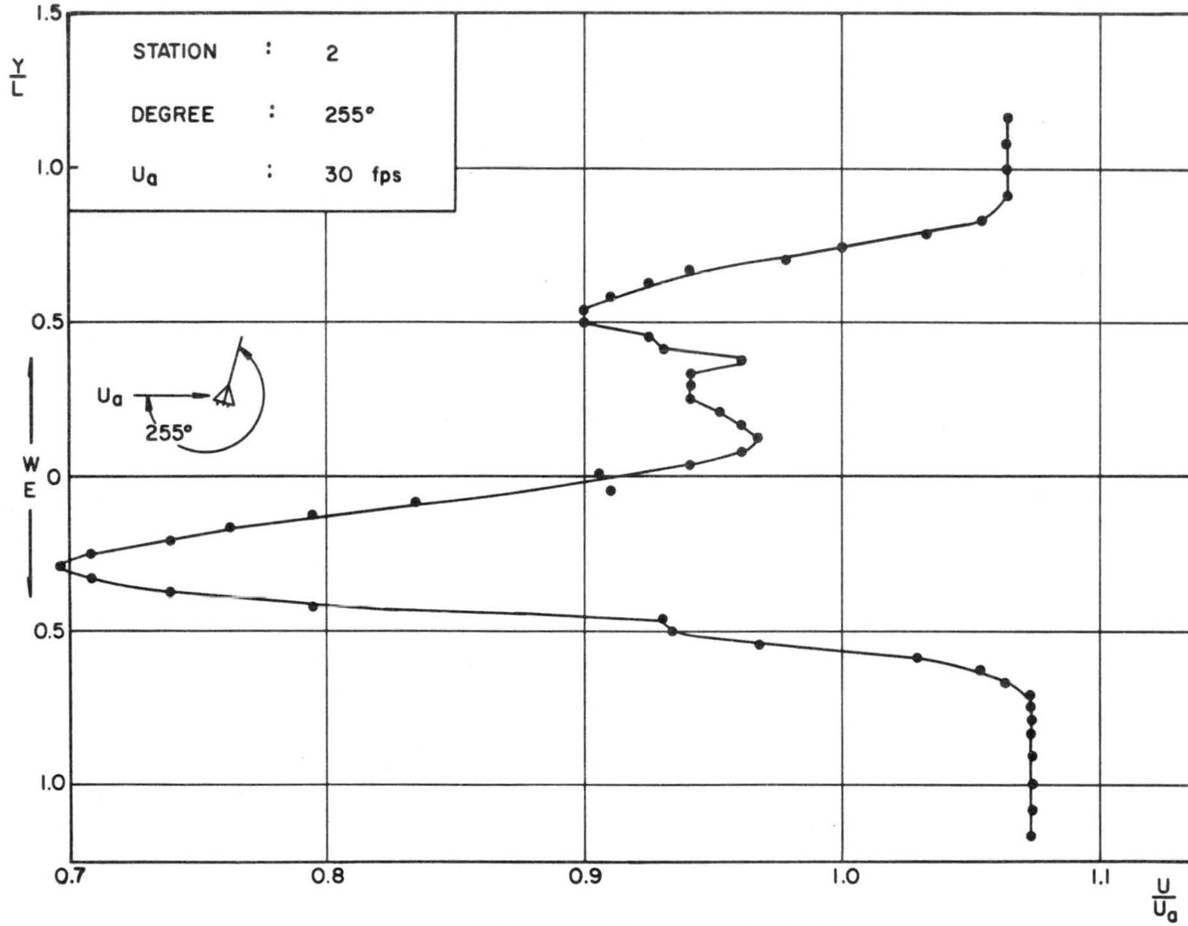

FIG. 59 TRANSVERSE VELOCITY PROFILE

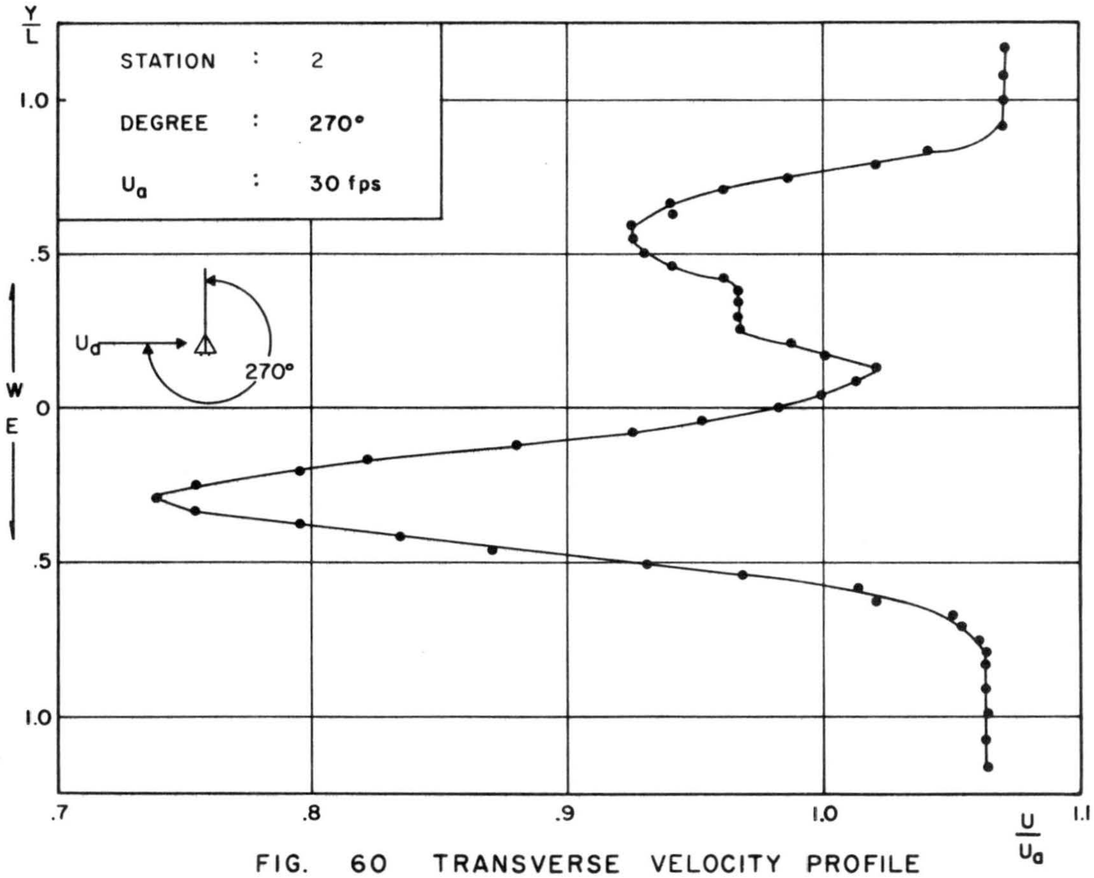

FIG. 60 TRANSVERSE VELOCITY PROFILE

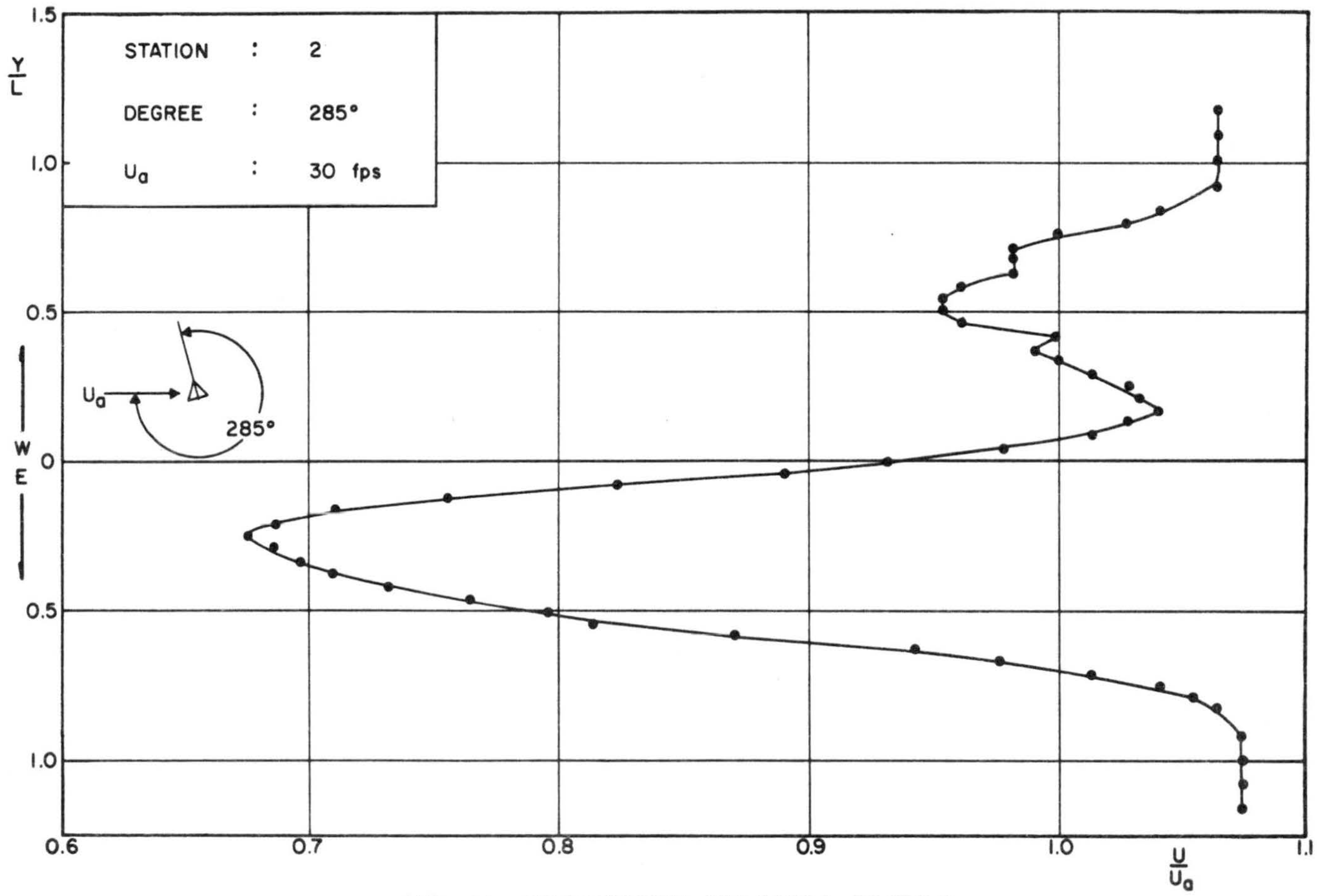

FIG. 61 TRANSVERSE VELOCITY PROFILE

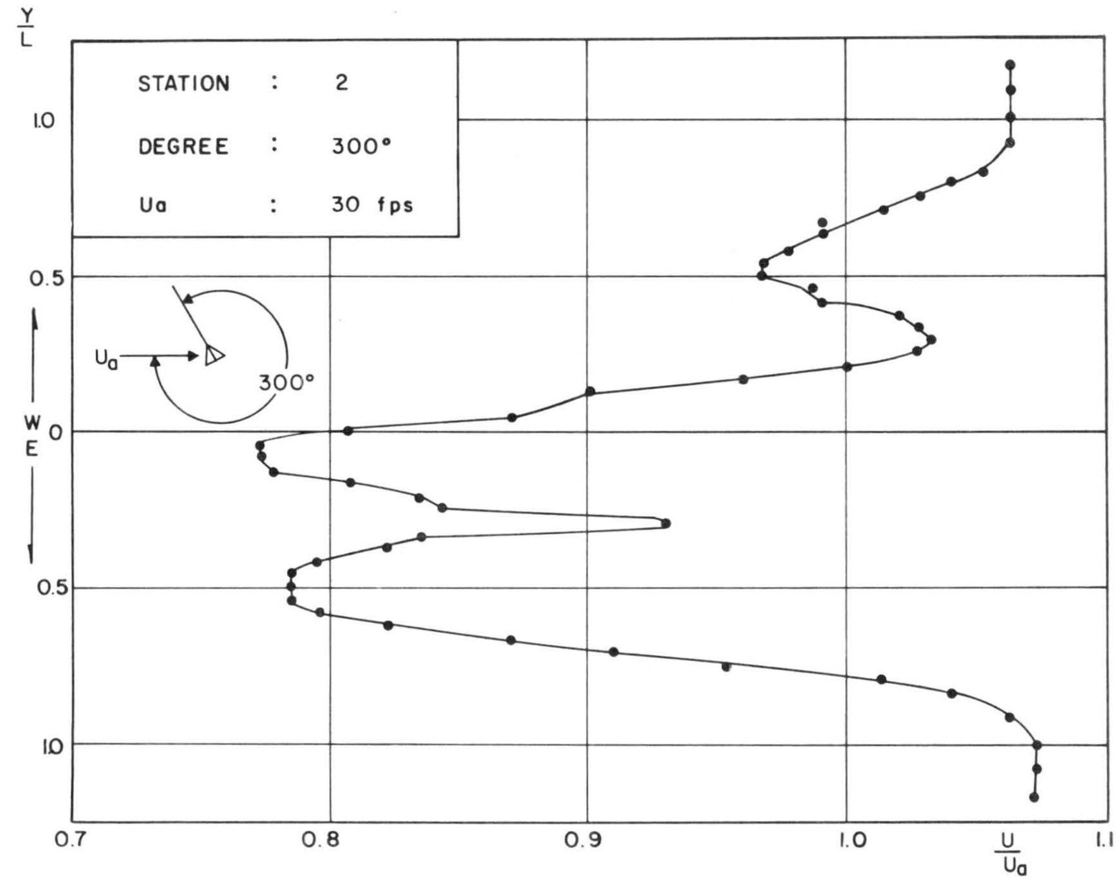

FIG 62 TRANSVERSE VELOCITY PROFILE

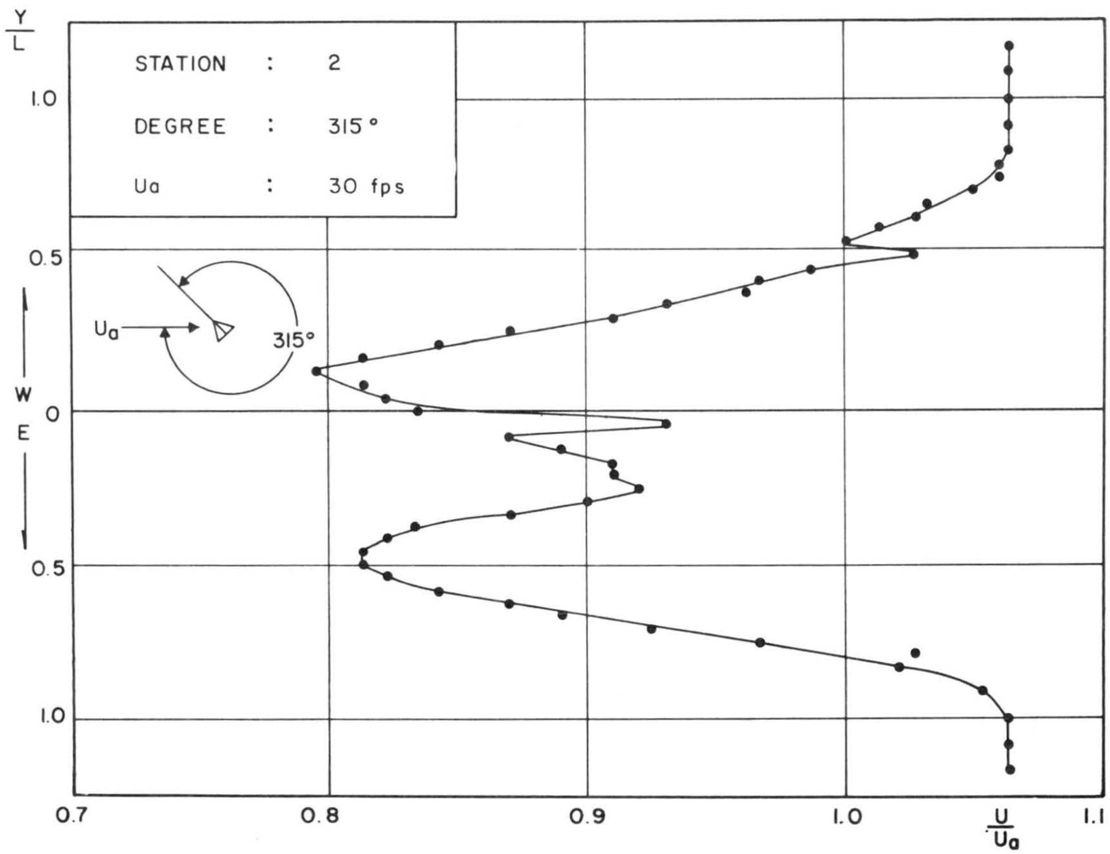

FIG. 63 TRANSVERSE VELOCITY PROFILE

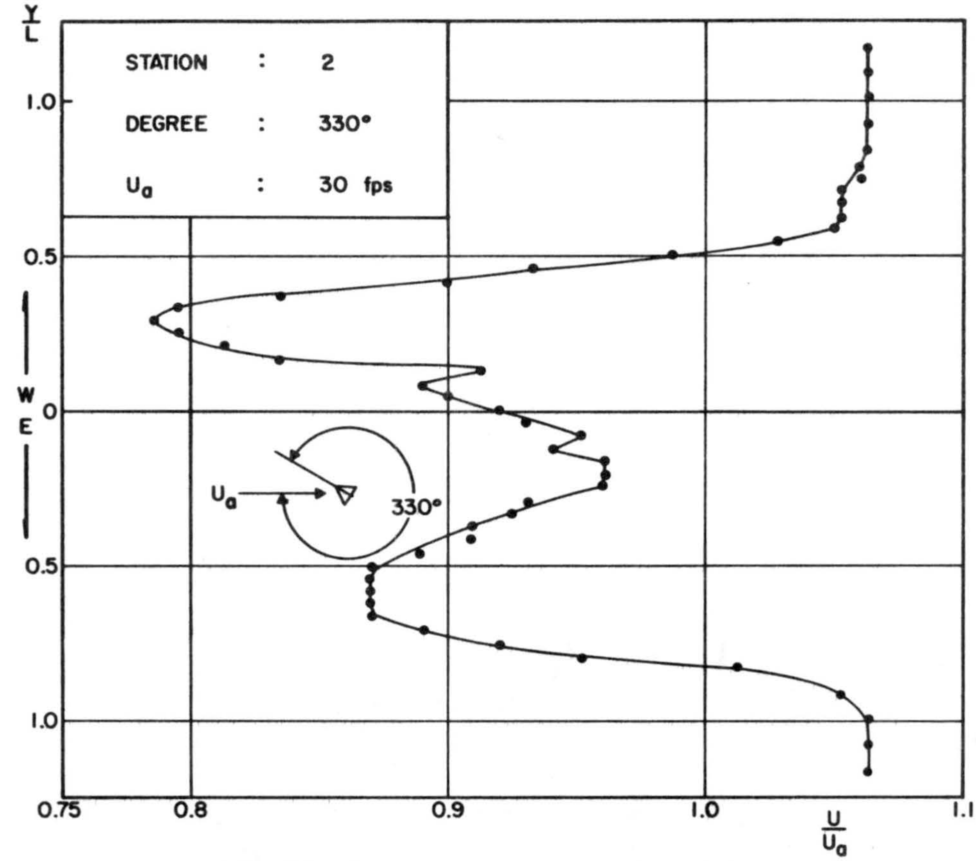

FIG. 64 TRANSVERSE VELOCITY PROFILE

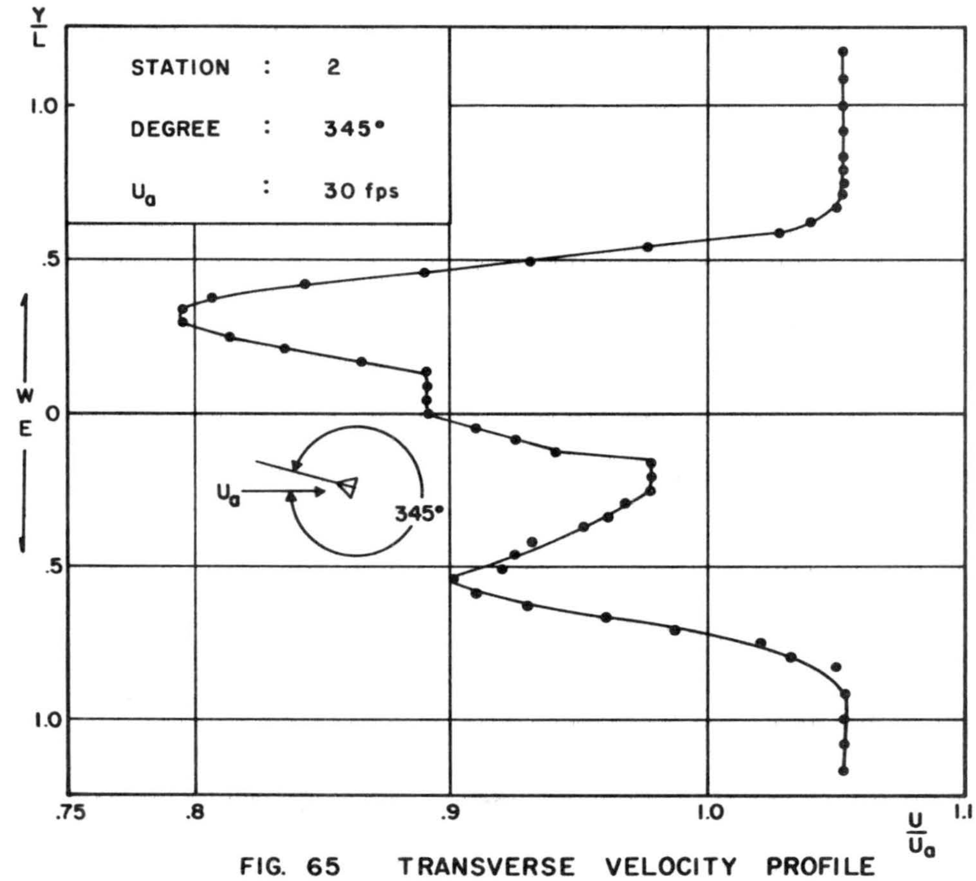

FIG. 65 TRANSVERSE VELOCITY PROFILE

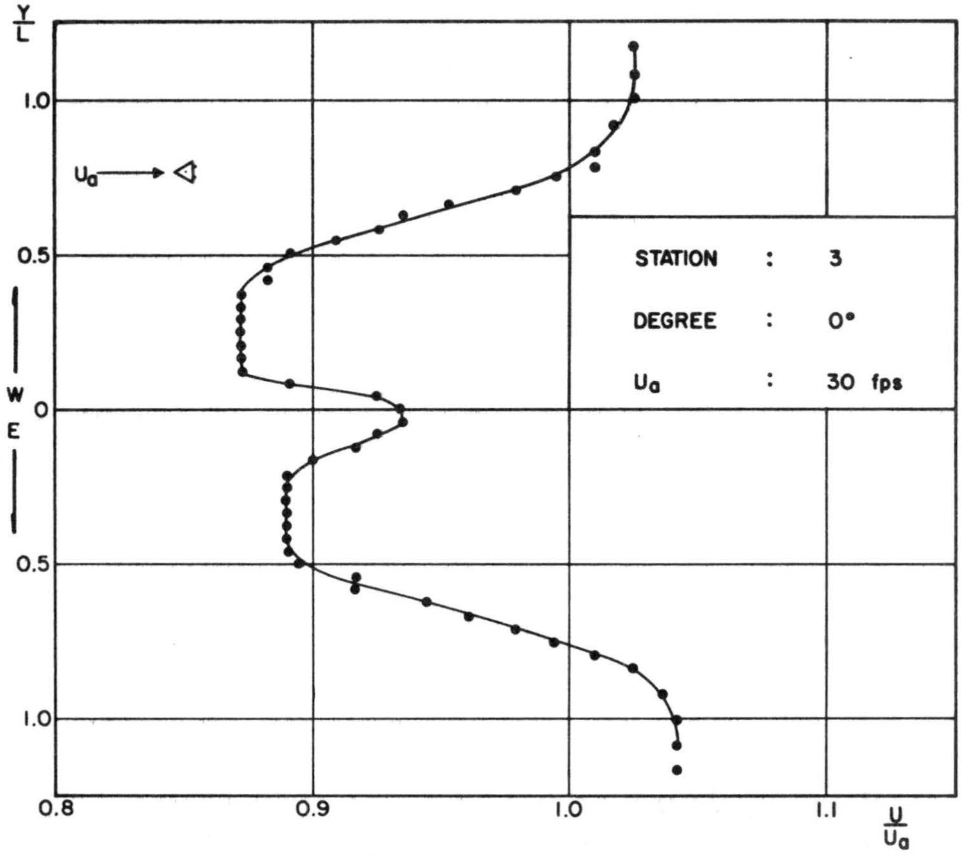

FIG. 66 TRANSVERSE VELOCITY PROFILE

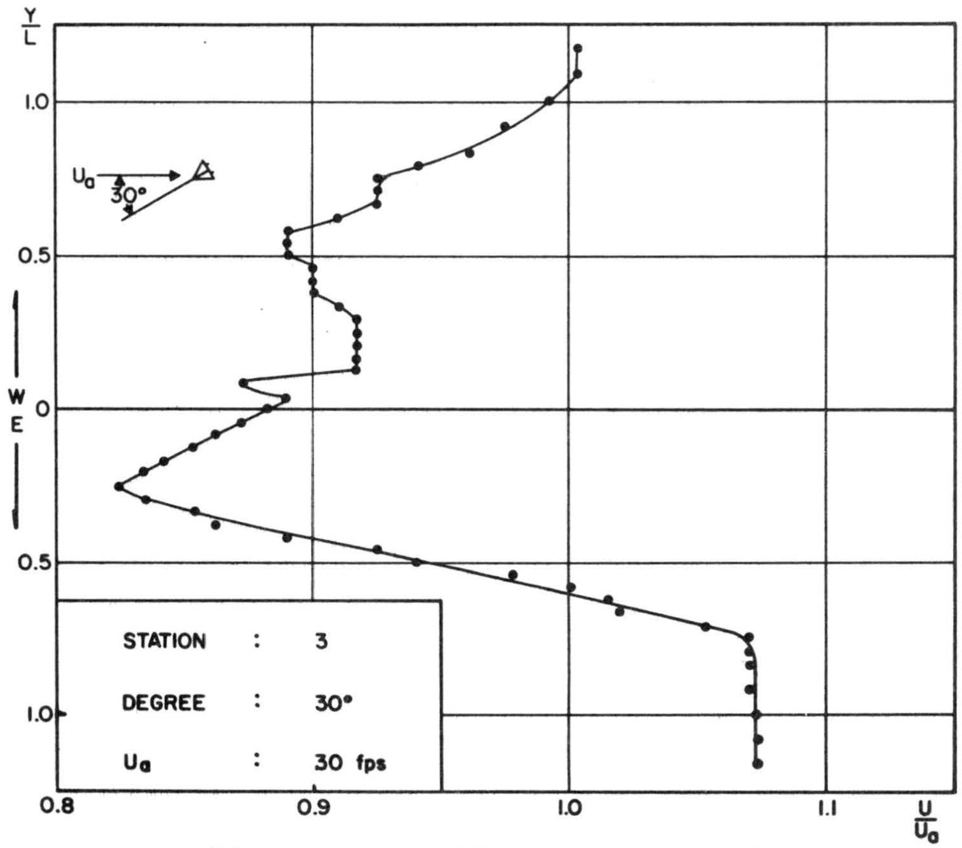

FIG. 67 TRANSVERSE VELOCITY PROFILE

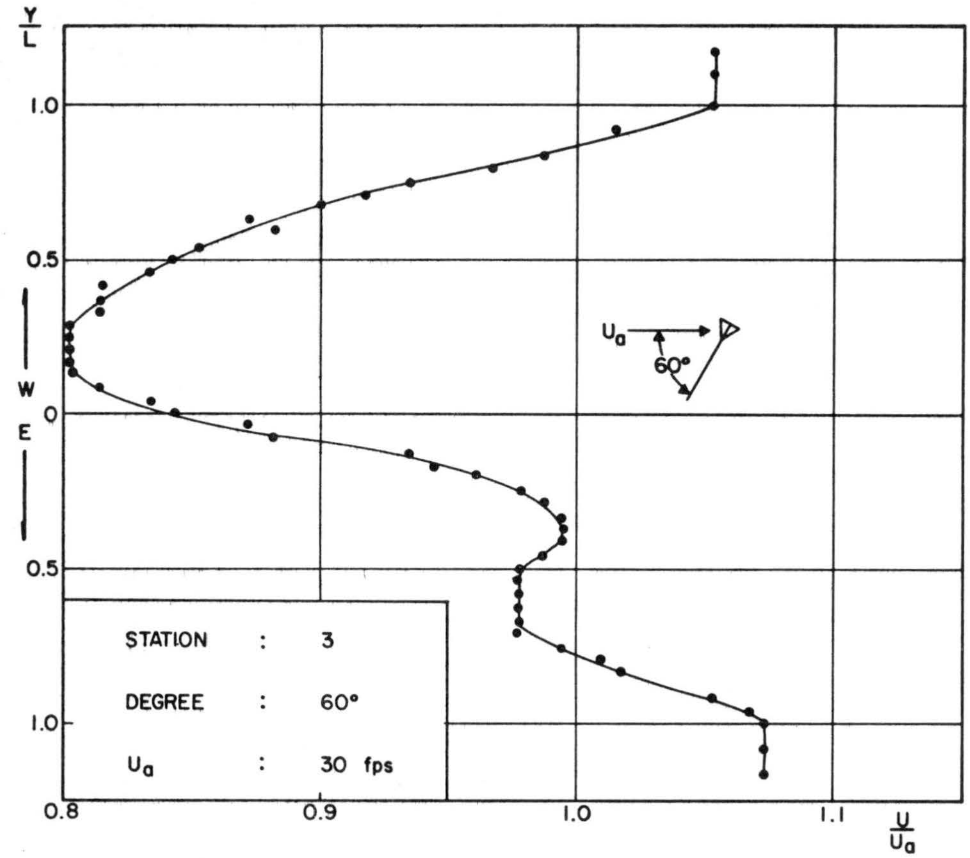

FIG. 68 TRANSVERSE VELOCITY PROFILE

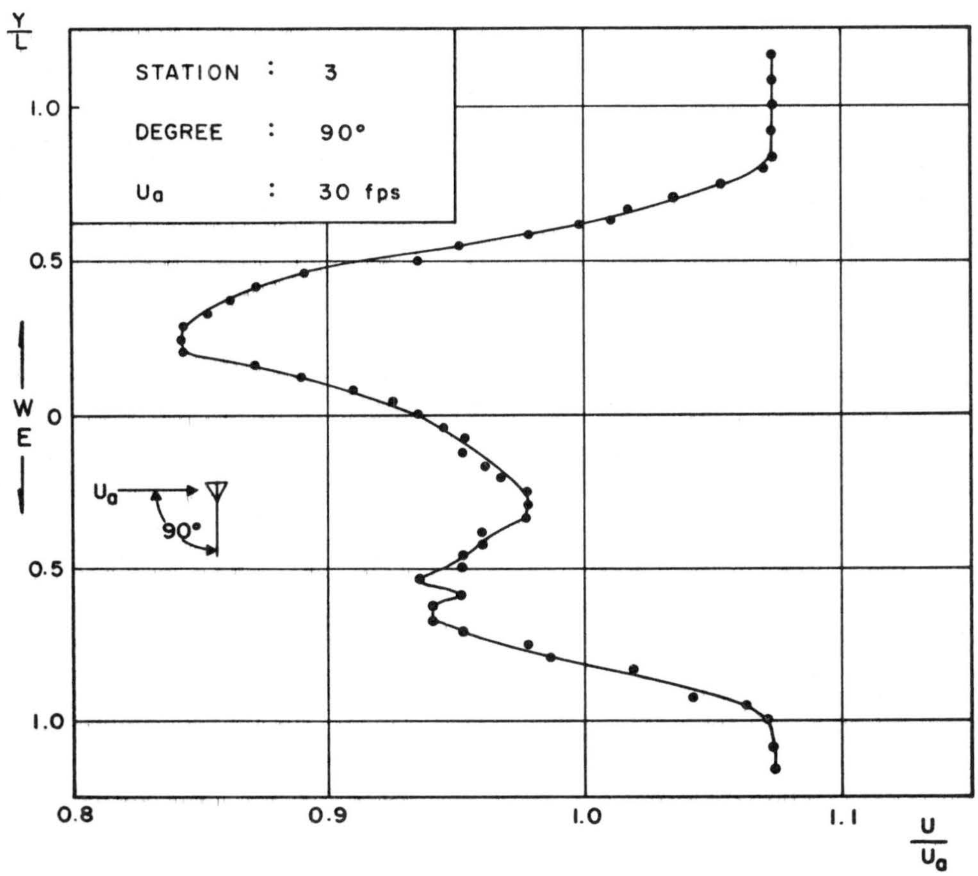

FIG. 69 TRANSVERSE VELOCITY PROFILE

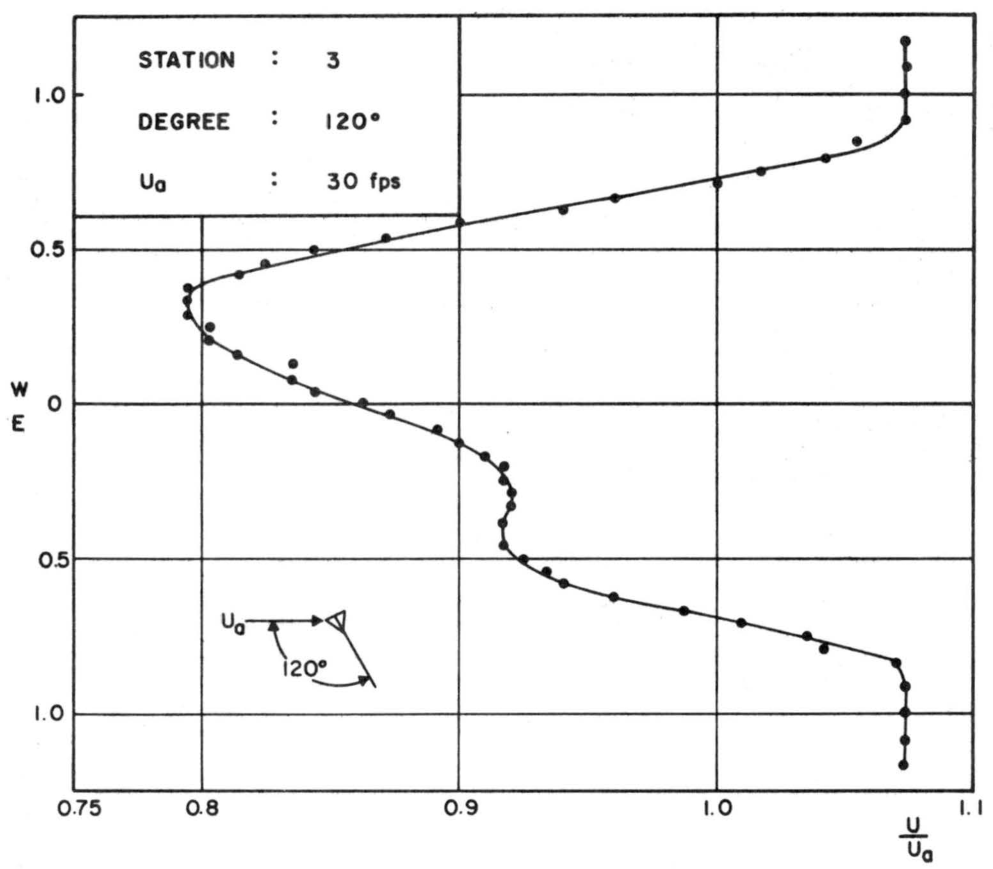

FIG. 70 TRANSVERSE VELOCITY PROFILE

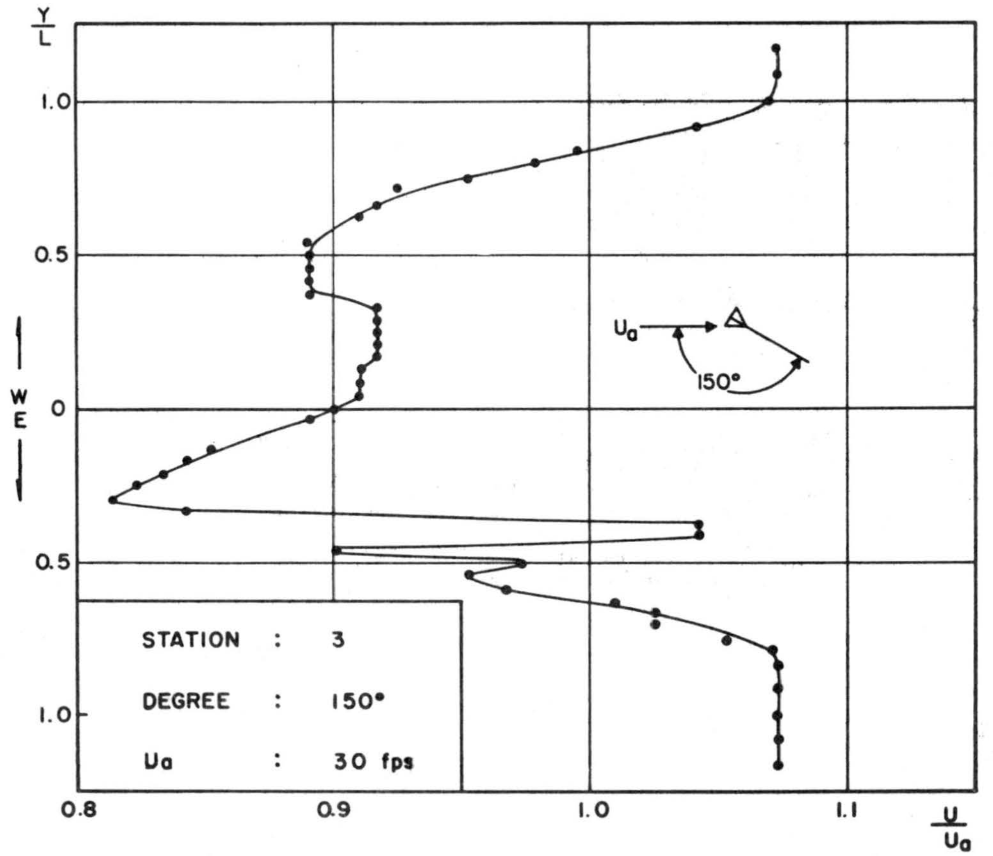

FIG. 71 TRANSVERSE VELOCITY PROFILE

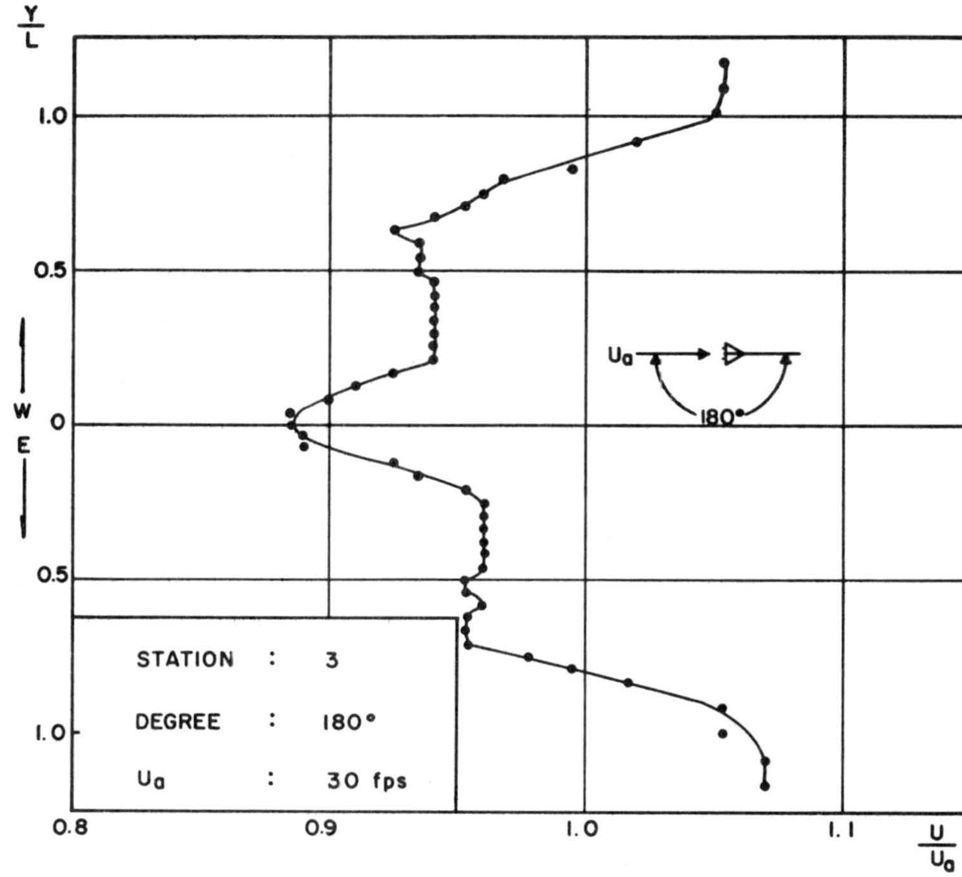

FIG. 72 TRANSVERSE VELOCITY PROFILE

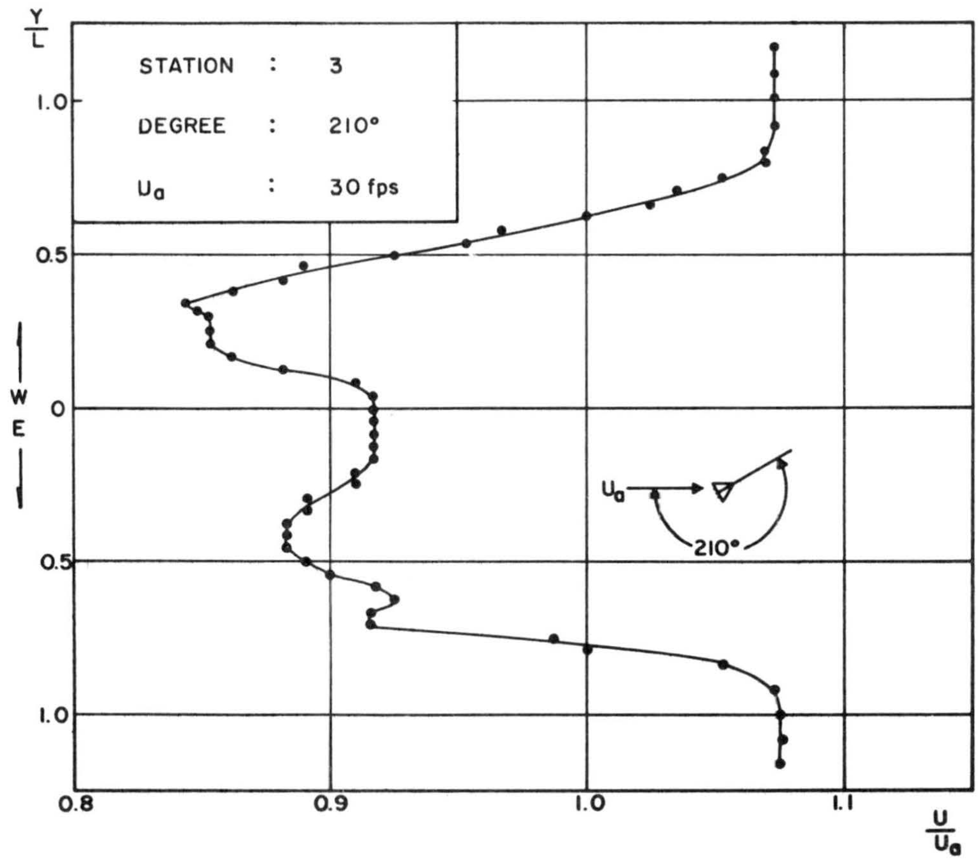

FIG. 73 TRANSVERSE VELOCITY PROFILE

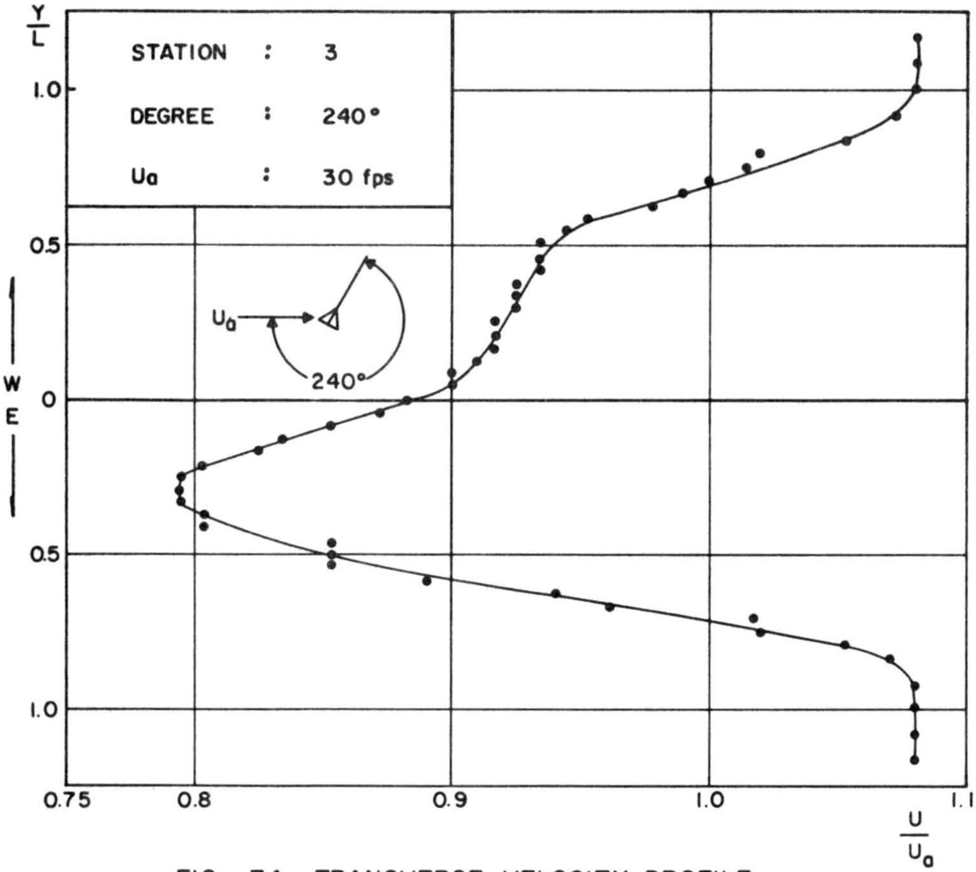

FIG. 74 TRANSVERSE VELOCITY PROFILE

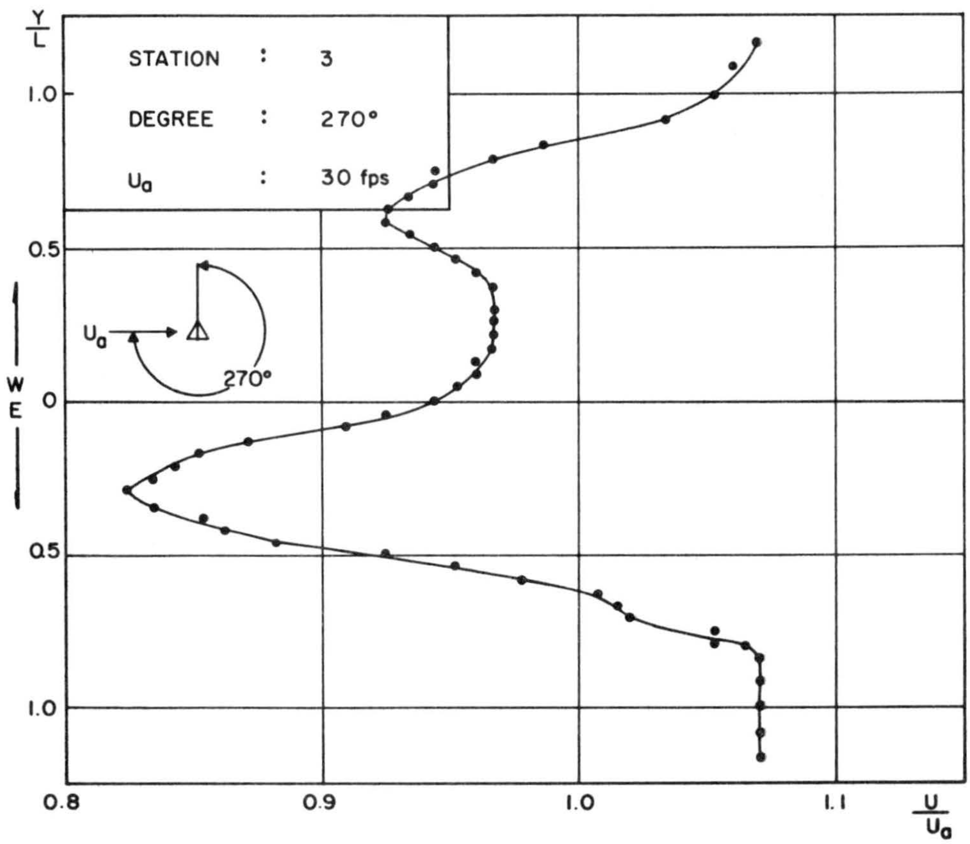

FIG. 75 TRANSVERSE VELOCITY PROFILE

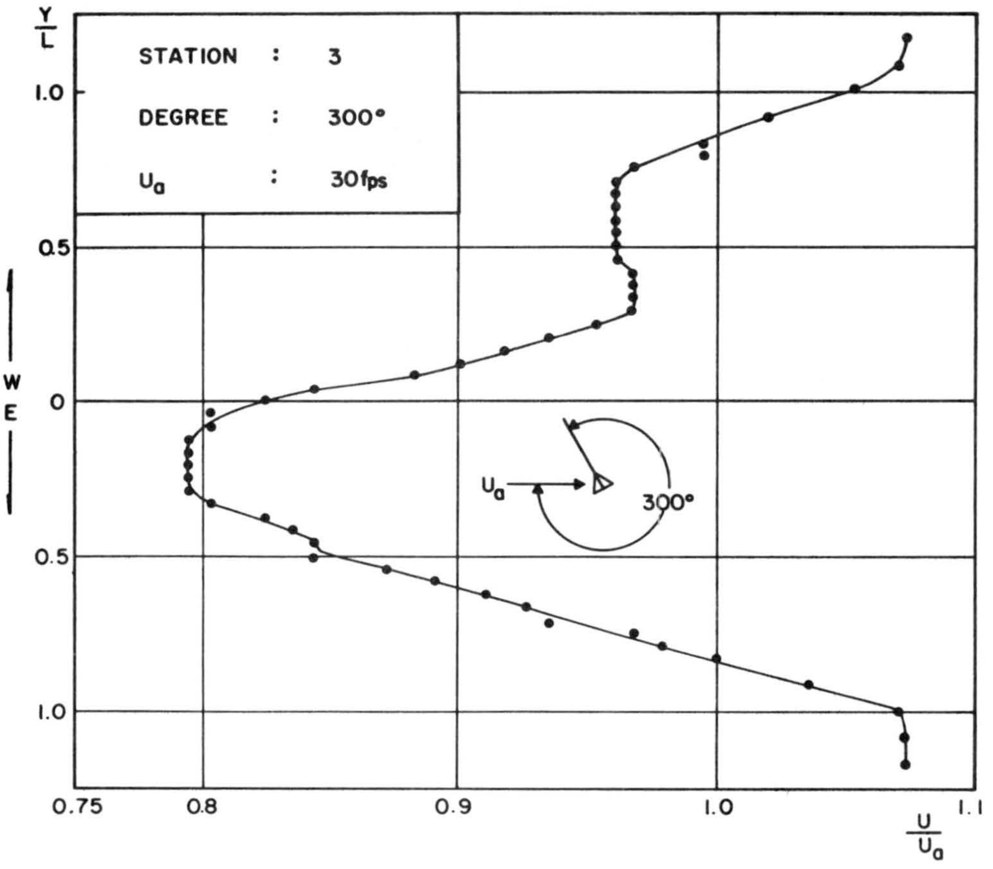

FIG. 76 TRANSVERSE VELOCITY PROFILE

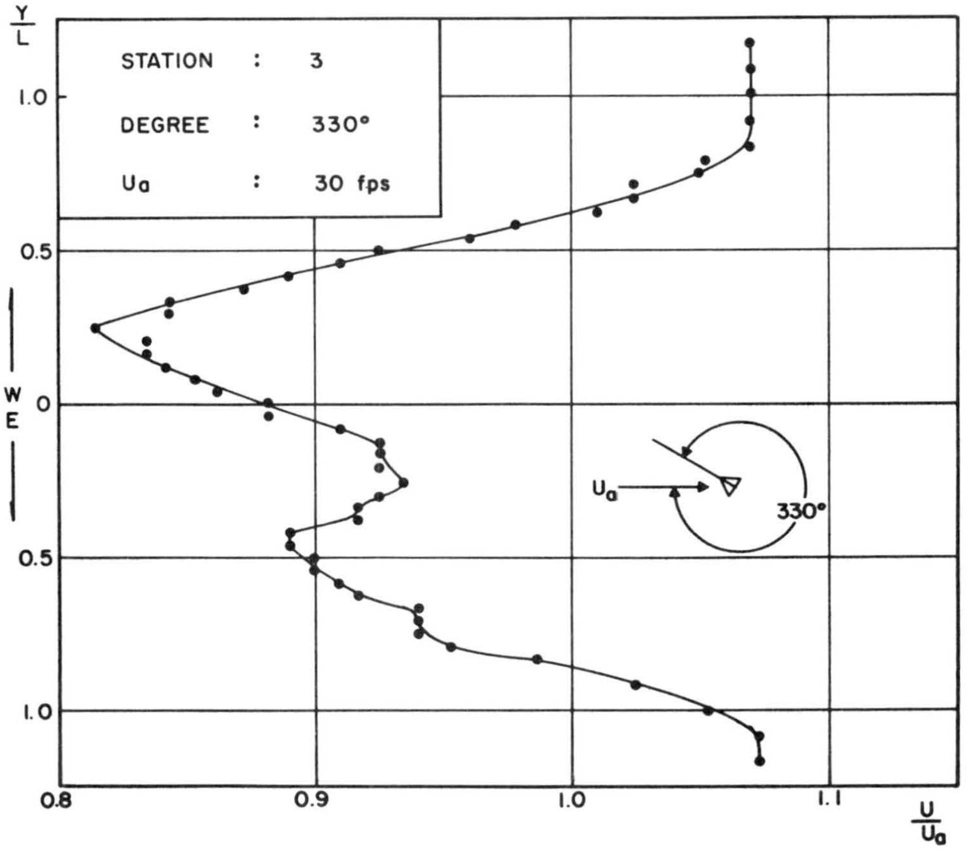

FIG. 77 TRANSVERSE VELOCITY PROFILE

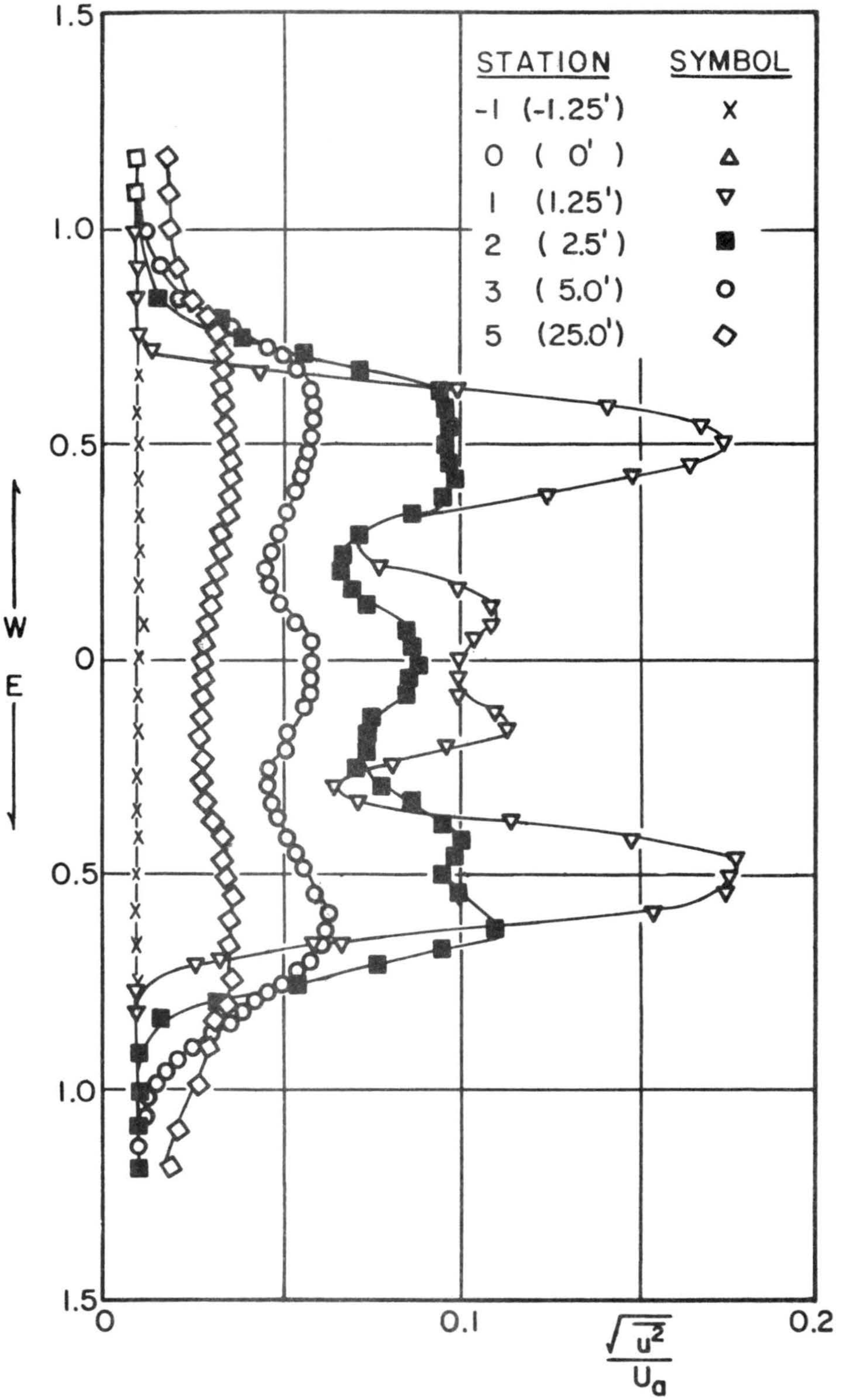

FIG. 78 TURBULENCE INTENSITY PROFILE